NUMERICAL SIMULATION OF RUBBER PANEL UNDER IMPACT LOADING

KAMSANI BIN KAMAL

RESEARCH REPORT SUBMITTED IN PARTIAL FULFILLMENT OF THE REQUIREMENTS FOR THE DEGREE OF MASTER OF ENGINEERING

FACULTY OF ENGINEERING

UNIVERSITY OF MALAYA

KUALA LUMPUR

2012

UNIVERSITI MALAYA

ORIGINAL LITERARY WORK DECLARATION

Name of Candidate: **Kamsani bin Kamal**

Registration/Matric No.: **KGH100006**

Name of Degree: **Master of Engineering**

Title of Project Paper/Research Report/Dissertation/Thesis ("this work"):

Numerical Simulation of Rubber Panel under Impact Loading

Field of study: **Mechanical Engineering**

I do solemnly and sincerely declare that:

(1) I am the sole author/writer of this work;
(2) This work is original;
(3) Any use of any work in which copyright exists was done by way of fair dealing and for permitted purposes and any excerpt or extract from, or reference to or reproduction of any copyright work has been disclosed expressly and sufficiently and the title of the work and its authorship have been acknowledged in this work;
(4) I do not have any actual knowledge nor do I ought reasonably to know that the making of this work constitutes an infringement of any copyright work;
(5) I hereby assign all and every rights in the copyright to this work to the University of Malaya ("UM"), who henceforth shall be owner of the copyright in this work and that any reproduction or use in any form or by any means whatsoever is prohibited without the written consent of UM having been first had and obtained;
(6) I am fully aware that if in the course of making this work I have infringed any copyright whether intentionally or otherwise, I may be subject to legal action or any other action as may be determined by UM.

Candidate signature: Date:

Subscribed and solemnly declared before,

Witness's Signature: Date:

Name:

Designation:

Abstract

This research report presents a numerical simulation of projectile impact on a rubber panel. The simulation is conducted in order to explore the possibilities of using rubber panel as additional safety device to sand materials which are currently used as “End Butt” at the 600 meters closed shooting range of Weapon Technology Division (WTD), STRIDE. The rubber panel should be able to stop and trap the bullet and should be light enough to be transferred from one position to the other position in the shooting range. Through simulation, we investigate the capability of rubber panel in resisting penetration of the bullet. The geometry and configuration of rubber panel capable to stop and trap the bullet are proposed. The proposed rubber panel should be suitable to be used in the shooting range. The numerical simulation is conducted using a commercial finite element code MSC. Dytran program which is available at WTD, STRIDE. The solver Lagrangian explicit method is used in the simulation and the failure behavior of contact problem is treated using Adaptive Contact Master-Slave Surface. The simulation result shows that the rubber panel is a potential material to be selected as additional safety device provided that appropriate geometry and configuration of the panel are chosen.

Abstrak

Laporan ini membentangkan satu kajian simulasi numerik hentaman peluru ke atas panel getah. Simulasi ini dijalankan untuk mengkaji atau mengenalpasti kebolehgunaan panel getah sebagai panel keselamatan tambahan kepada bahan pasir yang pada masa sekarang ini digunakan sebagai “*End Butt*” di lapangsasar tertutup 600 meter di Bahagian Teknologi Persenjataan (BTP), STRIDE. Panel getah ini mestilah boleh memberhenti dan memerangkap peluru dan juga mestilah cukup ringan untuk boleh dipindah-pindahkan daripada satu tempat ke satu tempat di dalam lapangsasar. Melaluli ujian simulasi, kami mengkaji keupayaan panel getah didalam menghalang penembusan peluru. Geometri dan konfigurasi panel getah yang boleh memberhenti dan memerangkap peluru adalah dicadangkan. Panel getah yang dicadangkan mestilah sesuai untuk digunakan di dalam lapangsasar. Ujian simulasi ini menggunakan kod finite element yang terdapat dipasaran daripada program MSC. Dytran yang terdapat di BTP, STRIDE. Kaedah penyelesaian “*Lagrangian explicit*” digunakan pada ujian simulasi ini dan di dalam kelakuan kegagalan pada permasalahan “*contact*” kaedah “*Adaptive Contact Master-Slave Surface*” telah dipilih. Hasil daripada ujian simulasi menunjukkan panel getah berpotensi digunakan sebagai panel keselamatan tambahan dengan syarat ianya hendaklah menggunakan atau mengaplikasikan geometri dan konfigurasi panel yang sesuai.

Acknowledgements

First and foremost I would like to express my highest gratitude and gratefulness to Allah S.W.T for His blesses and mercies, which enable me to finish this final project paper on time to fulfill the requirement of Master of Engineering degree.

From the deepest of my heart, I would like to say many thanks to my supervisor Dr. Andri Andriyana, senior lecturer of Department of Mechanical Engineering, University of Malaya, by accepting me as his student in performing and completing the final year project. His outstanding guidance and support has motivated and encouraged me to work much harder in completing this project. His comments and guidance are very useful for me to precede and finish this thesis.

Furthermore, I would like say thank you to Public Service Department of Malaysia for funding me in my master study. Special thanks to Director of Weapon Technology Division, STRIDE, in allowing me to use the MSC Dytran workstation and also gives me the moral supports and advices in finishing this project. Last but not least to all my friends from STRIDE and University of Malaya colleagues for their contribution, cooperation and support. Lastly, I would like to express my sincerest appreciation and warmest love to my wife and lovely daughters, whom for me has been my rock since I started my studies. They are very understanding, supportive and helpful in keeping up my struggle through all classes and finishing final project research. Without their blessings, achieving this goal would have been a near impossible.

Table of Contents

List of Figures

List of Tables

Nomenclatures

$\boldsymbol{A}$	Constant
a_n	Acceleration
$\boldsymbol{B}$	Constant
$\boldsymbol{C}$	Constant
$\underline{\underline{C}}$	Cauchy-Green stretch tensor
C	Damping matrix
CAD	Computer Aided Design
CAE	Computer-aided engineering
C_{ij}	Material parameter
$\boldsymbol{D}$	Constant
DRC	Defence Research Centre
DTC	Defence Technology Centre
d_n	Displacement
FEA	Finite Element Analysis
FMJ	Full metal jacket
$\underline{\underline{F}}$	Deformation gradient tensor
F^{ext}_n	Vector of External applied load
F^{int}_n	Vector of Internal load ($Cv_n + Kd_n$)
$F_n^{residual}$	Residual load vector
$\boldsymbol{G}$	Shear modulus
I_1, I_2, I_3	Invariants of the deformation tensor or strain invariants in terms of stretches
$\boldsymbol{K}$	Bulk modulus
K	Stiffness matrix
k	Volume modulus or bulk modulus
km	kilometre

LVC	Linear Viscosity Constant
M	Mass matrix
M^{-1}	Invert mass matrix
m/s	meter per second
mm	millimetre
NC	Nitrocellulose
NG	Nitroglycerin
PSTP	Pusat Sains Teknologi Pertahanan
STRIDE	Science and Technology Research Institute for Defence
$\boldsymbol{v}$	Poissons's ratio
v_{n}	Velocity
WTD	Weapons Technology Division
W	Strain energy potential
$\boldsymbol{W}$	Strain energy density function
X_{j}	Original geometry
x_{i}	Deformed geometry
YS	Yield Strength
1D	One-dimensional
2D	Two-dimensional
3D	Three-dimensional
$\lambda_1, \lambda_2, \lambda_3$	Ratio of extended length to the original length
λ_{ij}	Stretches
$\underline{\underline{\tau}}$	Stresses
$\underline{\underline{\sigma}}$	Second Piola-Kirchhoff stress tensor

CHAPTER 1: **Introduction**

1.1 Background of the Problem

STRIDE is one of the departments in Ministry of Defence of Malaysia. Previously it is known as Defence Technology Centre (DTC) from 1968 – 1972, Defence Research Centre (DRC) from 1972 – 1985, Pusat Sains dan Teknologi Pertahanan (PSTP) from 1985 – 2002 then Science and Technology Research Institute for Defence (STRIDE) from 2002 until now (Yunus 2009). The main functions of STRIDE are conducting research related to defence technology and testing and evaluating of equipments of Malaysian Armed Forces such as radio communications, materials, weapons, bullets, etc. STRIDE has 5 technical divisions. One of the divisions is known as Weapons Technology Division (WTD) based at Batu Arang, Selangor. The research and evaluation focus in this division is related to the weaponry and explosive technology. Under WTD there are 5 sections: Weapon Section, Ballistic Section, Ordnance Section, Propulsion Section and Weaponry Technical Support Section.

There are several types of weapon and bullet testing. One of the testing is firing activity. The objective of this activity is to study the functionality of the weapon or bullet and the resulting of bullet trajectory. For this purpose WTD has a closed or covered shooting range. The existing shooting range is 600 meters in length measured from the firing position. It has a tunnel-like construction with wall and roof made from concrete as illustrated in Figure 1.1.

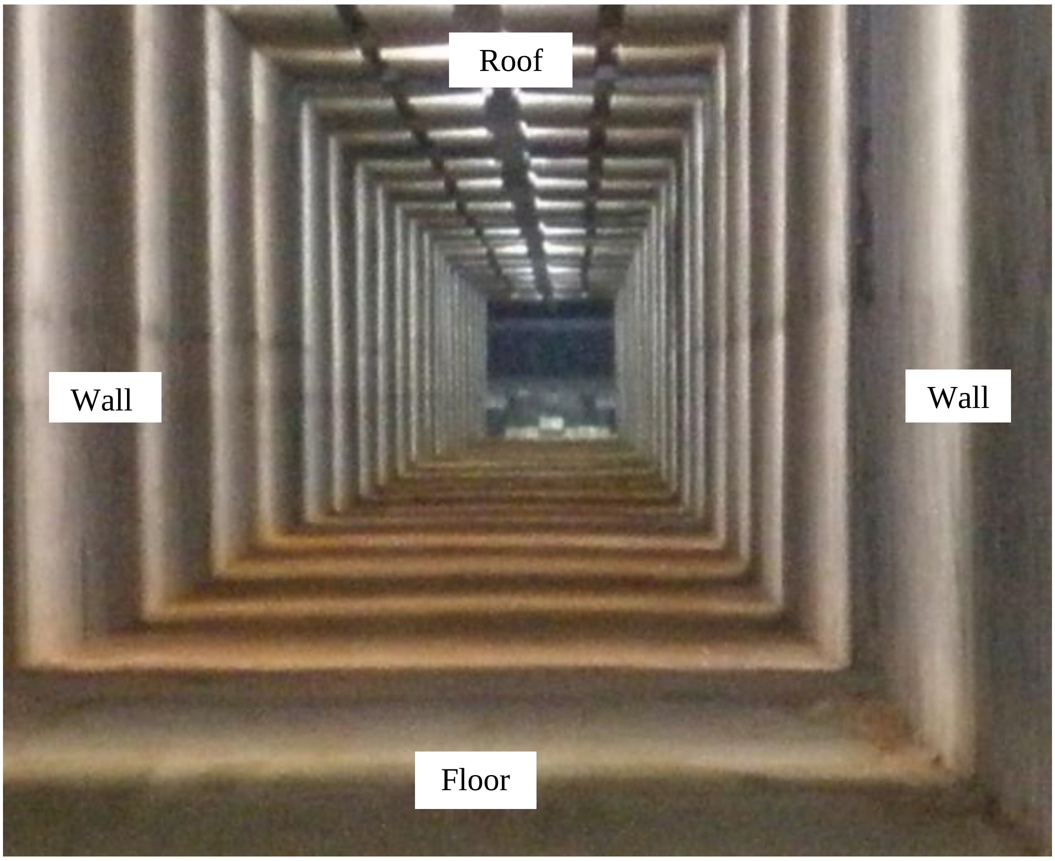

Figure 1.1: Tunnel-like construction of shooting range

Regarding the bullet used in WTD, the highest size of calibre or diameter of the bullet fired in this shooting range is 12.7 mm. During the test, the weapon is positioned at one end of the tunnel. In order to stop the tested bullet, an arrangement of sand in the sacks, known as “End Butt”, is permanently installed at another end of the tunnel. Since the firing position is also fixed, the shooting range cannot be modified, i.e fixed at 600 meters. The firing position cannot be transferrable because at this position all of the test and sensitive measuring equipment are being installed permanently. For example, the test weapon system has heavy mounting and fixed at this position. The requirement of muzzle velocity and environment measuring system has to be closed with the control room. The test weapon system and measuring equipment system are shown in Figure 1.2.

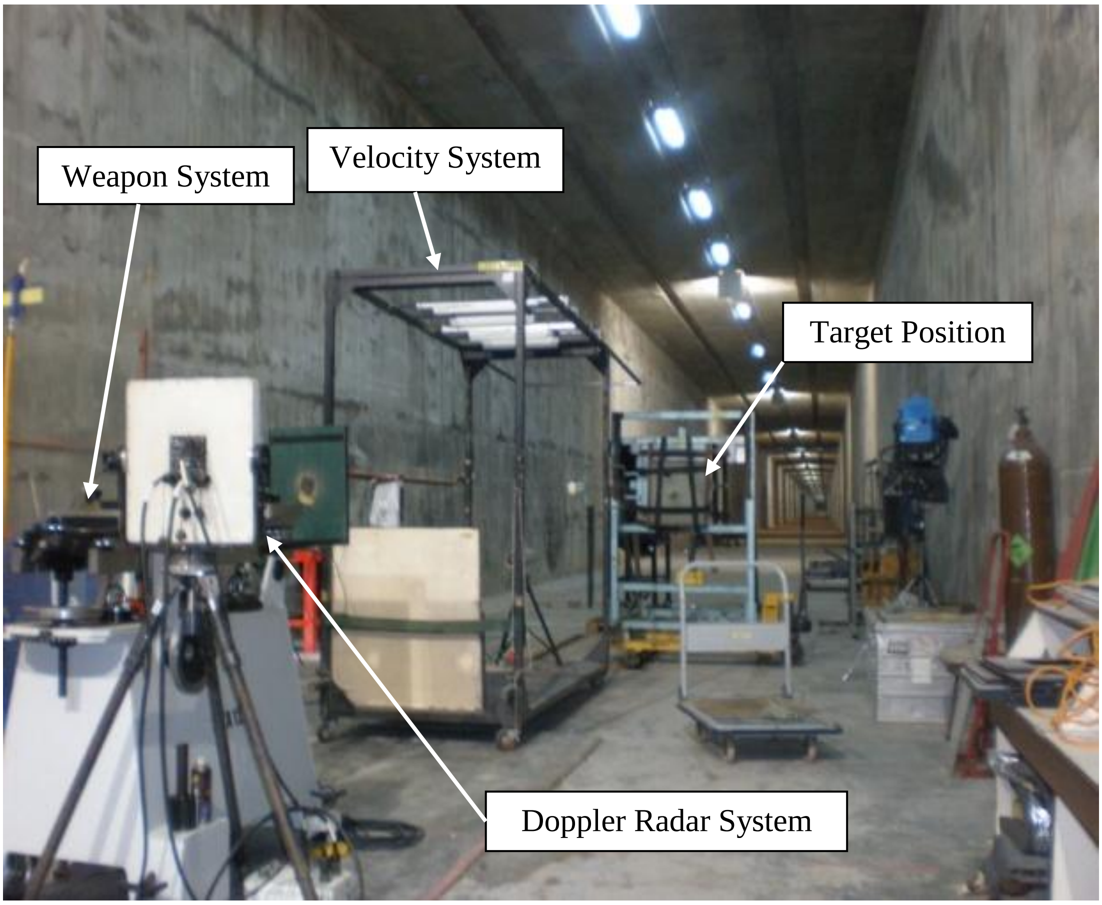

Figure 1.2: The position of test weapon and measuring equipment system

1.2 Problem Statement

In testing activity, when weapons fired from this firing position not all bullets will reach the end butt due to the height, angle of firing and the required distance of target. Furthermore, the target is positioned normally at 100 meters, 200 meters or 300 meters from the firing position. If the target is positioned at 100 meters or less, the bullet fired will not reach to the end butt. This bullet will hit the ground or hitting the wall of the range at first. This is very dangerous to the user and also damaging to the electric cables or others equipments around the closed shooting range.

The present material of end butt is using sand materials. They are stored in different sacks called sand bags. The sand bags are arranged in stacks occupying the whole area of end butt. The use of sand bags as a medium to stop the bullet has drawbacks which can be summarized as follow:

a. Sand dust will scatter and fly around the end butt area polluting the air when the bullet hits and tears the sand bags. This condition will increase the time require for clearance process, which is a part of safety procedures, required before conducting the subsequent test.

b. The broken sand bags have to be replaced regularly. In the current practice at STRIDE, all broken sand bags are replaced every six months. In order to increase the service duration of sand bags, which in turn will reduce the maintenance cost, the numbers of broken sand bags have to be minimised.

Figure 1.3: Sand out from sacks at the end butt

c. The sand bags arrays are not easily transferred to the new position according to the requirement of testing range.

To overcome problems mentioned above it is desirable to have a portable end butt, with a relatively small size in dimension, easy in handling and light weight. The existing and desired schematic diagram layouts are shown in the Figure 1.4 and 1.5 respectively.

For this propose, the study of potential material to be used as the above additional safety device has to be conducted. The safety device should be light weight and able to stop completely the bullet at the required distance of testing. Therefore the potential material should have sufficient damping capacity.

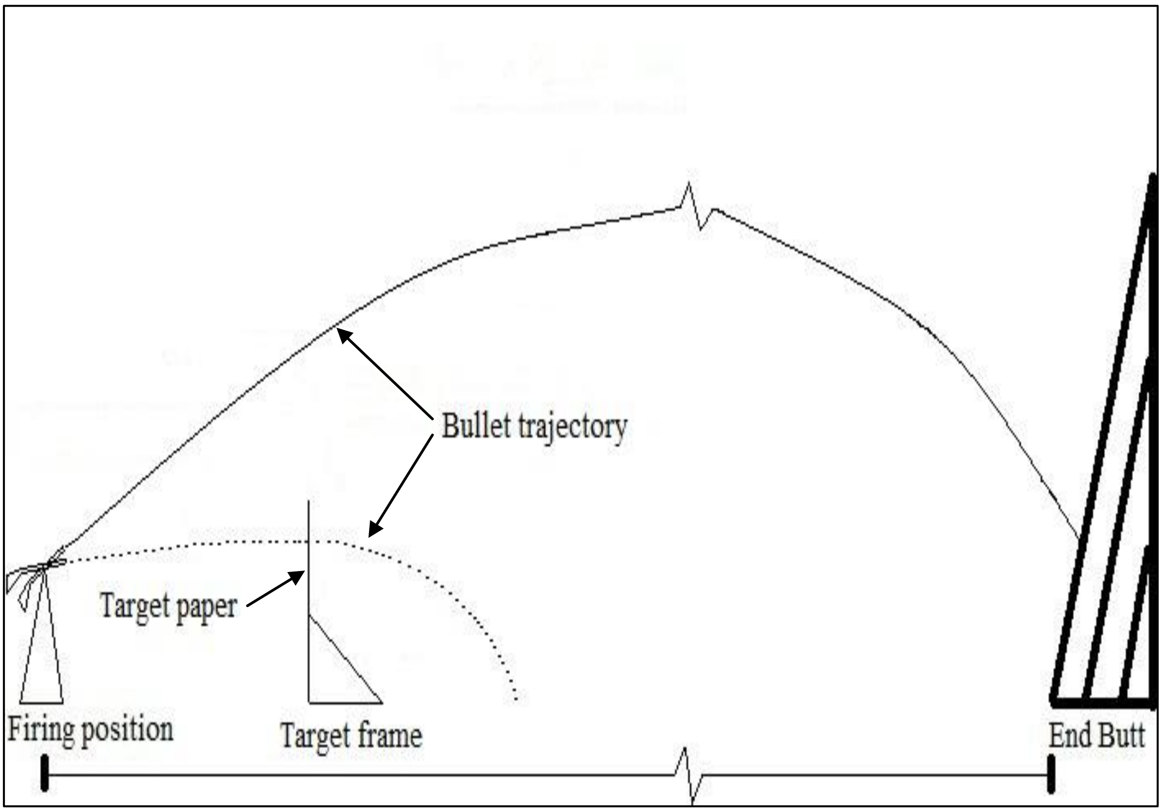

Figure 1.4: The existing schematic diagram layout of shooting range

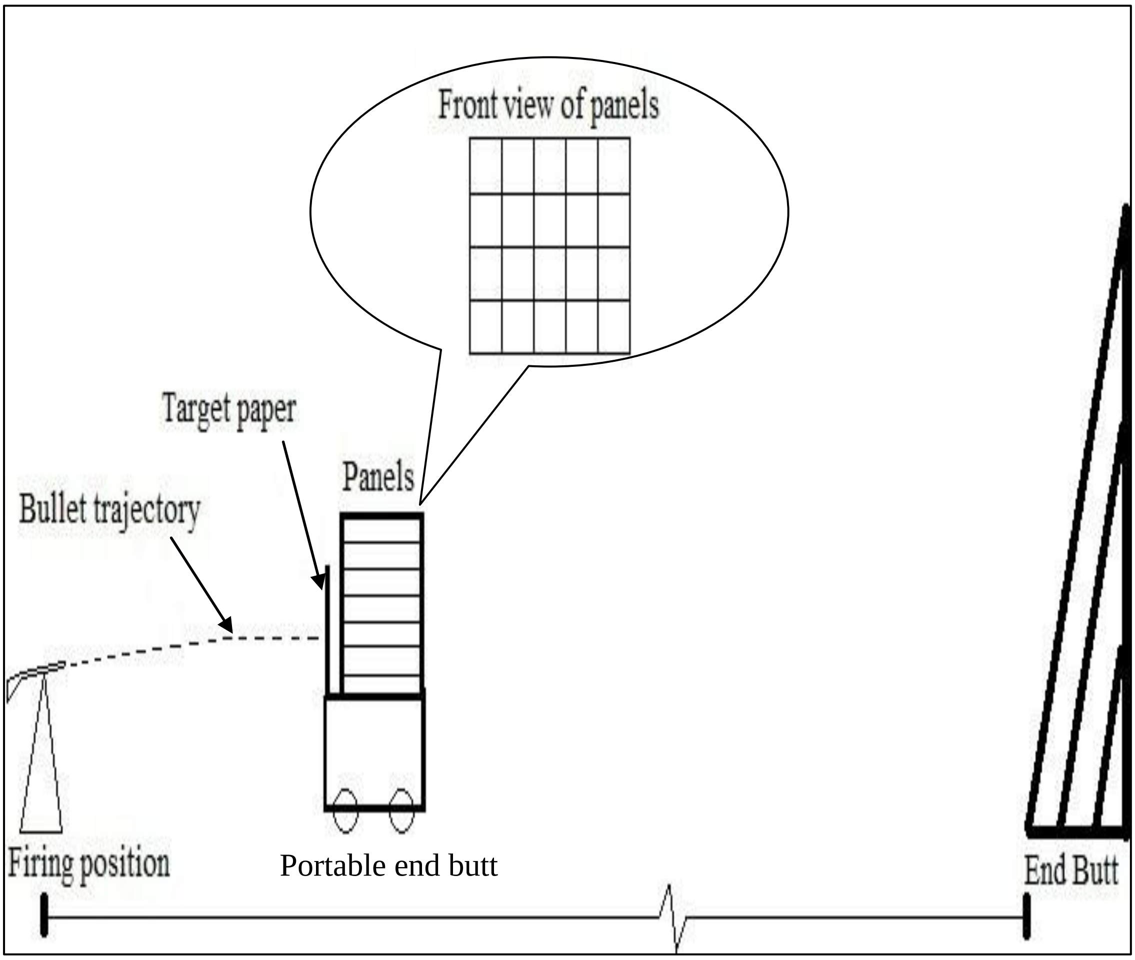

Figure 1.5: The desired schematic diagram layout of shooting range with portable rubber panel

1.3 Aims of the Study and Objectives

The objective of the present study can be summarized as follow:

a. To conduct the feasibility study on rubber material as a possible additional safety device (portable panel end butt).

b. To simulate the mechanical response of rubber material under impact loading condition.

c. To propose a new design of geometry and configuration of the portable rubber panel end butt.

1.4 Scopes of Study and Methodology

In the present study only numerical simulation method is considered. All material parameters involved in the simulation are obtained from the literature. The bullet calibre or diameter under consideration is 7.62 mm ball which is the one currently used at WTD, STRIDE.

The methodology conducted in this research is as followed:

a. Literature review on the FEA simulation materials under bullet impact.

b. Conducting the FEA penetration simulation on rubber materials.

c. Study on mechanical behaviour of materials.

d. Design new geometry and configuration of portable rubber panel.

e. Discussion of the results.

f. Conclusions and Recommendations.

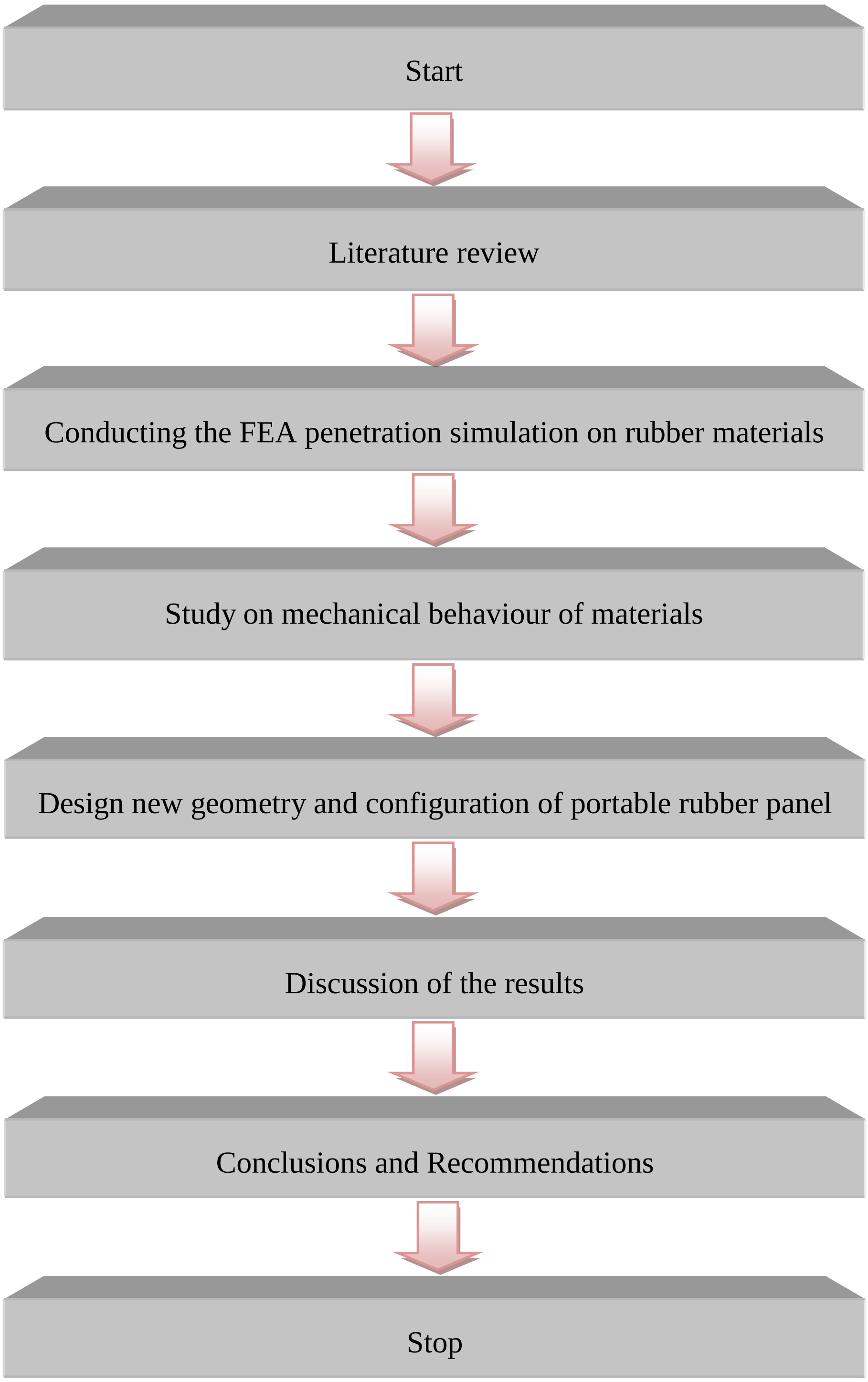

Figure 1.6: Methodology Flowchart

CHAPTER 2 : Literature review

2.1 Finite Element Analysis (FEA)

Many literatures stated the finite element analysis has started since 1940s. In 1941 Hrennikoff has developed the finite element analysis in the field of structural engineering and Mc Henry in 1943 used collection of bars and beams to solve the stresses in continuous solids (Reddy 1984; Logan 2002). It was known as one-dimensional (1D) finite element analysis. The two-dimensional (2D) finite element analysis was introduced in 1956 by Turner, Clough, Martin and Topp. They were solved the problems for truss elements, beam elements, and two-dimensional triangular and rectangular elements in plane stress. The three-dimensional (3D) finite element analysis was introduced by Martin in 1961, Gallagher et al. in 1962, and Melosh in 1963 (Logan 2002). They were studying the problems through 3D method by developing tetrahedral stiffness matrix. Since then, the finite element analysis has evolved and become the "must" tool in solving any engineering problems and become more important since the development of high speed computer. As known the finite element analysis is able to be used in analysing structural and non-structural problems. It is such as stress/strain analysis, buckling, vibration, heat transfer, fluid flow, and distribution of electric and magnetic potential.

The basic concept of the finite element analysis is an idea to simplify the complicated object by developing small pieces of simple blocks. Logan said in his book (Logan 2002), "The finite element method involves modelling the structure using small interconnected elements called finite elements. A displacement function is associated with each finite element. Every interconnected element is linked, directly or indirectly, to every other element through common (or shared) interfaces, including nodes and/or boundary lines and/or surfaces. By using known stress/strain properties for the material making up the structure, one can determine the behaviour of a given node in terms of the properties of every other element in the structure. The total set of equations describing the behaviour of each node results in a series of algebraic equations best expressed in matrix notation".

Generally before we can operate and run the finite element analysis programme and get the reliable results, we have to follow the procedures or steps in a finite element formulation of a problem. First of all we have to divide the models into the same system of finite element and choosing element type. The second step is defining the material behaviour on each element. The third step is defining the equations for the models such as loads and boundary conditions. The fourth step is solving the equations and the last step is obtaining the information required.

2.2 Review of Finite Element Analysis

Studying the mechanics of rubber under impact as additional safety device to sand material for 600 meters closed shooting range is a good innovation for WTD, STRIDE if able to materialise. Under this study we are using MSC. Software simulation workstation which is available at WTD, STRIDE. The FEA study on material under impact has been done before and most of it is for personnel protection, military vehicles, aerospace and other defence and civilian applications. They are still trying to solve and understand the mechanics of material that can give the best material choice to be used as bullet stopper. Types of materials they are studied such as composite, ceramics, aluminium plates, ductile steel and textiles. There are two methods of studying the materials under impact. First method is conducted through experimental firing in the laboratory and the second method is using FEA simulation software. In this study it will focus on FEA simulation only. There are many FEA software available in the market such as AUTODYN, LS-DYNA, IMPETUS, MSC. DYTRAN, ABAQUS, and etc. There are several studies on materials under impact have been done with FEA simulation and available in the journals. Most of them found that the result of experimental and the FE simulations gave a good agreement between them.

Borvik et al. (Børvik, Olovsson et al. 2011) studied on the normal and oblique impact on 20 mm thick AA6082-T4 aluminium plates. The bullets size is 7.62 x 63 mm NATO soft lead core and 7.63 x 63 mm APM2 hard steel core. The angle of impacts is 0º, 15º, 30º, 45º and 60º and the impact velocity is 830 m/s. They are trying to fine which angle of impact that can give the worst scenario when hit the plate material. They found that the angle that can give higher depth of penetration for both bullets is 0º to 60º. They are using LS-DYNA 3D non-linear FE simulation and using failure criterion of modified Johnson-Cook constitutive relation and the Cockcroft-Latham.

The FEA simulation of impact on ceramic composite armour material known as ultra high molecular weight polyethylene (UHMWPE) was done by Krishnan et al (Krishnan, Sockalingam et al. 2010). They are using LS-DYNA explicit finite element analysis and the material model Johnson-Holmquist was selected to model the impact phenomenon for ceramic material. The purpose of studying is to develop a finite element model as a predictive tool in design to balance the requirements given by weight, thickness and cost of body armour for a particular threat level.

The other study of impact on composites done by Gama et al (Gama and Gillespie Jr 2011). They studied the impact, damage evaluation and penetration of thick section composites. LS-DYNA explicit dynamic finite element analysis was used and the material model MAT162 was selected to simulate the progressive composite damage. They tried to develop a systematic model-experiment methodology in validating the finite element model from static to impact loading conditions. They also develop the 3D finite element model of the ballistic impact.

The study of impact by hemispherical-nose, cylindrical projectile on the lightweight composite sandwich panels consisting of fiber-reinforced E-glass polyester polymer facesheets and Divinycell H130 polymeric foam core was done by Hoo Fat and Sirivolu (Hoo Fatt and Sirivolu 2010). This paper is tried to develop an analytical model use to quantify the deformation and failure of composite sandwich panel subjected to high velocity impact of projectile. The result of transient deflection and velocity of the projectile and sandwich panel is fairly well between ABAQUS Explicit and continuum C3D8R elements and published experimental data.

Ong et al. (Ong, Boey et al. 2011) was using AUTODYN to design composite personnel armour by optimizing the role of each layer plays during projectile defeat. They investigating layered concept in armour plate technology based on fundamental shock physics to stop a projectile penetration. The studied using composite plate consisting of a very hard 1st layer, for the 2nd layer a wave spreading function, and shock absorbing place as the 3rd layer. They concluded that the sequence concept of the layering armour is fundamentally correct due to it performed better than the conventional armour steel of equivalent areal density.

Works on impact of various projectiles on ceramic/steel armour by using finite element analysis was done by Lamberts (Lamberts 2007). He tried to get high strain rates and high pressure by using various constitutive models. The study shows the

Johnson-Holmquist-Beissel model is the most appropriate to be used. In his study he used MSC. DYTRAN code.

The FEA simulation is also able to calculate the performance of plastics components under impact (Dean and Read 2001). They are working with the high value of stress and plastic strain when the plastics components received an impact. They found that for strain rate higher than 1 s^{-1}, errors in measurement occur associated with the generation of transient forces and difficulties to measurement strain.

Zeng et al. (Zeng, Pattofatto et al. 2010) study the perforation behaviour of sandwich plates with graded hollow sphere cores under impact using LS-DYNA. The material they were use for plate is 0.8 mm 2024 T3 aluminium alloy skin sheet and graded polymer. It is found that the first layer of skin sheet should be rather weaker than the core material. The weaker skin sheet material will folds into the core and cause much more energy to consume during perforation process. They were used finite element analysis to get the key of local information which is not experimentally available during the perforation process.

Iqbal et al. (Iqbal, Chakrabarti et al. 2010) studied the impact on ductile target by using 3D numerical simulation method using ABAQUS finite element analysis code. They studied the behaviour of Weldox 460 E steel and 1100-H12 aluminum targets when impacted with conical and ogive nosed steel projectiles respectively. The material is made in single and double layered target. The thickness for double layer target is same with a single layer target. They found that the monolithic material target has higher ballistic resistance than the double layered material target of the same thickness. This study shows the mechanics of perforation is quite complex and depends on various parameters including thickness and material properties of the target and shape of the projectile.

Rittel et al. (Dorogoy, Rittel et al. 2010) studied on polymethylmethacrylate (PMMA) plate under impact. They want to understand ductile failure and tensile failure. The effect of kinetic energy of projectile under angle trajectory of impact was also in their study. The ductile failure criterion enforces a straight trajectory in the initial velocity direction and the tensile failure criterion controls the deflection and ricochet phenomenon. They study by using ABAQUS explicit finite element code.

Qasim (Qasim H 2009) works on plastic deformation of a thin rectangular polycarbonate armour plate subjected to single and multiple impacts. The impacts were conducted on horizontal and diagonal path. He is using the result from LS-DYNA and compared with the experimental work. The results show close agreement between them.

Sareen (Ashish K. Sareen 1996) studied the impact and penetration of projectiles to a generic fluid-filled tank and a composite wing structure containing fuel cells. She is using MSC. DYTRAN finite element-code in her study. She found that the MSC. DYTRAN is a promising tool for improving ballistic tolerance designs and in guiding pre-test specimen setup.

Nyström et al. (Nyström and Gylltoft 2011) were studied in comparative numerical studies of projectile impacts on plain and steel-fibre reinforced concrete. They were using AUTODYN in studying the different amounts of fibres. The amount of fibres will influence the depth of penetration and crater formation on the front and rear face of a concrete target. He concluded that scabbing crater can be reduced in size by using fibre-reinforced concrete and the depth of penetration is only slightly less than the depth of penetration in plain concrete.

Duan et al. (Duan, Keefe et al. 2006) studied the influence of projectile-fabric friction and yarn-yarn friction during ballistic impact of a rigid sphere onto a square fabric panel. The result showed friction affected the fabric deformation within the impact region and also contribute in the fabric energy absorption. They used LS-DYNA explicit nonlinear FEA code in running the simulation.

Wang et al. (Wang, Miao et al. 2010) and Barauskas et al. (R. Barauskas 2005) worked on digital element approach for simulating impact and penetration of textiles and woven structures. They satisfied with the results found and the study can be done with simulation software.

Sands et al. (Sands, Fountzoulas et al. 2009) studied the influence of defects on the failure of laminates, for statically and dynamically testing in ceramic materials. They are using a transparent magnesium aluminate spinel (MgAl2O4) striking-ply backed by polycarbonate. The finite element analysis is used to predict unsuccessful designs and reduce the number of laminate configurations in experimental testing. They are using ANSYS/AUTODYN to simulate the penetration. According to them the result of simulation gave a good agreement with the experimental result.

Sauer (M 2011) studied the impacts of projectiles on fluid-filled aluminium plate containers. He was using LS-DYNA to simulate the penetration of high velocity impact. Lagrangian finite element method, non-commercial codes with explicit time integration was used. He found that the result has a good agreement with the experimental observations for deformation, water spread and residual velocity.

2.3 Polymer

Polymer is a material that can be in the form of crystalline and amorphous. Traugott Fischer (Fischer 2009) said "Rubber is a natural or synthetic polymer with a molecular structure that allows it to stretch by large amounts". A polymer consists of repeated units called as mers or monomers (McHenry 2010). Mer is referred to a unit of atoms or molecules of polymer foundation. A few molecular units or mers ($\leq$ 50) repeated as a group typically known as oligomer. Polymer is usually has more than 50 mers or maybe thousands of mers. Therefore, polymer is formed from many mers linked together and become a long chain. This can be called as macromolecules. The process of creating polymers properties is called the degree of polymerization. It has two processes which are known as addition polymerization and condensation polymerization (Donald R. Askeland 2003).

Polymer can be classified according to the molecular structure. It is known as a linear polymer, a branched polymer or a network polymer. A linear polymer has one backbone with no branches and it does not mean as a straight line. A branched polymer has smaller secondary chains which is emanating from the primary chain. The branched structure tends to lower the degree of crystallinity and density of the polymer. Cross-linking polymers is branched molecules are formed between separated polymer chain molecules.

The polymer in crystalline or in solids form such as plastics or o-ring, the chain of molecules are rigidly fixed in space and entangled between the polymer chains. Therefore it has higher density. The polymer in amorphous or in liquid form, the chain of molecules are freely in space. So it has low density.

The classification of polymers is based on thermal and mechanical properties. The mechanical properties of polymers such as modulus of elasticity, tensile, impact, and fatigue strength are the same with the parameters for metallic materials. Furthermore, polymers are highly sensitive to the rate of deformation, temperature and chemical in environment. The polymers can behave as brittle characteristic at the lower temperature, and will yielding and plastic deformation and totally elastic or termed as elastomers at the higher temperature.

The polymers can be classes as thermoplastic polymers, thermosetting polymers, and elastomers. Thermoplastic polymers have long, linear, or branched chains that are not cross-linked. This polymer is soften when heated therefore it can be repeated again and again to the other forms. Thermosetting polymers have long linear or branched chains that are strongly cross-linked. This polymer is irreversibility of the cross-linking reaction and it makes reprocessing of these polymers difficult. It behaves like the other brittle solid material. If the thermosetting polymer contains surface flaws or sharp notches, the stress will be high at these location to break covalent bonds and cause fracture to the polymer materials. Elastomers (or rubbers) can be thermoplastics or weakly cross-linked molecules thermosetting polymers and can be are distinguished by the large elastic elongation.

Viscoelasticity is a property of deformation of rubber and it has capacity of large elastic deformation. It is because this kind of property material has molecule structure like shape of coils spring. In deformation action, it is actually straightening these coils. The viscoelasticity property is in between elastic at low temperature and viscous or liquid like behaviour at high temperature.

Creep is a deformation at slow and steady process and increase in the deformation because of a constant load. It happen at above the glass transition temperature but it also can happen at room temperature and below. It is depend on the temperature and the load given. Usually this kind of deformation in polymers is called viscoelastic creep.

2.3.1 Constitutive Modelling

In the stress-strain relations of the hyperelastic material such as natural rubber is generally characterized by strain energy potentials. It is because natural rubber is a non-linear elastic isotropic behaviour and incompressible. In this study the define properties used in the software is according to Mooney-Rivlin function. From Zhao et al. and Leow et al. (Loew and Meier 2007; Li, Zhao et al. 2009) the Mooney-Rivlin function of strain energy potential is expressed as

$$W = \sum_{i+j=1}^{N} C_{ij}\ (I_1 - 3)^i (I_2 - 3)^j + \frac{1}{2} k\left(\sqrt{I_3} - 1\right)^2$$

where C_{ij} is a material parameter from the material test, k is the volume modulus or bulk modulus, I_1,I_2,I_3 are the invariants of the deformation tensor or the first order, second order and third order invariants strain values, respectively. The invariants are calculated from the principal stretch ratio λ_1, λ_2, and λ_3. The λ_1, λ_2, and λ_3 are defined as the ratio of extended length of the specimen to the original length of the specimen in three principal stress directions. The invariants are defines as

$$I_1 = \lambda_1^2 + \lambda_2^2 + \lambda_3^2$$

$$I_2 = (\lambda_1 \lambda_2)^2 + (\lambda_2 \lambda_3)^2 + (\lambda_1 \lambda_3)^2$$

$I_3 = (\lambda_1\lambda_2\lambda_3)^2$

In the uniaxial stress state, the principal stretch ratios λ_1, λ_2, and λ_3 are as

$\lambda_1 = \lambda_u$ and $\lambda_2 = \lambda_3 = 1/\sqrt{\lambda_1}$

where λ_u is the principal stretch ratio in the applied loading direction, λ_2, and λ_3 are the principal stretch ratios on the planes which is perpendicular to loading directions. Due to the material has incompressibility behaviour and constant volume, the I_3 invariant is 1, therefore the volume modulus or bulk modulus become 0 (Loew and Meier 2007).

2.4 Small Arms Ammunition

Naturally when said small arms ammunition it is for weapons such as pistols, sub-machine guns, rifles and machine guns. By definitions small arms ammunition is for calibre or diameter of bullet below 15 mm (Halsey 1982) or from other reference the diameter of bullet is below 20 mm (Omar 2003). Sometime small arms ammunition is also referred as a round of ammunition. The histories stated, small arms ammunition began since 1320 after the black powder was introduced (Halsey 1982). The function of ammunition is to incapacitate personnel or killing the animals through extensive wound effect on the body.

A complete round of ammunition consists of cartridge case, ignition system or cap, propellant and bullet (Donald E. Carlucci 2008). The typical overview of ammunition is shows in Figure 2.1.

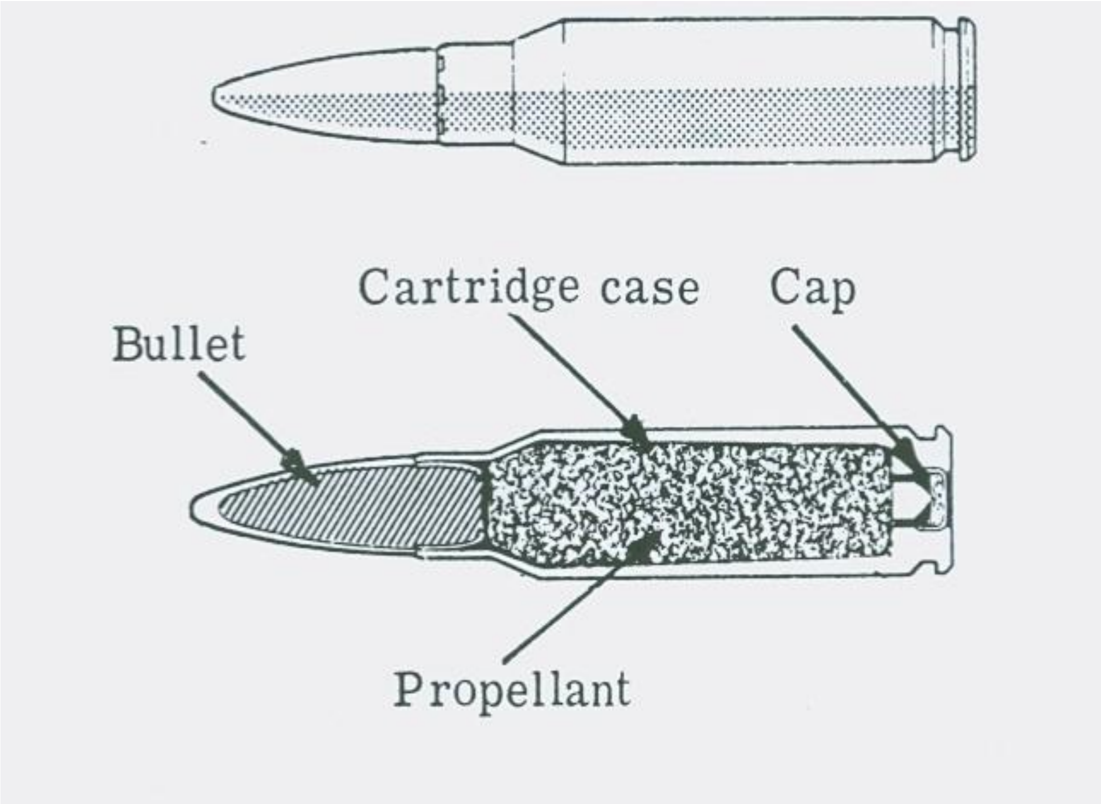

Figure 2.1: Typical round (Halsey 1982)

2.4.1 Cartridge Case

The functions of cartridge case are to accommodate the propellant charge, the ignition system and hold the bullet at its mouth. Beside that it also functions as a sealing system which means preventing gas from escaping to the rear side of barrel when the generated gas pushing bullet moves forward out of the barrel muzzle. A cartridge case is usually made from cartridge brass or cuprous-nickel or gilding metal. The alloy composition of cartridge brass is 70/30 copper zinc alloy in proportions, cuprous-nickel is a copper nickel alloy of about 80/20 in proportions and gilding metal is a copper zinc alloy of about 90/10 in proportions (Omar 2003).

2.4.2 Bullet

The function of bullet is to carry pure kinetic energy and transferring to the target when hit (Donald E. Carlucci 2008). Kinetic energy bullet for military purposes are fully jacketed or enveloped to cover an inner core metal. This is to achieve stability during flight and cause high wounding potential to the target. It is also to follow the Hague Convention guidelines 1900 (Halsey 1982). The conventional jacketed bullet is sometime described as a full metal jacket (FMJ) bullet. It is shown in Figure 2.2.

The jacket metal is usually from copper alloy such as gilding metals combination of 95% copper and 5% zinc. The inner core metal of the bullet is made from an alloy such as lead and antimony with ratio 9:1 to give a good bullet penetration and reasonable weight. The jacket does not fully cover the core of the bullet. It rolls over the base to leave the core exposed. The exposed part will provide what they called “set-up” or the base of bullet expanding during firing in assisting the jacket or envelope to engrave with the “land” inner part of the barrel. The expand bullet base subjected to gas pressure enable the earliest seal of gas to be formed. This is to prevent the excessive amounts of gas from escaping through the front of the bullet. High velocity bullets are made tapered or known as “boat-tailed” towards the base of the bullet. This is to reduce drag of the bullet in flight.

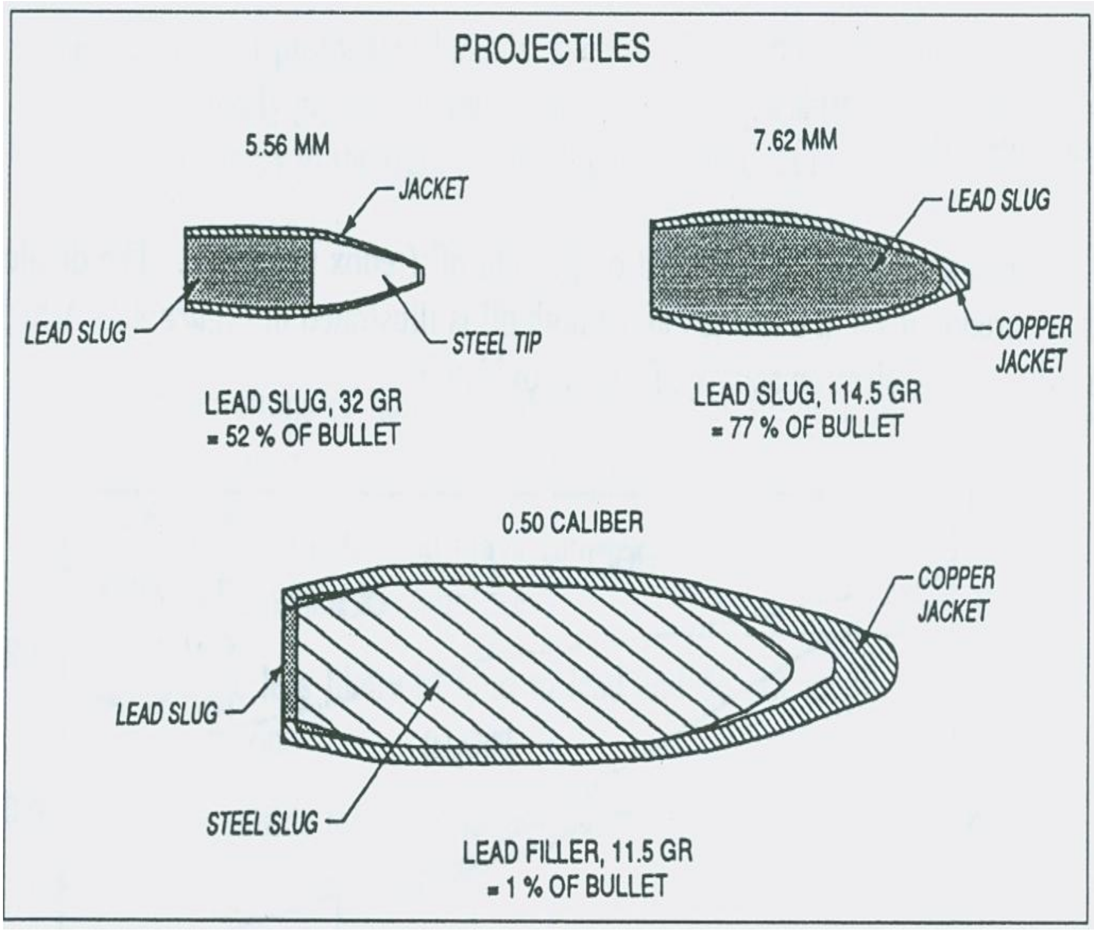

Figure 2.2: Diagram of bullet jacket and core

2.4.3 Ignition System

The ignition system functions when the percussion cap composition is crushed by a firing pin to produce flame. The flame then passing through the fire holes to burn the main propellant. The most used ignition system known as berdan cap and boxer cap (Omar 2003). The berdan cap consists of a cap that fits over and anvil in the base of cartridge case. The boxer caps manufactured incorporates a brass anvil assembly on the top of the closing disc or it consists a cap incorporates its own built-in anvil. The ignition composition commonly based on mercury fulminate and for the present day it is made from lead styphnate.

2.4.4 Propellant

Propellant used in the small arms ammunition normally has two types. It is known as single base propellant and double base propellant. The single base propellant is based on nitrocellulose (NC) only. NC may be in the form of flakes, grains or cylinders depending on the rate of burn desired. Double base propellant contained approximately 90% NC and 8% Nitroglycerin (NG). The advantage of double base propellant is it is more energetic but produces greater flame temperature than single base propellant. The other disadvantage is it increases erosion at the inner part of the barrel particularly at commencement of rifling.

2.5 Technical Data Bullet 7.62 mm, 5.56 mm, and 9 mm

Bullet 7.62 mm and 5.56 mm is purposely for rifle which is able to hit target at the long distance. Bullet 7.62 x 51 mm ball is able to reach target at distance more than 2 km and still carries sufficient energy to incapacitate target while bullet 5.56 mm is able to reach target up to 1 km (C J Marchant Smith 1982). The muzzle velocity of these bullets is high: about 800 m/s for bullet 7.62 mm and 900 m/s for bullet 5.56 mm.

Pistol and submachine-gun normally have bullet diameter or calibre 9 mm. It is for engaging closer target for about 100 meters in range since the muzzle velocity is lower: about 400 m/s. The summary technical data of bullet 7.62 mm, 5.56 mm and 9 mm is shown in Table 2.1.

BulletType	Muzzel Velocity	Muzzel Energy	Bullet Weight
7.62 x 51 mm Ball M80	854 m/s	3519 J	9.65 g
5.56 x 45 mm Ball M193	975 m/s	1692 J	3.56 g
5.56 x 45 mm Steel Core SS109	930 m/s	1708 J	4.00 g
9 x 19 mm Parabellum	396 m/s	583 J	7.45 g

Table 2.1: Bullet Data (Terry J Gander 2000)

2.6 MSC. Dytran Code

STRIDE has bought MSC. Software in 2007 with the purpose to develop the capability of research in material designs by using the computer-aided engineering (CAE). The MSC. Software Corporation which is formerly known as MacNeal-Schwendler Corporation has been supplying the sophisticated computer-aided engineering tools since 1963 (1997). The products of MSC. Software cover the engineering disciplines such as structural analysis, heat transfer, crash dynamics, electromagnetic field analysis and graphics pre- and post-processing. The main product is MSC. Nastran used finite element structural program for linear analysis, vibration and classic dynamic and the original development of this software began in 1966 (1997). The other software products marketed by the MSC Software Corporation are MSC. Marc, MSC. Dytran, MSC. Patran, MSC. Marc Mentat, MSC. Adams, MSC. Fatigue, and etc.

In calculating the mechanical response on impact simulation, the finite element analysis code MSC. Dytran is used. According to the MCS. Dytran 2005 r3 Theory Manual (2006) the solution technique of this program uses the Lagrangian explicit method to solve the equation of motion and it as follows.

The equation of motion

$$Ma_n + Cv_n + Kd_n = F_n^{ext}$$

where M is the mass matrix, C is the damping matrix and K is the stiffness matrix. The a_n is acceleration, v_n is velocity, d_n is displacement and $F^{ext}{}_n$ is vector of external applied loads.

Then the equation can be written as

$$Ma_n = F_n^{ext} - F_n^{int}$$

$$a_n = M^{-1}F_n^{residual}$$

where F_n^{int} is vector of internal load ($Cv_n + Kd_n$) and $F_n^{residual}$ is residual load vector ($F_n^{ext} - F_n^{int}$).

The acceleration found by inverting the mass matrix (M^{-1}) and multiplying it by the residual load vector ($F_n^{residual}$).

From the MCS. Dytran 2005 r3 Theory Manual (2006) an explicit method does not require matrix decomposition or matrix solution. The loop is carried out for each time step as shown in the Figure 2.3 and it follows in calculating the material response. Since the accelerations assumed to be constant over the time step, therefore the time step has to be chosen small. In the reason of stability, it must be chosen smaller than the smallest natural period in the mesh. It is means that the time step has to be smaller than the time for a stress wave to travel through the smallest element.

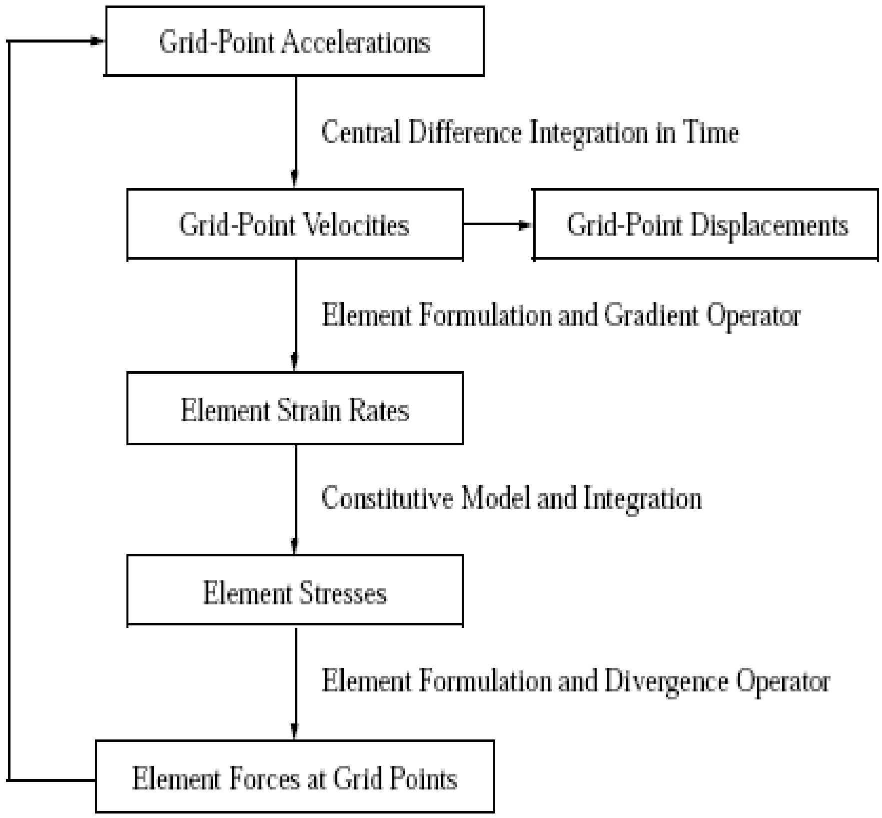

Figure 2.3: Loop of Explicit Method for each time step (2006)

MSC. Dytran is used also for studying sheet metal forming, contact analysis and plastic container forming. MSC, Dytran actually has two solving techniques known as Lagrangian method solver and Eulerian mothod solver. The solving method can be used either one or both and can couple the methods to define an interaction.

According to the MCS. Dytran 2005 r3 Theory Manual (2006) the Lagrangian method solver is used commonly for engineering applications or structural modelling. With the Lagrangian method solver the grid points are located on the body. The elements of material with constant mass connect the grid points forming a mesh. As the body deforms, the grid points will move with the body and the elements (mesh) distort as shown in Figure 2.4. The Lagrangian method solver is then calculating the motion of elements of constant mass. The Lagrangian processor is used explicit formulation and allows large deflection with material and geometric non-linearities.

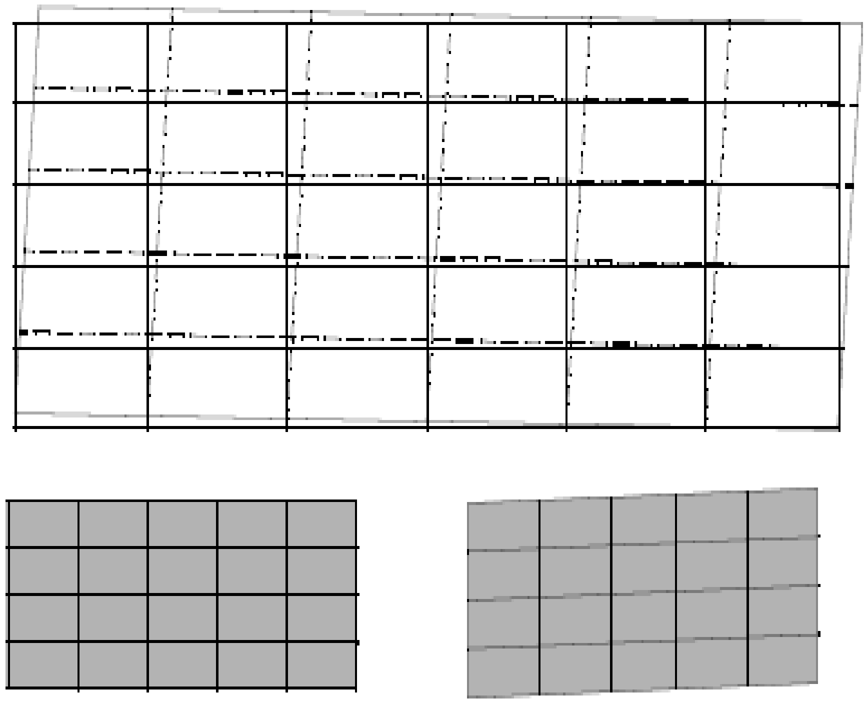

Figure 2.4: Lagrangian Solver Method (2006)

According to the MCS. Dytran 2005 r3 Theory Manual (2006) the Eulerian method solver is used for analyses fluids or materials undergo very large deformation or Fluid Modelling. With Eulerian method solver the grid points remain fixed in space and the elements are simply partitions of the space defined by connected grid points, defining fixed volumes or elements. The Eulerian mesh is a ‘fixed frame of reference’. The material of the body moves through these Euler elements mesh, the mass, momentum and energy of the material is transported from one element to another as shown in Figure 2.5. The Eulerian solver calculates the motion of material through elements of constant volume. The Eulerian processor is essentially an explicit inviscid computational fluid dynamics code.

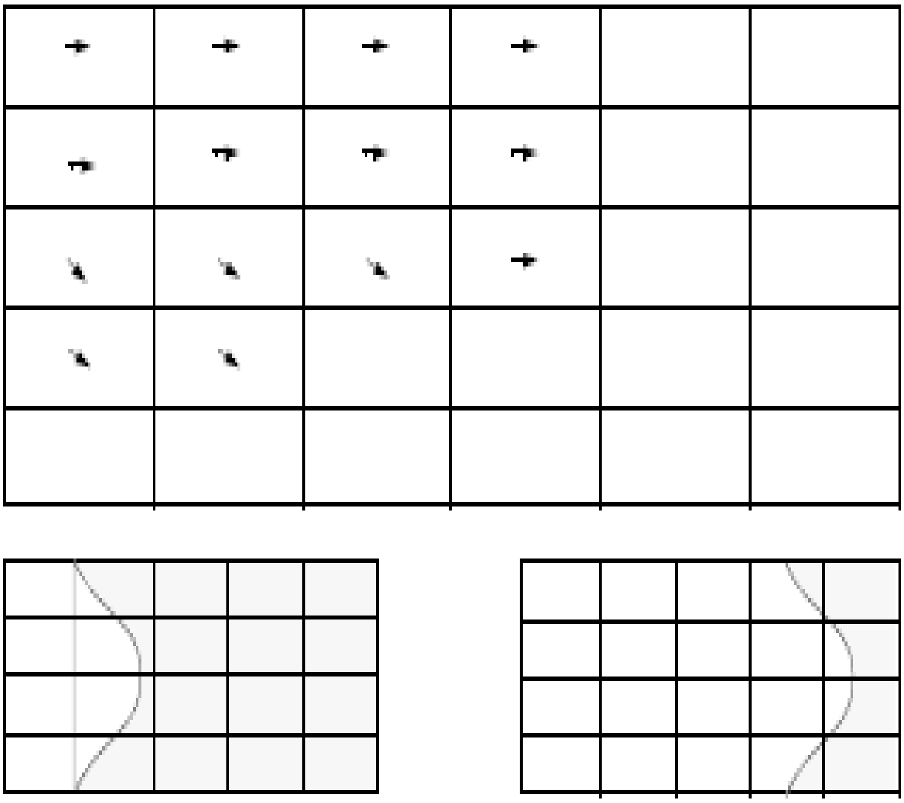

Figure 2.5: Eulerian Solver Method (2006)

In this study we are using Adaptive Contact under Contact from load and boundary condition menu. Adaptive contact is selected to command the failure behaviour between the bullet and the panel material model. From the MCS. Dytran 2005 r3 Theory Manual (2006), it allows a penetrating object to go through a closed surface after elements in its path have failed, without causing holes in its connectivity. Any contact failure behaviour requires master/slave designations for the contacting surface. In this simulation the bullet is designated as master and the panel material model as slave. Every time step, MSC. Dytran will checks the adaptive contact for the grid points of the bullet to see if any have penetrated into the element of the panel material model. If penetration is found, a force is applied on the bullet grid in the direction opposite the penetration. An equal and opposite force is also applied to the grids which are connected to the element being penetrated. What makes the contact adaptive is its ability to allow the projectile to punch through the hole created when the elements in front of it have failed. When an element in the contact region fails, the adaptive contact algorithm stops applying force to it and also stops applying force from it on the penetrating object (2006).

2.6.1 Constitutive Model RUBBER1

The material behaviour in the MSC Dytran followe to Mooney-Rivlin hyperelastic model. It can be used with Lagrangian solid elements only. In the MSC. Dytran theory manual (2006), “The strain energy density function is defined according to the Mooney-Rivlin model:

$$\boldsymbol{W}(I_1, I_2, I_3) = \boldsymbol{A}(I_1 - 3) + \boldsymbol{B}(I_2 - 3) + \boldsymbol{C}\left(\frac{1}{I_3^2} - 1\right) + \boldsymbol{D}(I_3 - 1)^2$$

The constants $\boldsymbol{A}$ and $\boldsymbol{B}$, and Poissons’s ratio $\boldsymbol{v}$ are the input parameters for the model. The constants $\boldsymbol{C}$ and $\boldsymbol{D}$ are related to the input parameters as:

$$\boldsymbol{C} = \frac{1}{2}\boldsymbol{A} + \boldsymbol{B}$$

$$\boldsymbol{D} = \frac{A(5\boldsymbol{v} - 2) + B(11\boldsymbol{v} - 5)}{2(1 - 2\boldsymbol{v})}$$

I_1, I_2, and I_3 are strain invariants in terms of stretches. Stretches are defined as:

$$\frac{\delta x_i}{\delta X_j} = \lambda_{ij}$$

where x_i and X_j are respectively, the coordinates of the deformed and the original geometry.

For rubber-like materials, the shear modulus $\boldsymbol{G}$ is much less than the bulk modulus $\boldsymbol{K}$. In this case,

$$\boldsymbol{G} = 2(\boldsymbol{A} + \boldsymbol{B})$$

The stresses are computed as:

$$\underline{\underline{\tau}} = (det\underline{\underline{F}})^{-1} \times \underline{\underline{F}} \times \underline{\underline{\sigma}} \times \underline{\underline{F}}^{T}$$

Where σ is the second Piola-Kirchhoff stress tensor:

$$\underline{\underline{\sigma}} = 2(\partial W/\partial \underline{\underline{C}})$$

The Cauchy-Green stretch tensor $\underline{\underline{C}}$ is defined as:

$$\underline{\underline{C}} = \underline{\underline{F}}^{T}\underline{\underline{F}}$$

where $\underline{\underline{F}}$ is the deformation gradient tensor

$$\underline{\underline{F}} = \frac{\delta \vec{x}}{\delta \vec{X}}$$

In terms of principal stretches λ_1, λ_2, λ_3 (for example, the stretches in the coordinate system where all shear strains and shear stresses varnish) the expressions for the deformation gradient tensor $\underline{\underline{F}}$, and the Cauchy-Green stretch tensor $\underline{\underline{C}}$ simplify to

$$\underline{\underline{F}} = \begin{bmatrix} \lambda_1 & 0 & 0 \\ 0 & \lambda_2 & 0 \\ 0 & 0 & \lambda_3 \end{bmatrix}, \qquad \underline{\underline{C}} = \begin{bmatrix} \lambda_1^2 & 0 & 0 \\ 0 & \lambda_2^2 & 0 \\ 0 & 0 & \lambda_3^2 \end{bmatrix}$$

The strain invariants I_1, I_2, and I_3 read

$$I_1 = \lambda_1^2 + \lambda_2^2 + \lambda_3^2$$

$$I_2 = \lambda_1^2\lambda_2^2 + \lambda_2^2\lambda_3^2 + \lambda_3^2\lambda_1^2$$

$$I_3 = \lambda_1^2 \lambda_2^2 \lambda_3^2$$

The stresses can be written as

$$J\tau_{ii} = \lambda_i \frac{\partial W}{\partial \lambda_i}$$

Where $J = \lambda_1 \lambda_2 \lambda_3 = \frac{dV}{dV_0}$

CHAPTER 3 : Methodology

The main purpose of this study is to investigate the depth of penetration of the bullet in the rubber panel. We set the properties of bullet constant such as the bullet dimension, bullet initial velocity and bullet weight. First of all, the models of bullet and target panel are drawn using the Computer Aided Design (CAD) SolidWorks 2007 Software. The data of the bullet properties, the rubber properties and the reinforce material properties are obtained from the available references. The simulation modelling is carried out in three-dimensions (3D). The numerical simulation is carried out with the MSC. DYTRAN software with solver Lagrangian explicit finite element code and the failure behaviour command of penetration is using Adaptive Contact Master-Slave Surface.

3.1 The MSC-Dytran Environment

Before running the simulation, the sequence of setting the model and to retrieve the result in the MSC. Dytran environment have to follow steps as stated below. First, the model of the bullet and the model of the panel have to be loaded. Second step is the models have to be meshed according to the appropriate element shape. Third step is creating the material properties and input the data of material use in the analysis. Then the forth step is to assign the model with the material property created in step three. The fifth step is assigned the boundary condition and the initial velocity to the models. In this step the failure behaviour of material is also assign to the models. Step sixth is selecting the output data required in the analysis menu and time duration to run the analysis. The last step is run the analysis using the MSC-Dytran Explorer. The data of penetration can be retrieved from MSC-Dytran Explorer. If we want to view the image of penetration, we can use the Result menu by using the .arc file. The environment of MSC-Dytran is shown in Figure 3.1. and the MSC.Dytran Explorer is shown in Figure 3.2.

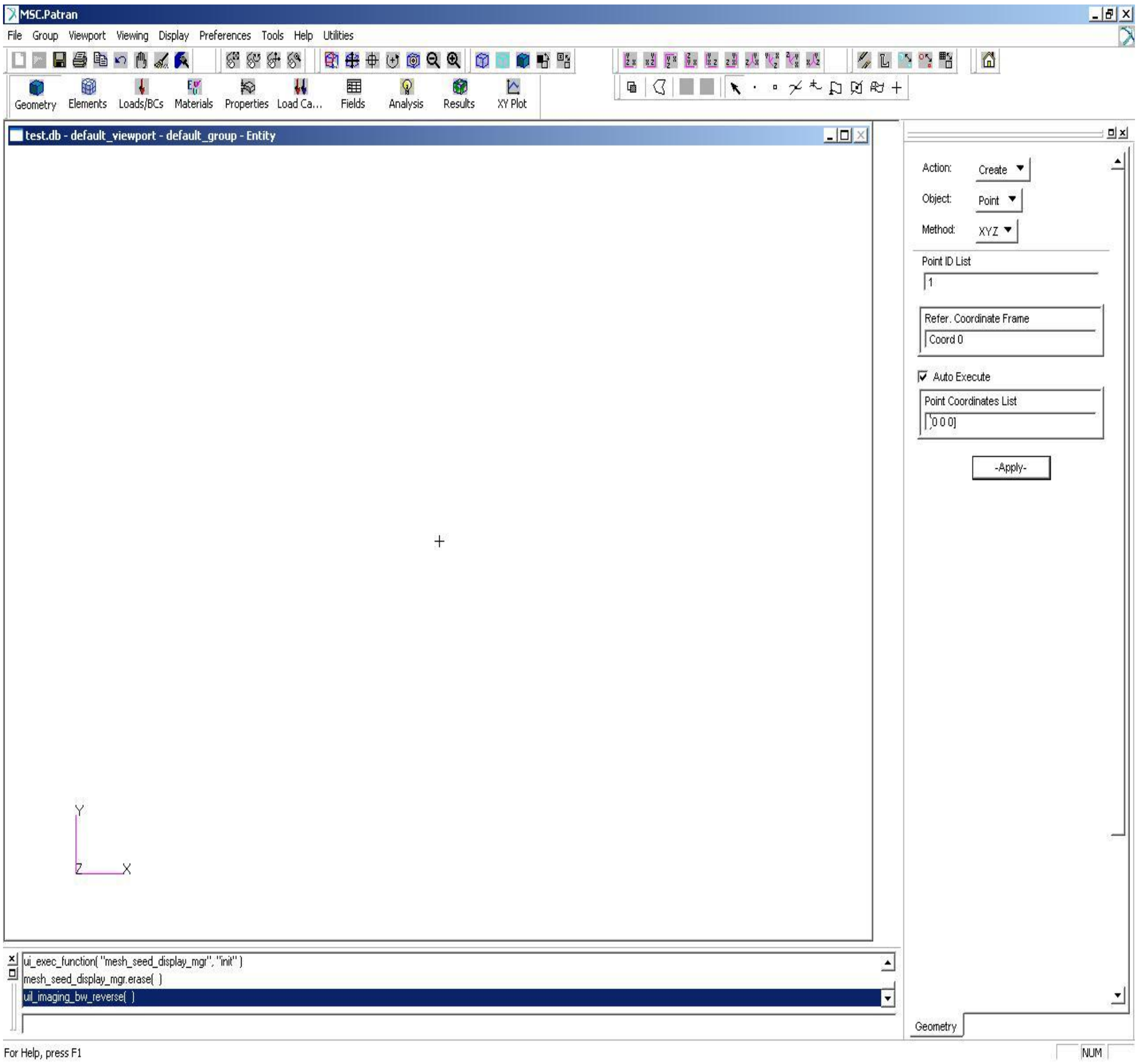

Figure 3.1: The MSC. Dytran environment

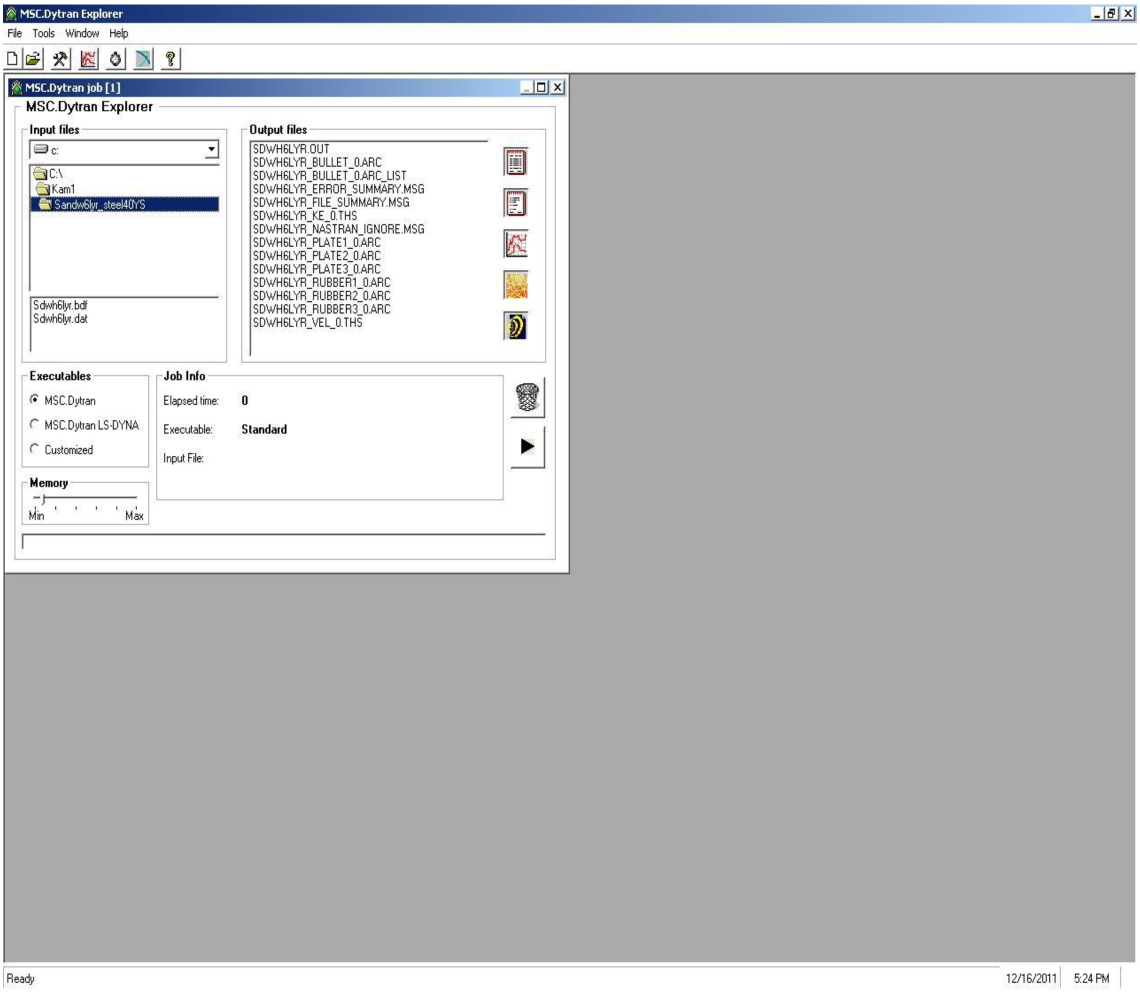

Figure 3.2: The MSC. Dytran Explorer environment

3.2 Bullet

There are wide varieties of bullet diameter or calibre in the market. But the bullet calibre or diameter studied is only the bullets use in the WTD, STRIDE shooting range. Most of the bullets type used in the WTD, STRIDE shooting range are used by Malaysian Army. These bullets called full metal jacket (FMJ) type. The diameter of bullet choose in this study is 7.62 mm since it carried the highest energy when comparing with the diameter bullet 5.56 mm and 9 mm. Therefore bullet 7.62 mm has the higher energy of penetration capability than the diameters bullet 5.56 mm and 9 mm. The data of bullet used in this study shows in Table 3.1.

Bullet Type	Muzzel Velocity	Muzzel Energy	Bullet Weight
7.62 x 51 mm Ball M80	854 m/s	3519 J	9.65 g

Table 3.1: Data of Bullet 7.62 mm (Terry J Gander 2000)

3.2.1 Bullet Model

The model of the bullet illustrated in Figure 3.3 corresponds to the outer shape dimension of 7.62 x 51 mm NATO Ball M80 (with a soft lead core). The dimension of the ogivel nose part is 76.2 mm in radius, the overall length is 28.633 mm, and the diameter is 7.62 mm (Terry J Gander 2000).

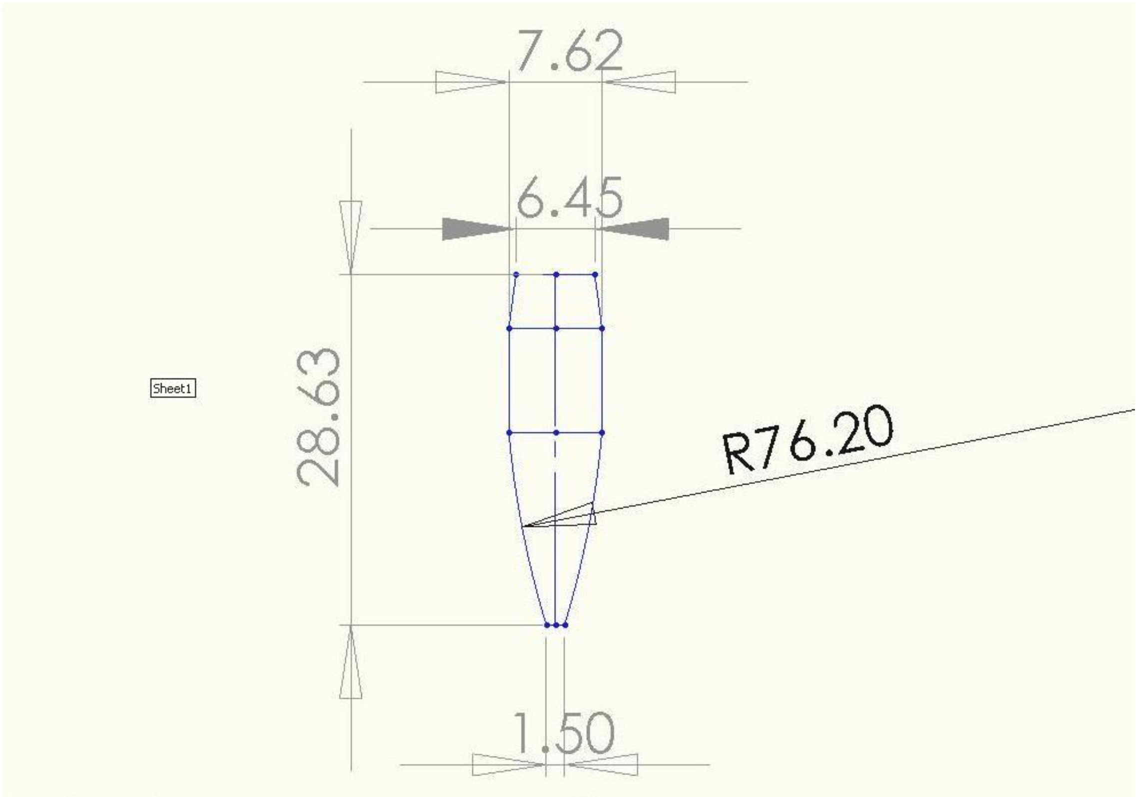

Figure 3.3: Bullet drawing and dimensions

The mesher of bullet model is assigned as surface type and using tetrahedral elements shape with paver meshing algorithm with Tria 3 topology. The total number of shell element counted is 255 elements. The finite element solid model shown in Figure 3.4 and the wire mesh frame shown in Figure 3.5.

The material constitutive model of bullet is assigned as Rigid (MATRIG) body which means it does not deform during impact. The bullet model assigned as a rigid body because to make sure that the panel will receive the highest energy on impact. If the bullet breaks the energy will reduce and make the depth of penetration reduce. The initial velocity assigned to the model of bullet is 800 m/s. This initial velocity is assigned at the node of the elements shown in Figure 3.6. In the Adaptive Contact Master-Slave Surface failure behaviour, the bullet is assigned as master.

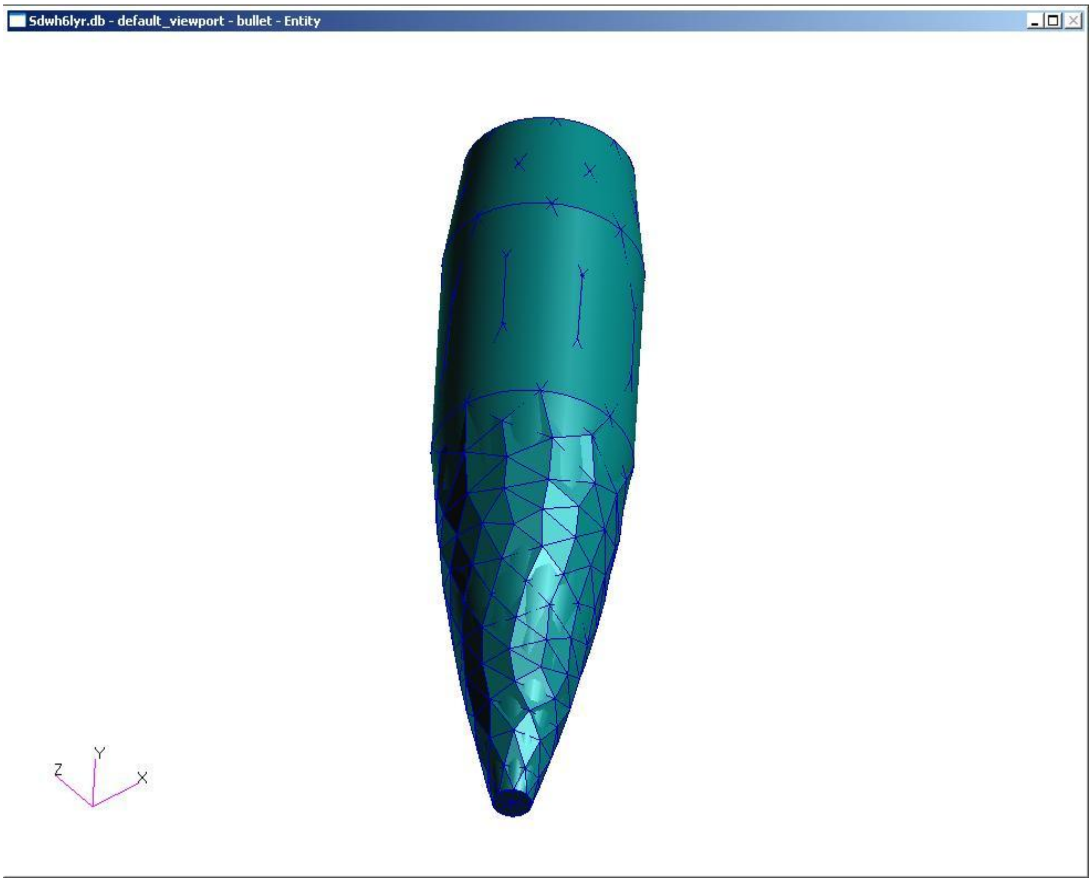

Figure 3.4: The view of solid finite element model

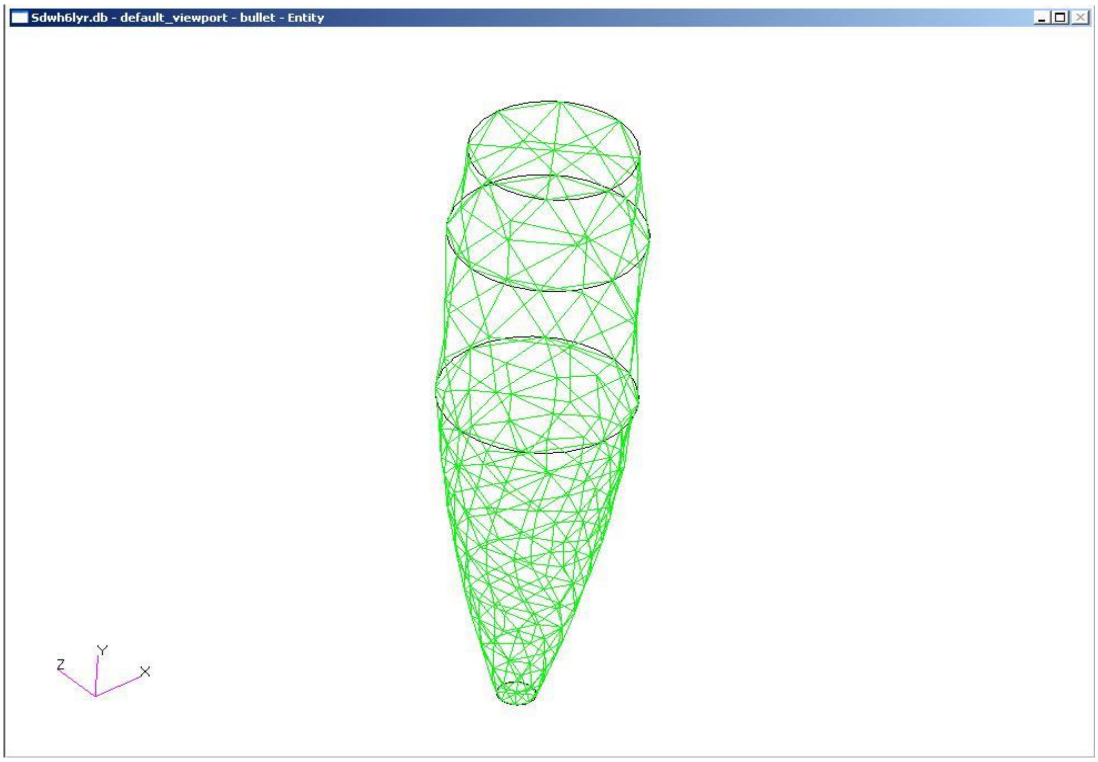

Figure 3.5: The example view of wire mesh frame of the bullet model

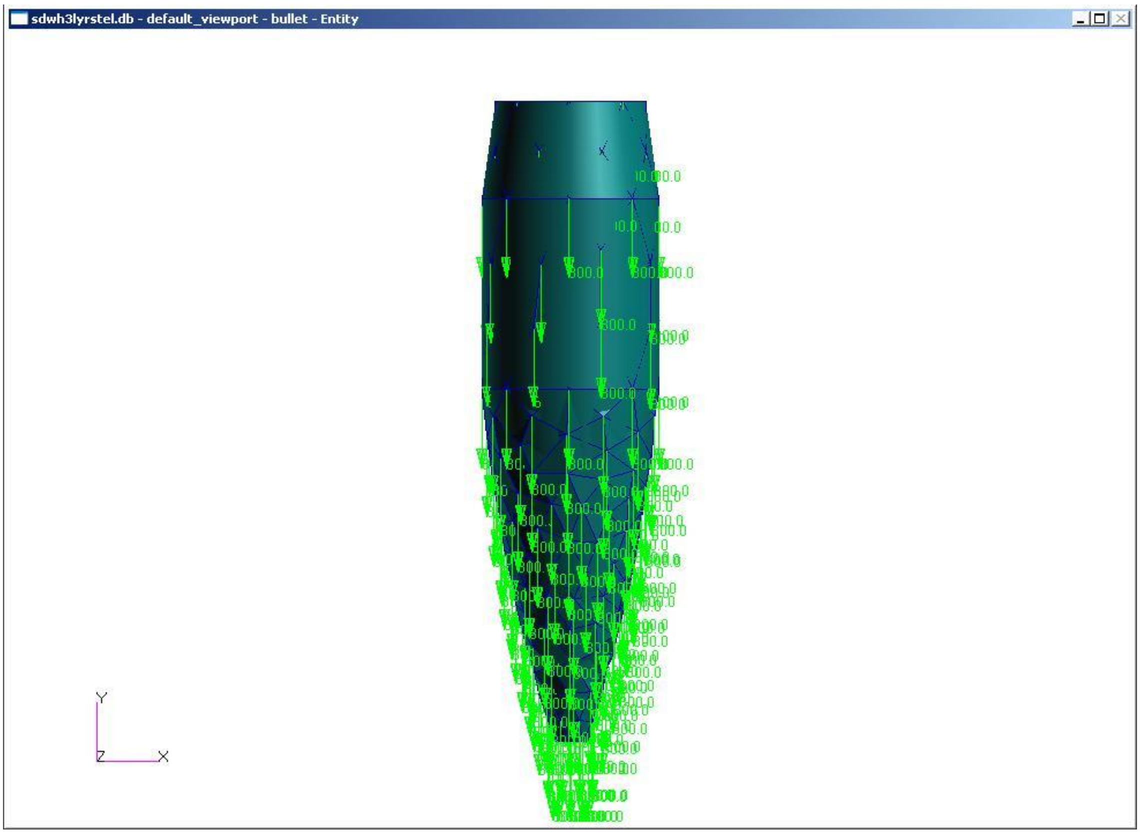

Figure 3.6: The initial velocity is assigned at the node of the elements

3.3 Material Panel

The material use in this study is rubber and the reinforce material. The first study is totally concentrated with the rubber panel. Since the rubber alone is not sufficient to stop the bullet penetration (500 mm thickness), the reinforce material is introduced. The reinforce material under study has two types of material. It is known as Steel Alloy 4140 and Stainless Alloy 304. The panel will be assembled in sandwich between rubber-reinforce material. At the end of study we will select between these two reinforce material which one is the best that can be used with the rubber panel.

3.3.1 Rubber Material

The properties data of the rubber material are obtained from the available references and shown in Table 3.2. The rubber panel model is drawn in 3D and the dimension of the panel is 100 mm in length, 100 mm in width. In the study, the rubber panel model has different thickness per model. The thickness of the panel model is 200 mm, 300 mm, 400 mm and 500 mm.

The rubber panel is uniformly meshed using hexahedron eight-noded shape with IsoMesh algorithms. The mesher is compact or dense at the centre part of panel from upper surface to the bottom surface. The numbers of element is 8000 elements and the example plot of mesh is shown in Figure 3.7. The boundary condition of the panel is fully fixed on every finite element node at the edge of the panel. All edges of the rubber are constrained in all degrees of freedom.

The material entry of the constitutive model is a user define material model Rubber(RUBBER 1) with the element type is Lagrangian solid (2006). The RUBBER1 is following the failure behaviour of a Mooney-Rivlin rubber model which more suitable for hyperelastic material (2006). All setting of the calculation simulation is by default. The rubber panel material is assumed as isotropic.

Serial	Property	
1	Density	1.1 kg/m^3
2	Constant A	0.89 Mpa
3	Constant B	0.46 Mpa
4	Poisson Ratio	0.5 or 0.49999

Table 3.2: Properties of Rubber Material (Roberts 1977)

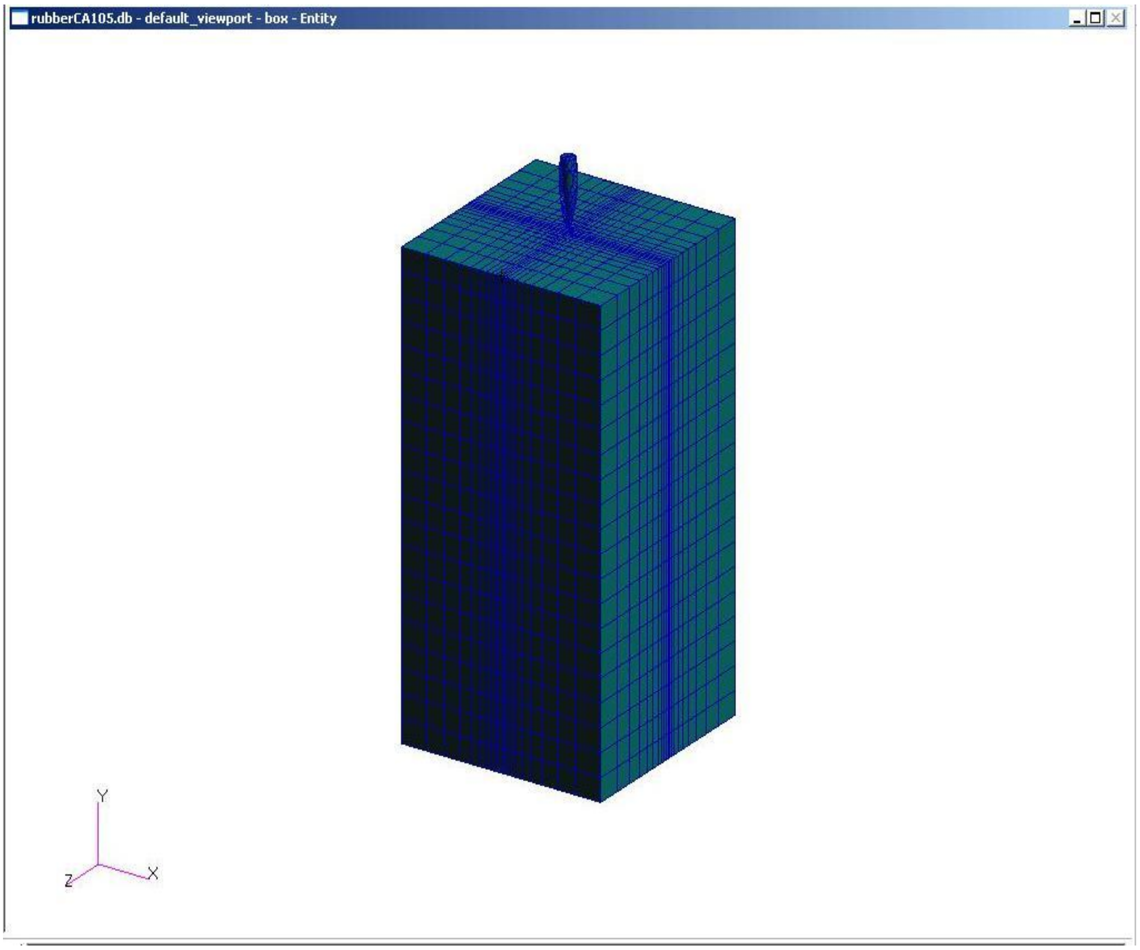

Figure 3.7: The example view mesh of Rubber Panel

3.3.2 Plate Material

After studying the rubber panel, the next work consist in using sandwich panel i.e combination between rubber materials and reinforce materials. The reinforce material is in the form of thin plate. The sandwich panel has 200 mm in length and 200 mm in width. The thickness of the plate is 5 mm. The dimension of length and width is different for this sandwich panel with the rubber panel because 200mm x 200 mm is easier to handle. The plate is assembled in sandwich with rubber. The selection of the 5 mm plate thickness is because it is the normal thickness for plate available in the Malaysian market. The properties of the plates show in Table 3.3.

Serial	Property	Material	
		Steel Alloy 4140	Stainless Alloy 304
1	Density	7850 kg/m^3	8000 kg/m^3
2	Elastic Modulus	207 GPa	193 GPa
3	Poisson Ratio	0.3	0.3
4	Yield Stress	290 MPa (hot roll)	515 MPa (cold work)
5	% of plastic elongation	0.2	0.4

Table 3.3: Properties of Plates (Callister 2007)

The material entry of constitutive model of plate is a user define material model ElasPlas (DYMAT 24) for piecewise Linear Plasticity with the element type is Lagrangian solid (2006). All setting of the calculation simulation is by default. The material is assumed as isotropic. The meshing element is same as per rubber panel mesher, it is the uniform mesh hexahedron eight-noded shape with IsoMesh algorithms.

The mesh element number for plate is 800 elements. The failure effect of the model is come from the Maximum Plastic Failure which is the % of Plastic Elongation. Same as rubber panel all edges of the plate are constrained in all degrees of freedom. The yield failure model is check using Von Mises profile.

3.4 The Setting of Depth of Penetration Simulation on Rubber Panel

In the penetration study, the models are arranged in vertical position. The bullet is position above and centre of the panel surface with some small distance. The distance between the bullet and the panel surface is 2 mm. We set the angle of impact is normal incidence (0° obliquity) to the top surface of the panel. MSC. Dytran is simulate only single impact event and is assigned to hit at the centre of the panel in the vertical path. In the failure behaviour material of Adaptive Contact Master-Slave Surface, the bullet is assigned as master and the rubber panel is assigned as slave.

The depth of penetration study started with different value of Constant A with thickness of the panel 500 mm. After that, the simulation continues with different thickness of rubber panel 400 mm , 300 mm, and 200 mm. The value of Constant A is increasing started from 1.0 x 0.89 MPa, then 1.2 x 0.89 MPa, 1.4 x 0.89 MPa, 1.6 x 0.89 MPa, 1.8 x 0.89 MPa, and 2.0 x 0.89 MPa. The result then collected on every simulation testing panel. This analysis is trying to fine the best value of Constant A which can give the suitable depth of penetration and the bullet not perforate the rubber panel.

The other variable input is studied. It is the Linear Viscosity Constant (LVC). The LVC is considered as the dampers property in the rubber panel. Adding value into this input is to reduce the effect hyperelastic of the rubber material. The LVC values are set from 0.01, 0.001, and 0.0001. We study the effect of LVC by maintaining the rubber panel plate thickness at 500 mm and Constant A at value 1.4 x 0.89 MPa.

3.5 Design of New Material for End Butt

The new design of new material for end butt is consist of rubber and plate metal. Adding plate is a requirement in design in order to increase the capability of absorbing energy from bullet impact during penetration. The rubber and plate are arranged successively to form a sandwich panel as illustrated in Figures 3.5 to 3.7. The dimension of this design is 200 mm in length, 200 mm in width. The thickness of the rubber panel is kept constant at 50 mm and the thickness of the plate also is kept constant at 5 mm. The total thickness of new design is depending on the number of layers use. The purpose of layers is to make the design of new material for end butt more compact. We are doing the simulation for both plate material properties.

The arrangement of bullet, panel position and the angle of impact are the same with the explanation given in section 3.4. The geometry of the bullet and assigned properties are similar with the previous simulation. The difference is only on total number of shell element which is increasing to 367 elements as per given by default.

The first design is started with total 4 layers of rubber-plate in sandwich pattern arrange alternately. In this sandwich panel has 2 layers of rubber and 2 layers of plate. The total numbers element for this design during simulation is 5600. The total thickness of the 4 layers is 110 mm. We are simulating the same thing with the second and third design but with 6 layers and 8 layers accordingly. The second design has total numbers element is 8400 with total thickness of 165 mm. The third design has total numbers element is 11200 with total thickness of 220 mm.

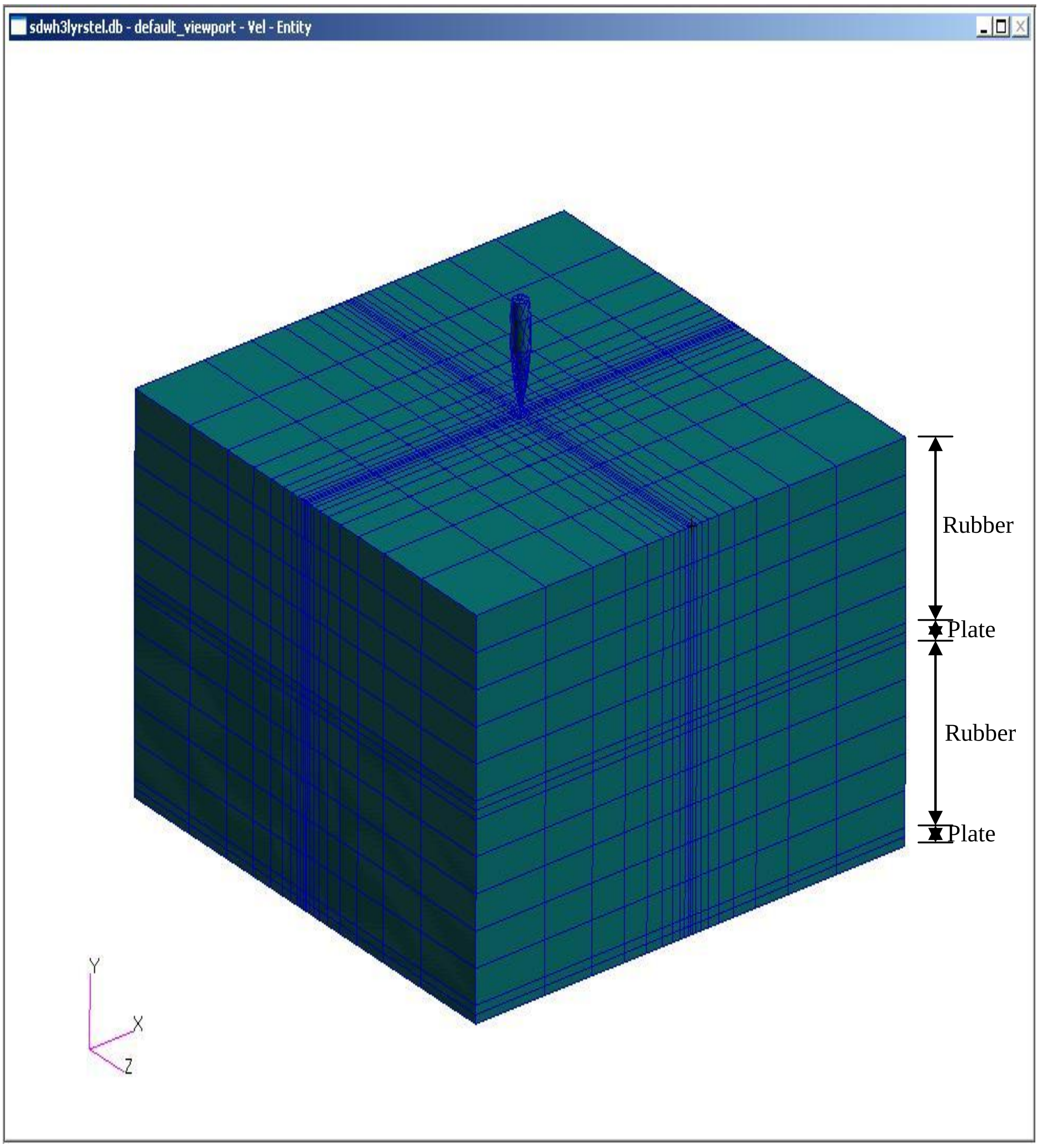

Figure 3.8: View of mesh elements and Sandwich panel 4 layers

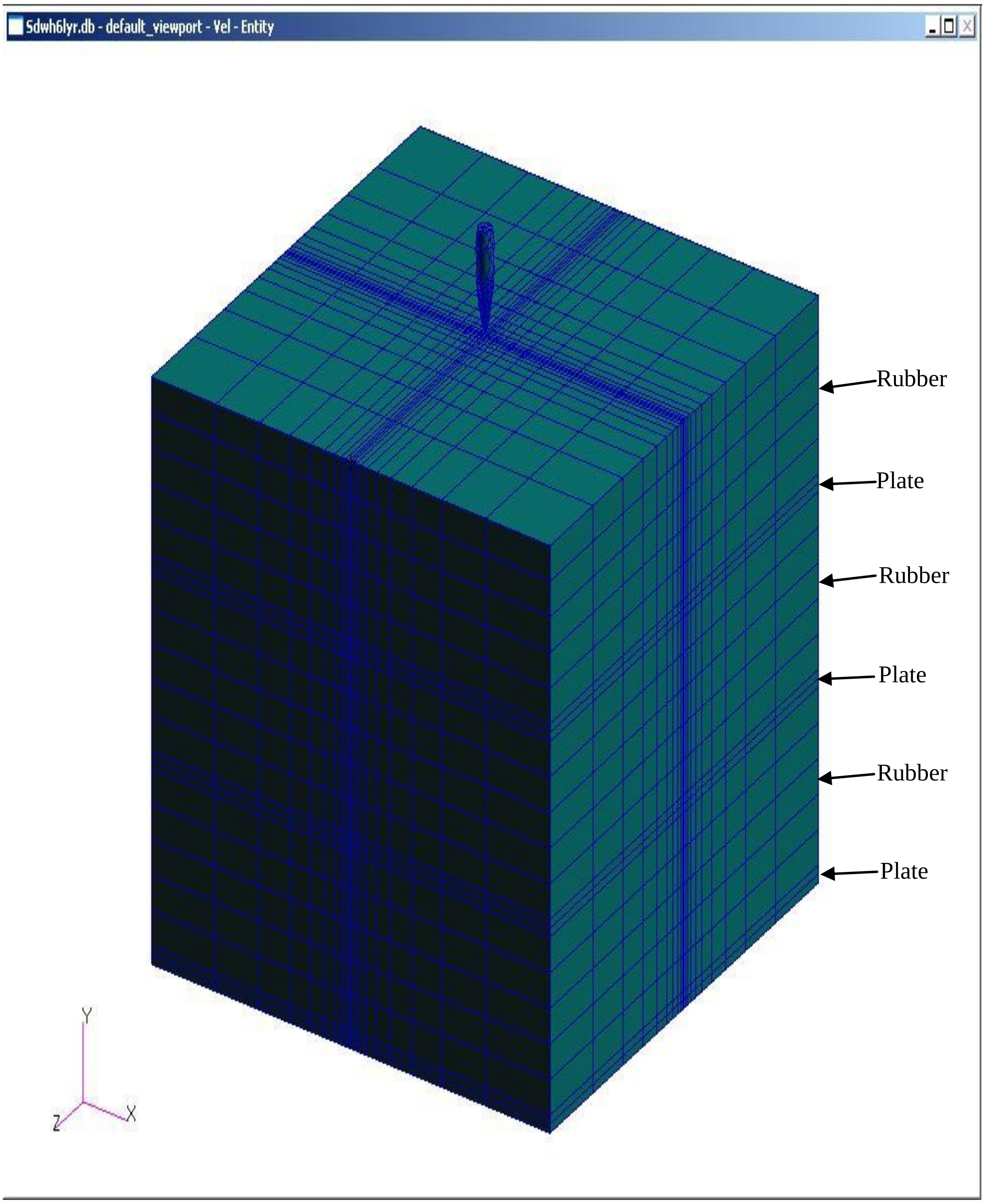

Figure 3.9: View of mesh elements and Sandwich panel 6 layers

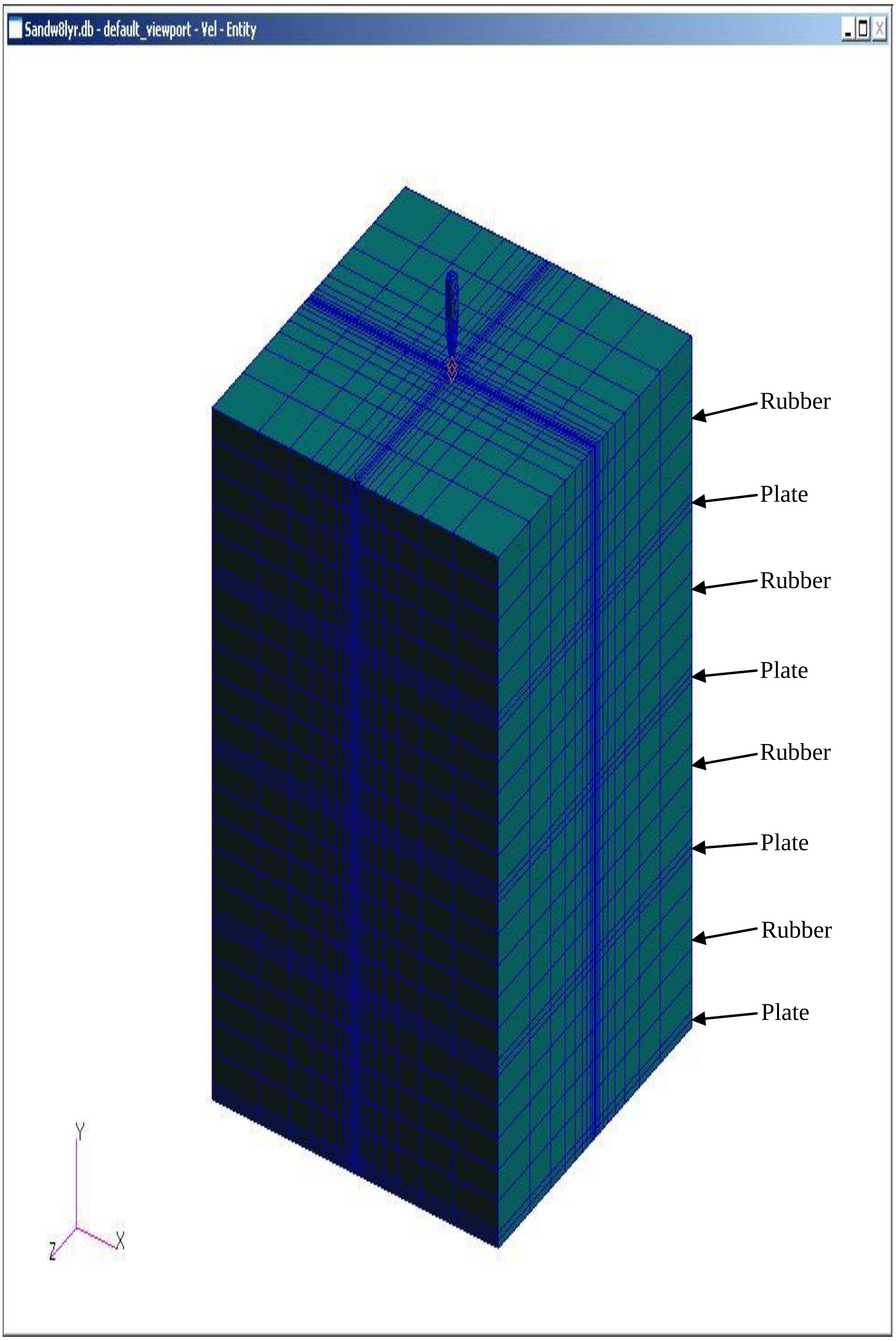

Figure 3.10: View of mesh elements and Sandwich panel 8 layers

CHAPTER 4 : Results and Discussions

In this chapter, we present the results and discuss the finding of the study. As mentioned previously, the new material will be used as additional safety device to sand. For that, Natural Rubber Filled material was selected to be studied. The numerical simulation was conducted to study the capability of rubber panel in resisting the penetration of the bullet impact. Then study the response of rubber panel if the properties of material have changed. The final result needed is the depth of penetration of the bullet in the material.

The input data required to run the simulation is the initial velocity of bullet is set 800 m/s, the weight of bullet is set 9.65 g, the dimension of bullet is constant and the bullet is set as a rigid body. The variable input of material properties of Natural Rubber Filled, Steel Alloy 4140 and Stainless Alloy 304 material are as per in Chapter 3 above.

The results are based on the panel thickness, different values of Constant A of rubber property, different values of Linear Viscosity Constant (LVC) of constitutive material property, design of rubber panel in layers when combine in sandwich with the other plate materials and different values material properties of plate.

4.1 Result for Rubber Panel

4.1.1 Depth of Penetration into the Different Panel Thickness

4.1.1.1 Rubber Panel Thickness is 500 mm

Figure 4.1 shows how the depth of penetration is affected by the Constant A for rubber. It is found that the bullet penetrates and perforates the rubber panel when Constant A is set with value 1.0 x 0.89 MPa and 1.2 x 0.89 MPa. Increasing the value Constant A to 1.4 x 0.89 MPa makes the depth of penetration reduces to 327 mm from the rubber panel surface. Increasing further the value of Constant A from 1.6 x 0.89 MPa, 1.8 x 0.89 MPa, and 2.0 x 0.89 MPa, the bullet is only able to penetrate the rubber panel up to 21.8 mm, 22 mm and 19 mm respectively.

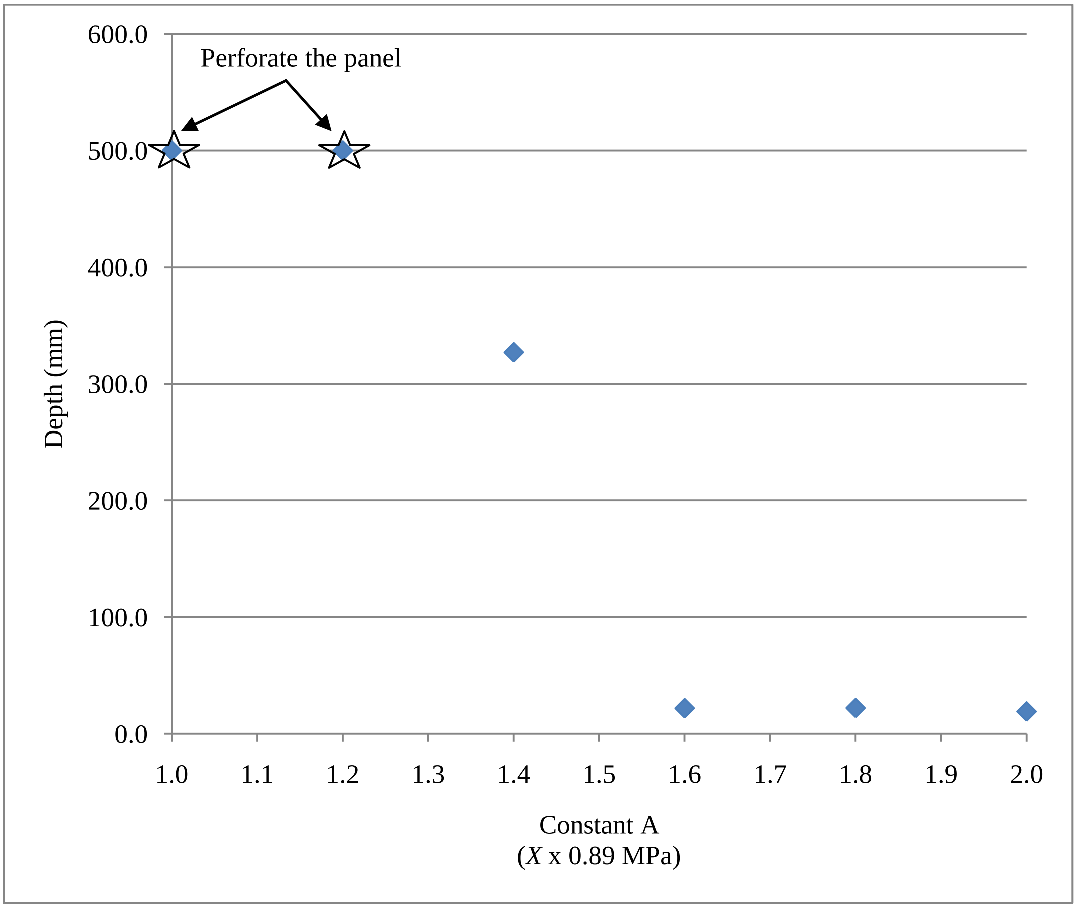

Figure 4.1: Penetration vs Constant A of Rubber Panel Thickness 500 mm

4.1.1.2 Rubber Panel Thickness is 400 mm.

Figure 4.2 also shows how the depth of penetration is affected by the Constant A for rubber. The Constant A is set with 1.4 x 0.89 MPa, 1.5 x 0.89 MPa and 1.6 x 0.89 MPa. It is found that for Constant A 1.4 x 0.89 MPa, the bullet is penetrated and perforated the rubber panel. The result for Constant A at 1.5 x 0.89 MPa, is same with Constant A 1.4 x 0.89 MPa which is penetrated and perforated the rubber panel. The result for Constant A at 1.6 x 0.89 MPa, it is only penetrating 22 mm of the rubber panel.

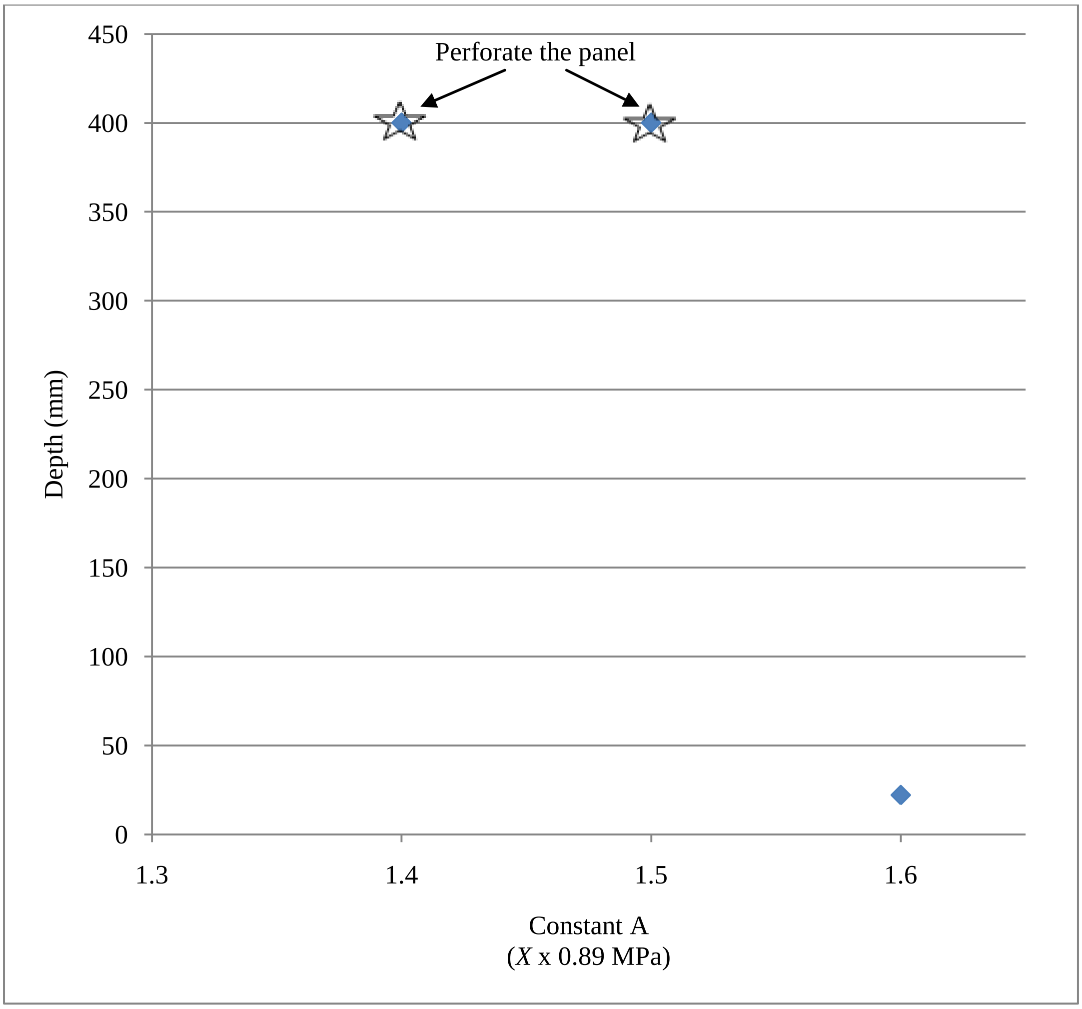

Figure 4.2: Penetration vs Constant A of Rubber Panel Thickness 400 mm

4.1.1.3 Rubber Panel Thickness is 300 mm.

Figure 4.3 also shows how the depth of penetration is affected by the Constant A for rubber. Values of Constant A are set with 1.4 x 0.89 MPa, 1.6 x 0.89 MPa and 1.8 x 0.89 MPa. It is found that the result for Constant A at value 1.4 x 0.89 MPa and 1.6 x 0.89 MPa, the bullet is penetrate and perforate the rubber panel. Constant A set at 1.8 x 0.89 MPa, the depth of penetration is 153 mm.

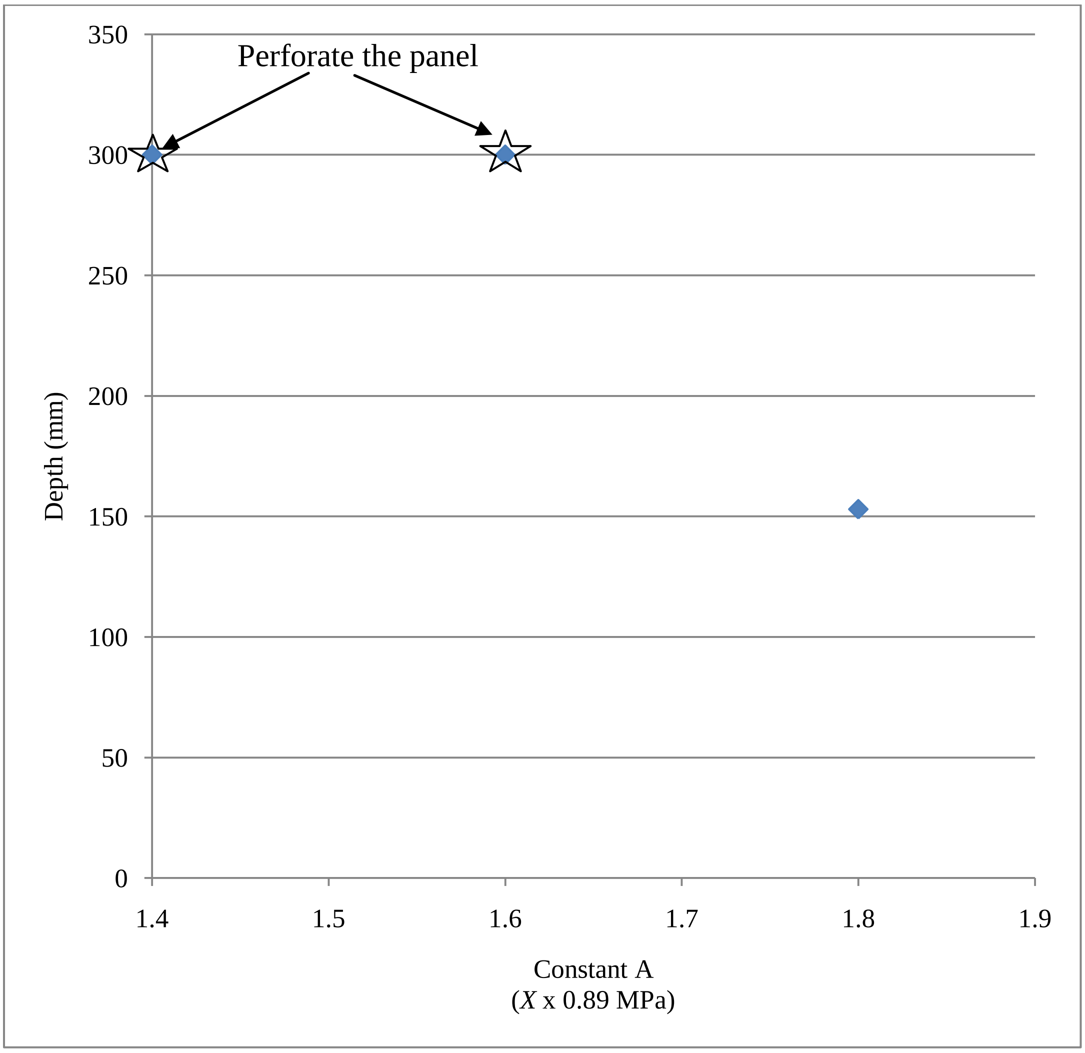

Figure 4.3: Penetration vs Constant A of Rubber Panel Thickness 300 mm

4.1.1.4 Rubber Panel Thickness is 200 mm.

Figure 4.4 also shows how the depth of penetration is affected by the Constant A for rubber. The value of Constant A is set with 1.40 x 0.89 MPa, 1.5 x 0.89 MPa, and 1.6 x 0.89 MPa. It is found that the bullet is penetrate and perforate all the rubber panel for all values of Constant A.

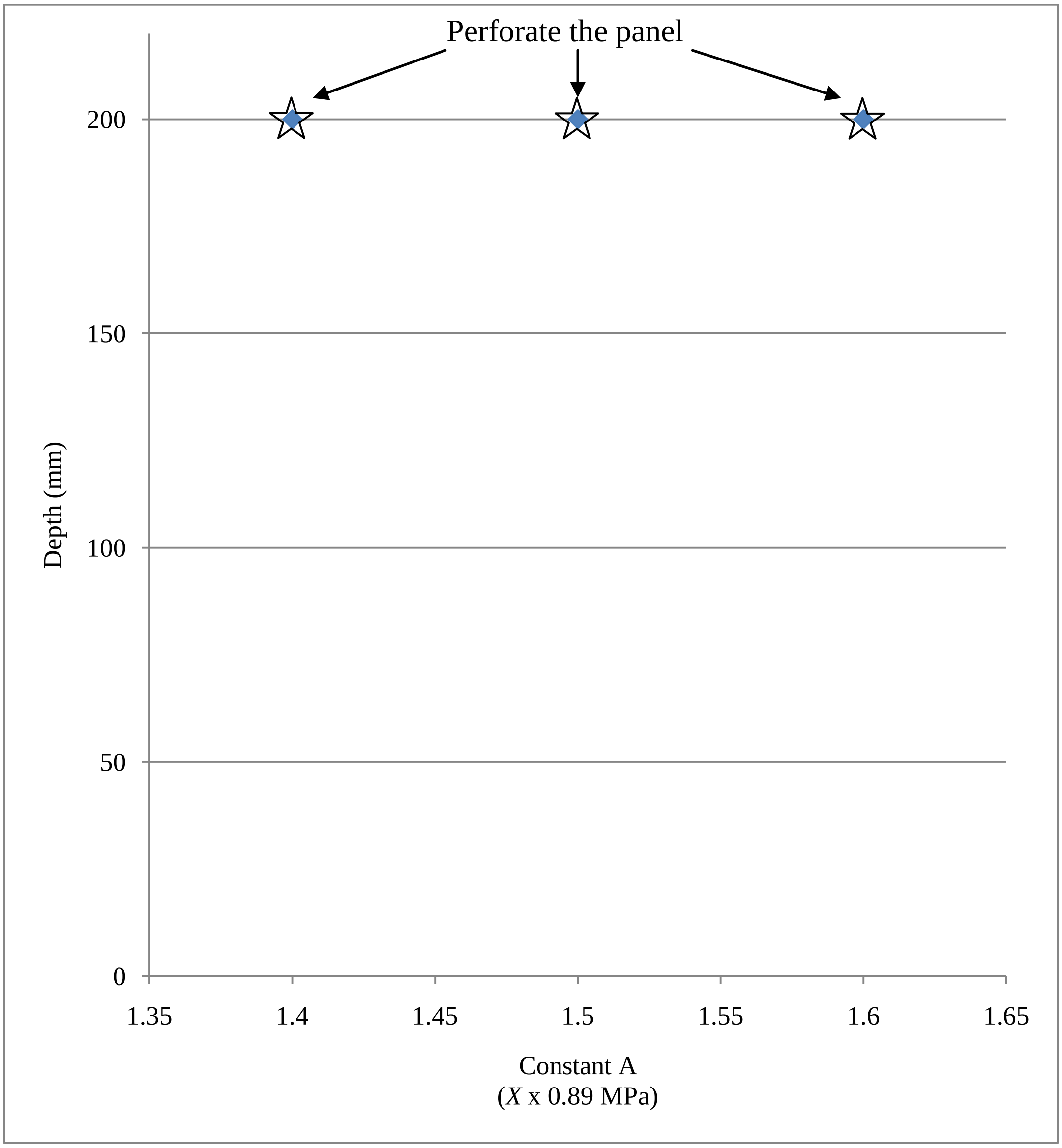

Figure 4.4: Penetration vs Constant A of Rubber Panel Thickness 200 mm

4.1.2 Effect of Linear Viscosity Constant (LVC) on the Depth of Penetration

Figure 4.5 shows how the depth of penetration is affected by the LVC for rubber. In this simulation, the Constant A parameter is maintained at 1.4 x 0.89 MPa and the thickness of the rubber panel is 500 mm. It is found that for value LVC is 0.0001, the bullet is penetrating deeper when compared with value LVC 0.01 and value LVC 0.001. The depth of penetration value for LVC 0.0001 is 250 mm before exit at the side of the panel. For values LVC 0.01 and LVC 0.001, the depth of penetration is only 22 mm.

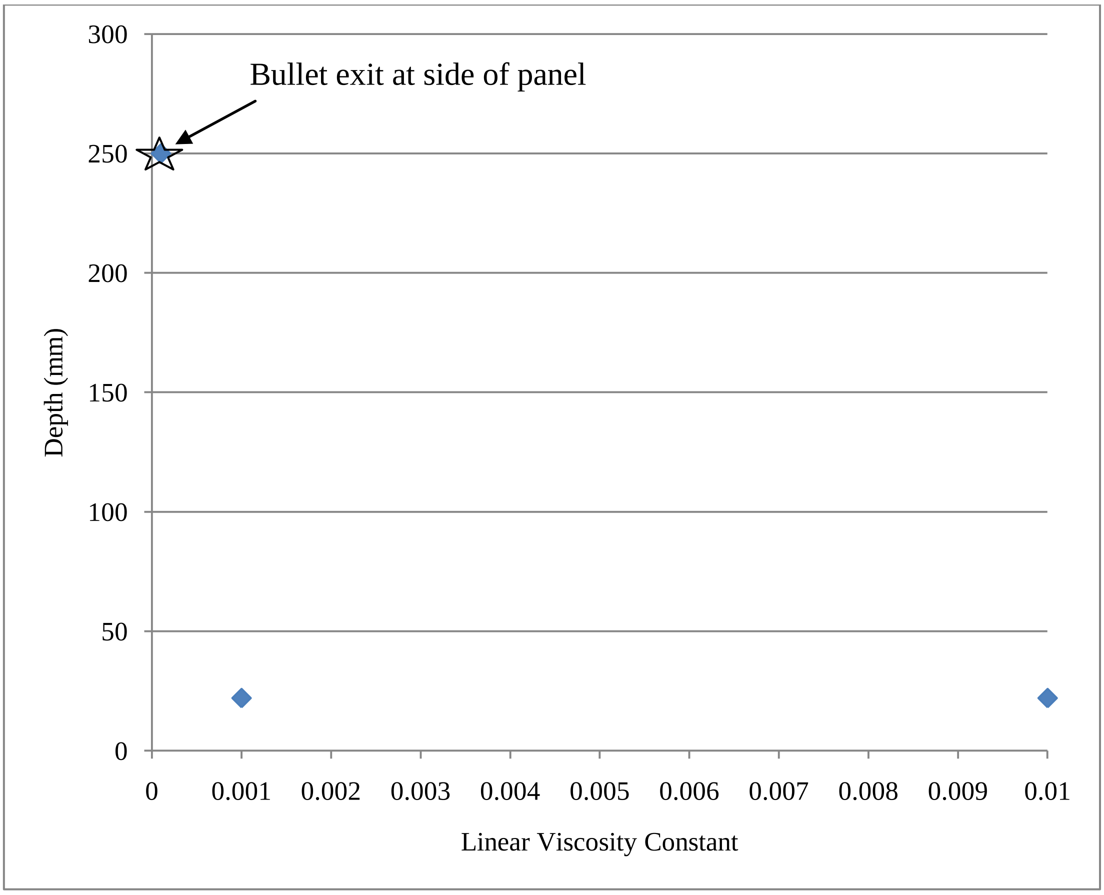

Figure 4.5: Depth of Penetration vs Linear Viscosity Constant (LVC)

4.2 Discussion for Rubber Panel Result

The results of penetration show that for rubber panel thickness of 500 mm, the depth of penetration is reduced when the value of Constant A rubber property increasing. At the first two value of Constant A the bullet is penetrating and perforating the rubber panel, but for Constant A of 1.4 x 0.89 MPa the bullet penetrate the rubber panel and stop at 327 mm from the front panel surface. The bullet is unable to penetrate more than 22 mm in depth for Constant A of 1.6 x 0.89 MPa, 1.8 x 0.89 MPa, and 2.0 x 0.89 MPa.

The depth of penetration for various thickness of rubber panel of 400 mm, 300 mm, and 200 mm is investigated. The selections of Constant A are set between 1.4 x 0.89 MPa to 1.8 x 0.89 MPa. Observation on the result for thickness 400 mm shows that none of the value Constant A can be used. Indeed, for Constant A of 1.4 x 0.89 MPa and 1.5 x 0.89 MPa the bullet penetrates and perforates the panel. For Constant A of 1.6 x 0.89 MPa it allows partial penetration of the bullet into the rubber panel.

Result for the thickness of rubber panel 300 mm shows, the bullet is penetrate and perforate the panel for Constant A of 1.4 x 0.89 MPa and 1.6 x 0.89 MPa. The penetration of the bullet is 153 mm for Constant A of 1.8 x 0.89 MPa. The results for thickness of rubber panel 200 mm show that the bullet penetrates and perforates the rubber panel. This result shows that this rubber panel thickness cannot be used to stop the bullet.

Most of the results show that the bullet always rebound back when reached the maximum depth of penetration as shown in the Annex. As we know rubber is a hyperelastic or non-linear elastic material. This kind of material is able to store and release energy again after impact. The constitutive model of Rubber(RUBBER1) in the MSC Dytran is purely for hyperelastic material to introduce the damping effect, the

Linear Viscosity Constant (LVC) is used. In this simulation testing the values of LVC selected are 0.01, 0.001 and 0.0001. The result shows that by applying the values LVC in the property input, the material is able to reduce the rebound effect as shown in Figure 4.6. For value LVC 0.01 and LVC 0.001, both values are also given the same result of penetration. Therefore we choose the value 0.01 of LVC to be put in the rubber material property menu.

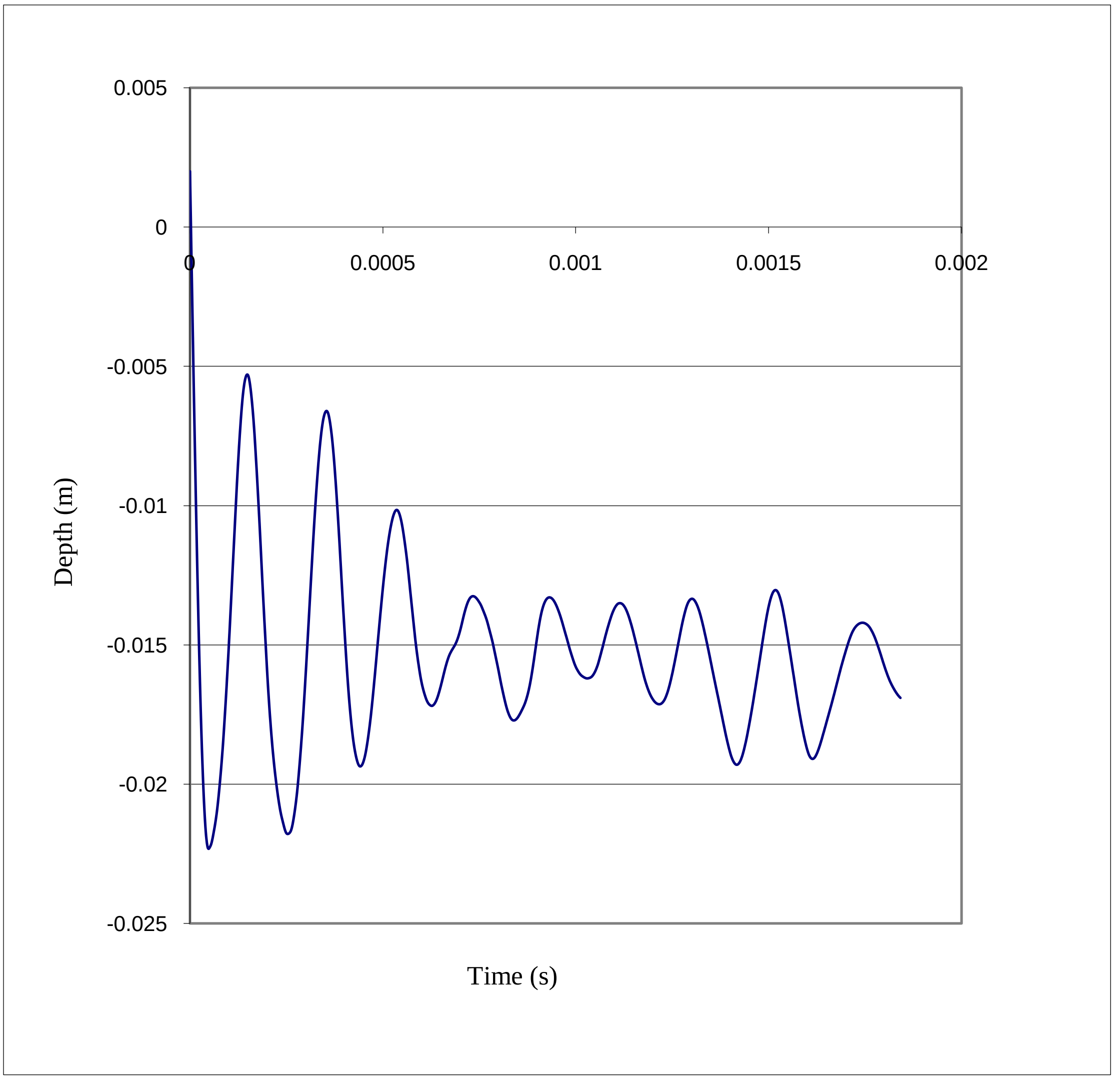

Figure 4.6: Bounce effect reducing by time shows on graph Penetration vs Time for Linear Viscosity Constant 0.01.

In this simulation testing, different types of rubber material have been considered. The different types of rubber are known from different value of Constant A input. The results show depth of penetration is reduced with the increasing of Constant A. Therefore, the best parameter of rubber panel refers to the results of simulation is Constant A 1.4 x 0.89 MPa with the panel thickness 500 mm. Referring to the thickness 500 mm for the rubber panel, it is too large to handle and difficult in process of manufacturing. Due to that the rubber alone as a panel is not sufficient. Therefore, the panel consists of sandwich structure between rubber and reinforcing material is proposed.

4.3 Result for Sandwich Panel

In this study we consider 4 Layers, 6 Layers and 8 Layers of sandwich panels. 4 layers panels means it has 2 rubber layers and 2 plate layers, for 6 layers panel it has 3 rubber layers and 3 plate layers and for 8 layers panel it has 4 rubber layers and 4 plate layers. Every rubber panel thickness is 50 mm and every plate panel is 5 mm. For the plate material, 2 different materials are considered in this study: Steel Alloy 4140 and Stainless Alloy 304.

4.3.1 Depth of Penetration for the Different Sandwich Panel

4.3.1.1 Sandwich Panel of Rubber-Steel Alloy 4140

Figure 4.7 shows how the depth of penetration is affected by impacting the bullet on the Rubber-Steel Alloy 4140 sandwich panel. It is found that the 4 layers panel is penetrated up to 65 mm, and the bullet is bounced back out from the front surface of the panel. The 6 layers panel has depth of penetration 164 mm and for the 8 layers panel the bullet penetrate up to 106 mm.

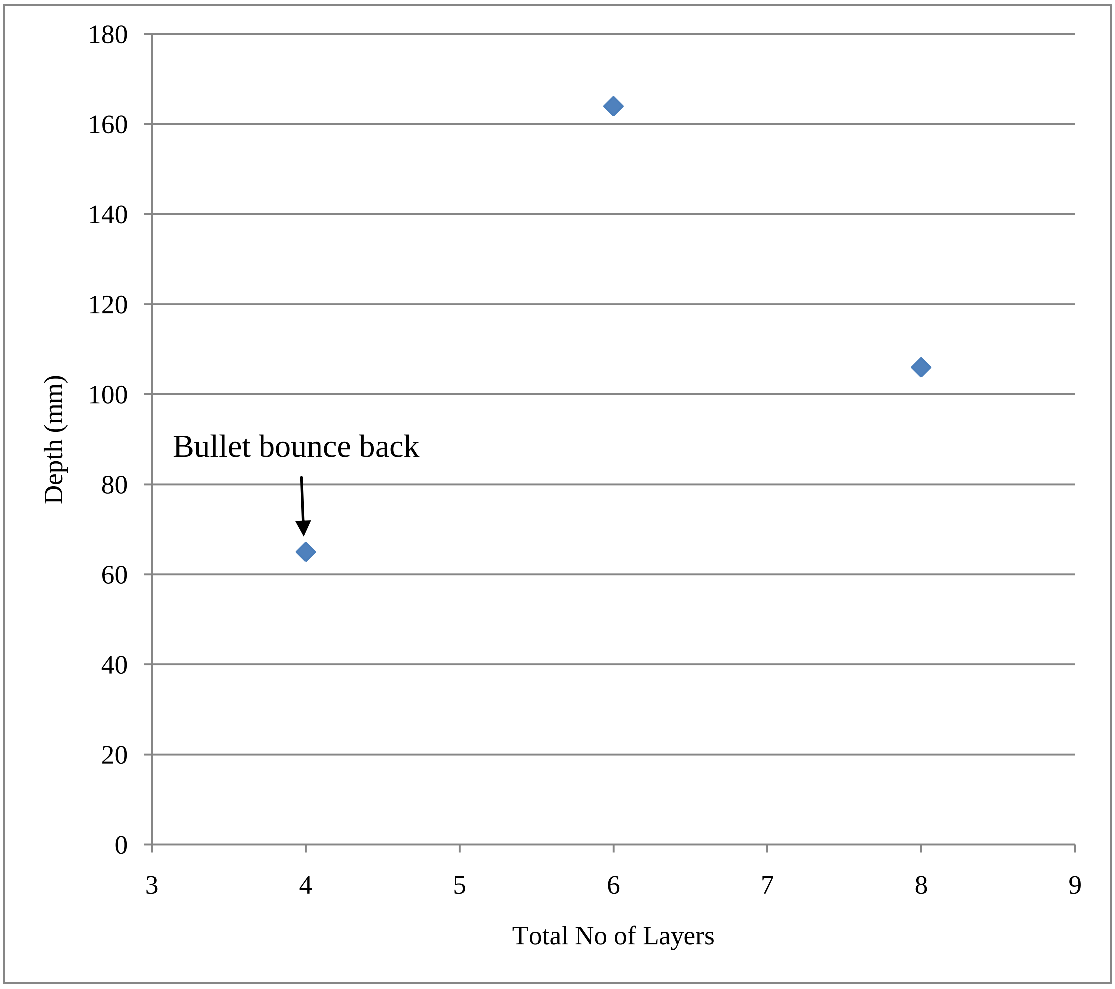

Figure 4.7: Depth of Penetration vs Total No of Layers of Sandwich Panel Rubber-Steel Alloy 4140

4.3.1.2 Sandwich Panel of Rubber-Stainless Alloy 304

Figure 4.8 shows how the depth of penetration is affected by impacting the bullet on the Rubber-Stainless Alloy 304 sandwich panel. It is found that for the 4 layers panel, the bullet penetrate and perforate the sandwich panel. The 6 layers panel is penetrated up to 130 mm and the 8 layers panel is penetrated up to 166 mm of the sandwich panel.

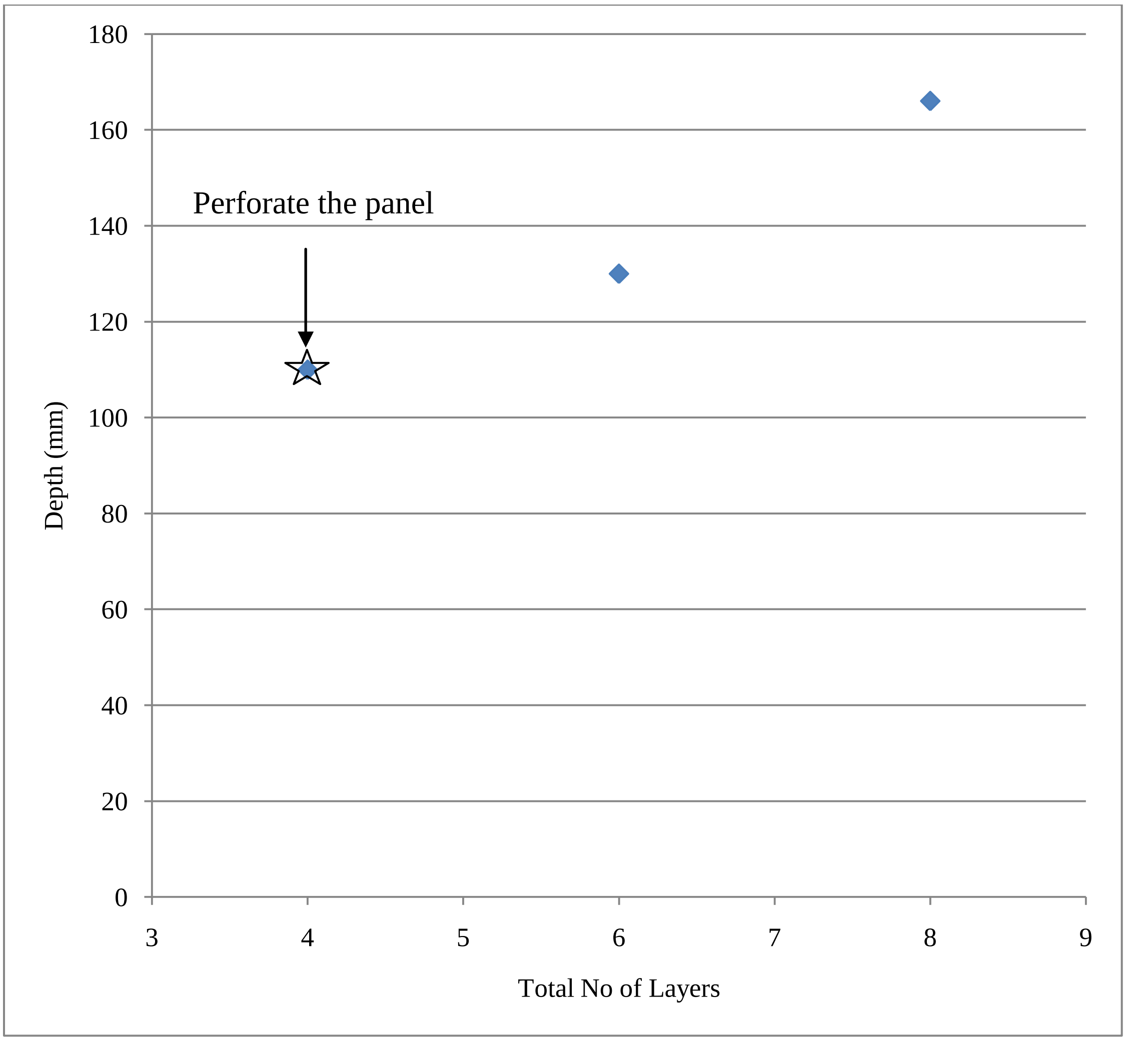

Figure 4.8: Depth of Penetration vs Total No of Layers of Sandwich Panel Rubber-Stainless Alloy 304

4.3.2 Effect of Plate Yield Strength (YS) of Steel Alloy 4140

The sandwich panel selected in this testing is 6 layers panel with total thickness 165 mm. In this simulation test, the yield strength of the Steel Alloy 4140 is reduced 20% for every step. The value of YS is 290 MPa, 232 MPa, 174 MPa, and 116 MPa. Figure 4.9 shows how the depth of penetration is affected by the Yield Strength (YS) of the Steel Alloy 4140 sandwich panel. It is found that the depth of penetration for YS 290 MPa is 155 mm, YS 232 MPa is 105 mm, YS 174 MPa is 114 mm, and YS 116 MPa is 165 mm. For YS 116 MPa the bullet has perforated the panel.

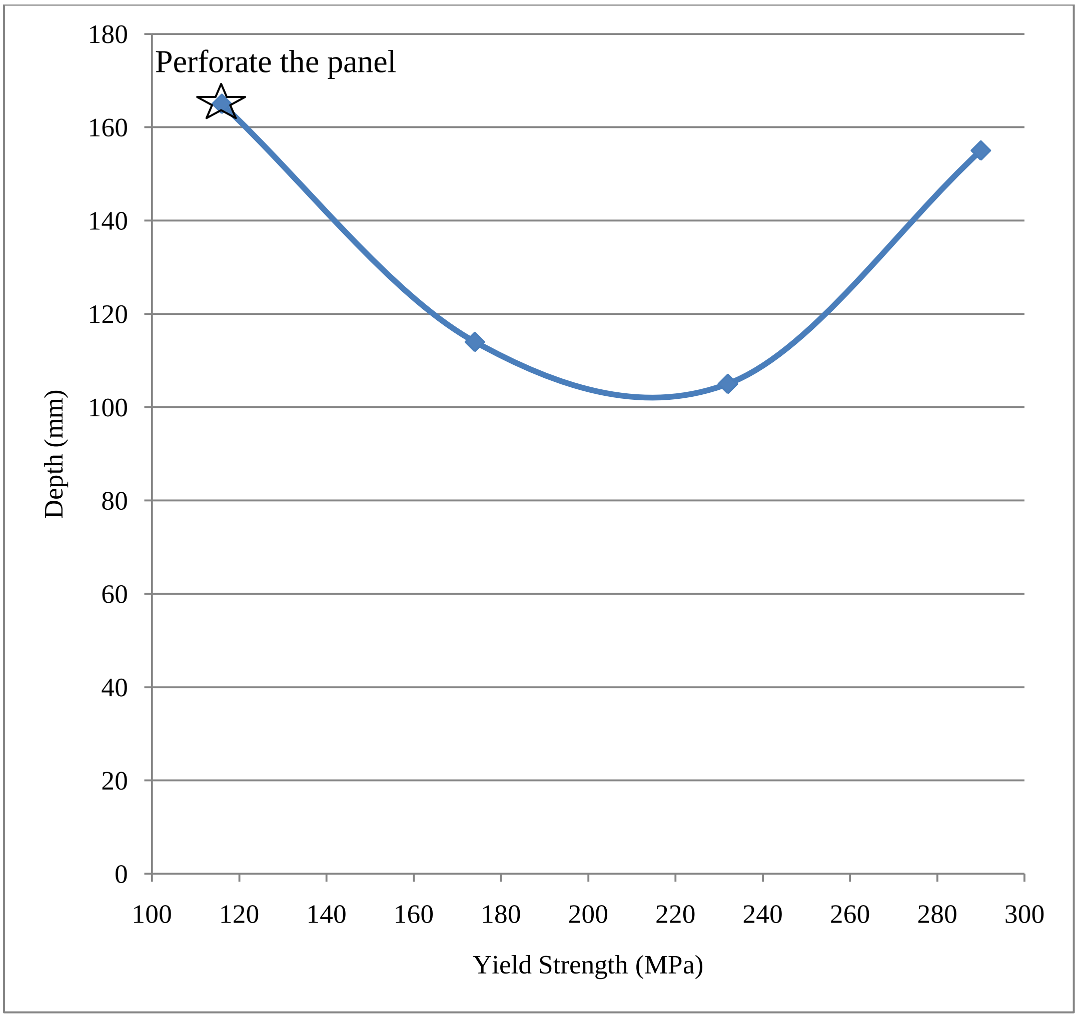

Figure 4.9: Depth of Penetration vs Yield Strength of Sandwich Rubber-Steel Alloy 4140 Panel 6 Layers

4.3.3 Effect of % of Plastic Elongation of Steel Alloy 4140

The sandwich panel selected in this testing is 6 layers panel with total thickness 165 mm. In this simulation test, the % of Plastic Elongation of the Steel Alloy 4140 is increased for every step. The values are increased to 0.2, 0.4, 0.6 and 0.8. Figure 4.10 shows how the depth of penetration is affected by the % of Plastic Elongation of the Steel Alloy 4140 sandwich panel. It is found that, the depth of penetration for % of Plastic Elongation 0.2 is 155 mm, % of Plastic Elongation 0.4 is 119 mm, % of Plastic Elongation 0.6 is 112 mm, and % of Plastic Elongation 0.8 is 140 mm.

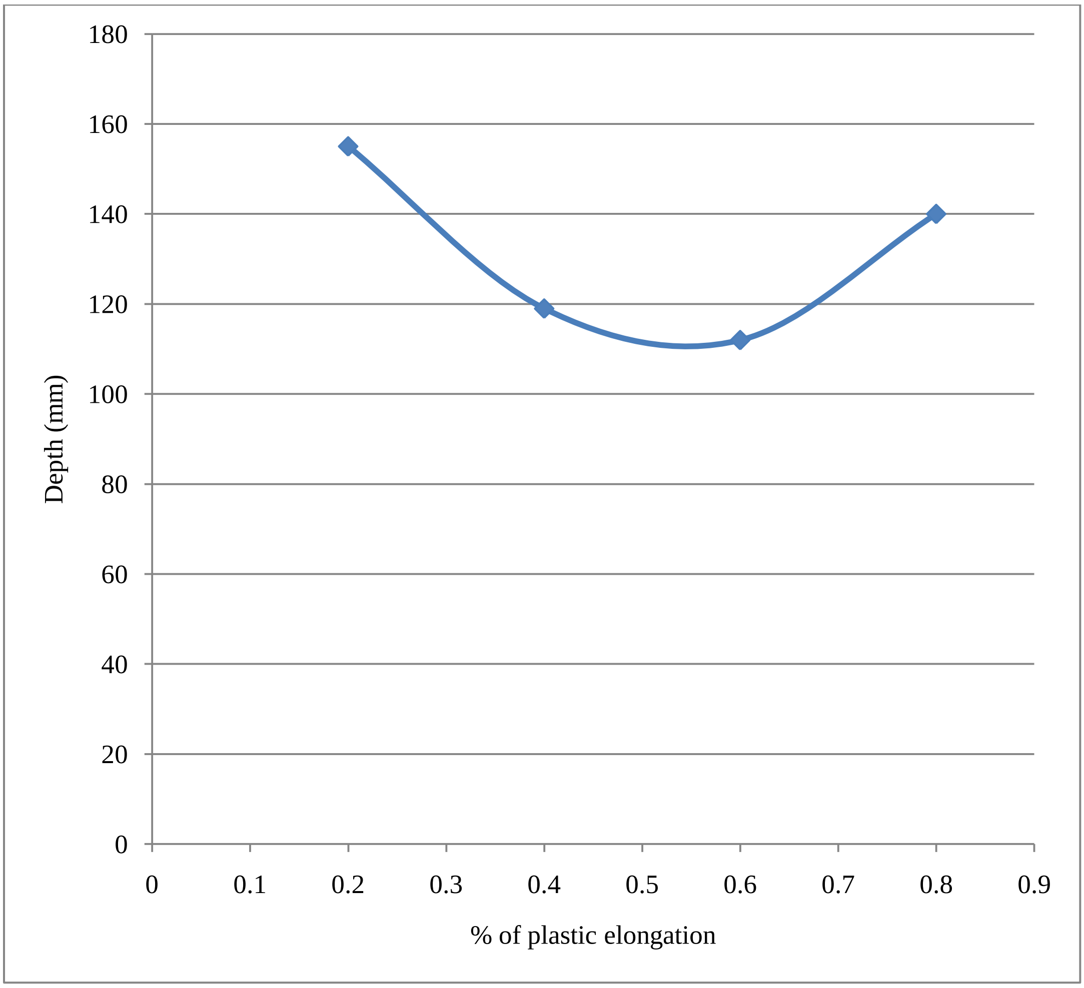

Figure 4.10: Depth of Penetration vs % of Plastic Elongation of Sandwich Rubber-Steel Alloy 4140 Panel 6 Layers

4.4 Discussion for Sandwich Panel

The sandwich panel design is introduced because if only rubber alone is used, its capability in resisting bullet penetration is not sufficient as per describe above. For that reason we propose a design with 3 different sandwich panels consisting different number of layers. The total thickness of 4 layers is 110 mm, 6 layers is 165 mm and 8 layers is 220 mm. The parameter properties of the rubber are the same with the data given in Table 3.2 and the properties of the plates given in Table 3.3.

The results for the 4 layers panel show that the depth of penetration for sandwich panel of rubber-Steel Alloy 4140 is 65 mm. From the graph in the Appendix, it shows that the bullet is bounce back and off the panel from the front surface. For the sandwich panel of rubber-Stainless Alloy 304, the bullet penetrates and perforates the sandwich panel. Therefore, for safety reason both panels are not suitable to be used as a bullet stopper.

The results for the 6 layers sandwich panel show that the sandwich panel of rubber-Steel Alloy 4140 and sandwich panel of rubber-Stainless Alloy 304 are able to stop the bullet. The depth of penetration into the panels is 164 mm and 130 mm respectively. The bullet is trapped at the second last and the last layer of the panel. These panels are not suitable to be used because the bullets are able to reach the second and last layer of the panel. If the bullet has higher velocity, it may perforate the panel.

The results for the 8 layers of sandwich panel show that both panels are able to stop the bullet. The depth of penetration is 106 mm for sandwich of rubber-Steel Alloy 4140 panel and 166 mm for sandwich of rubber-Stainless Alloy 304 panel. For the rubber-Steel Alloy 4140 panel, the bullet is stopped at layer no 4. For the rubber-Stainless Alloy 304 panel, the bullet is stopped at layer no 6. These results show that the 8 layers sandwich panel for both type of reinforce material selection are suitable to be used as the bullet stopper and trap. Between the two, the rubber- Steel Alloy 4140 is more suitable to be used because it is capable to stop bullet at layer no 4.

The further study is done by varying the YS and % of Plastic Elongation in order to investigate their effect of depth of penetration. The study is started with reducing the YS and keeps maintaining the rubber parameters and % of Plastic Elongation. The second study is increasing the % of Plastic Elongation and keeps maintaining the YS and the rubber parameters. In this study the parameters property of the rubber is keep maintained as per in Table 3.2 and the original properties of the plate material is as per in Table 3.3. The simulation is conducted using the 6 layers of sandwich panel with the reinforce plate of Steel Alloy 4140 only.

The results for reducing the YS show that the depth of penetration is reducing before it is increasing again at about 50% of the original of YS. The results for increasing the % of Plastic Elongation show that the depth of penetration is reducing before it is increasing again at about 0.5% of Plastic Elongation of the original data. From the simulation, both results show that the change in the YS and % of Plastic Elongation of reinforce material will have the effect on the depth of penetration.

By comparing the depth of penetration between the panels of rubber alone and the sandwich panel, the depth of penetration for sandwich panel is much lower than the rubber panel. The rubber panel alone requires the thickness of 500 mm which is larger than the sandwich panel of 220 mm in thickness. For that, the sandwich panel is easier to handle in the shooting range due to small in size. Furthermore, the value use of Constant A is also lower for the sandwich panel, therefore it does not require excessive carbon black filler.

In this study we are selecting rubber as the main material because it is easily available in Malaysia. Indeed, Malaysia supplies rubber of about 46% of the world need and cultivates rubber about 2 to 4 million acres or about 65% of total land used for cultivation (Kishore 2010) . The price of this material is relatively cheap. Therefore, the cost in producing the rubber panel is low.

CHAPTER 5: Conclusions and Recommendations

5.1 Conclusions

In this study, the numerical simulation of rubber panel under impact loading was considered. The rubber panel will be used as a potential additional safety device during the firing test conducted at WTD, STRIDE. Indeed, the current practice of firing test has several drawbacks including those related to safety, maintenance cost and pollution issues as detailed in Chapter 1. The additional safety device should be portable, with a relatively small size in dimension, easy in handling and light weight. Moreover, it should be capable to stop completely the bullet during the test, i.e. it should have sufficient damping capacity. Considering the above requirements, rubber materials are chosen as the potential material for the panel.

The numerical simulations on the feasibility study of rubber materials used as portable panel have been successfully conducted using MSC. Dytran software available at WTD, STRIDE. The Mooney-Rivilin hyperelastic strain energy was used during the simulation to represent the rubber failure behaviour. The effect of different material parameters including damping capacity on the depth of penetration was investigated. Based on this result, the chosen material parameters of rubber to be used in the design of the new panel are A = 1.4 x 0.89 MPa, B= 0.46 MPa, LVC=0.01.

The numerical simulations on mechanical responses of rubber material under impact loading were investigated. Different types of rubber were considered. Through study, it was found that the depth of penetration is reduced with the increasing of parameter A. However the result show that the rubber alone as a material for panel is not sufficient. Indeed, the required panel geometry will be too large (500 mm in thickness) to be used in practice at WTD, STRIDE. Moreover, producing such massive rubber panel would be difficult. Therefore, it was proposed that the panel should consist of sandwich structure between rubber and reinforcing materials. For simplicity two type of steel were considered: Steel Alloy 4140 and Stainless Alloy 304.

For each type of reinforcing material, 3 types of sandwich arrangement were investigated: 4 layers sandwich panel, 6 layers sandwich panel and 8 layers sandwich panel. The result shows that 8 layers panel give better result than 4 or 6 layers. Further numerical simulations on the effect of the yield strength and % of plastic elongation of reinforcing material on the depth of penetration were established. It was found that the depth of penetration reduces when both yield strength and % of plastic elongation increase before the penetration increases for further increase of yield strength and % of plastic elongation.

To conclude, all of the objectives of the study are achieved.

5.2 Recommendations

The following are suggested for future investigation:

1. The numerical results should be validated and compared with experimental observations. Therefore, appropriate experimental set-up to probe the mechanical response of rubber panel under impact loading is required.

2. In real engineering applications, many industrial rubber components exhibit strong viscoelastic response. Therefore, the validity of hyperelastic constitutive equation to describe rubber behaviour should be evaluated. In the case where strong viscoelastic response is observed, additional subroutine describing the viscous effect should be developed and implemented into MSC. Dytran.
3. The effect of temperature on the behaviour of the rubber panel should be investigated.
4. Further investigation on the optimum geometry and configuration of rubber panel is needed. For this purpose the comprehensive studies involving cost analysis of materials fabrication and maintenance should be conducted.
5. The current workstation available at WTD, STRIDE should be improved in order to get accurate results within relatively short period of time.

BIBLIOGRAPHY

(1997). MSC/DYTRAN User's Manual Version 4.0. USA, The MacNeal-Schwendler Corporation.

(2006). MSC. Dytran 2005 r3 Theory Manual, MSC. Software Corporation, 2 MacArthur Place Santa Ana, CA 92707.

(2006). MSC. Dytran 2005 r3 User's Guide. USA, MSC. Software Corporation.

Ashish K. Sareen, M. R. S., Bell Helicopter Textron, Inc. Fort Worth, Texas (1996). Evaluation of an Analytical Design Tool for Ballistic Dynamics Simulation. 1996 MSC World User's Conference Proceedings, Newport Beach, CA, The American Helicopter Society.

Børvik, T., L. Olovsson, et al. (2011). "Normal and oblique impact of small arms bullets on AA6082-T4 aluminium protective plates." International Journal of Impact Engineering **38**(7): 577-589.

C J Marchant Smith, P. R. H. (1982). Small Arms & Cannons, Brassey's Defence Publishers.

Callister, W. D. (2007). Materials Science and Engineering: An Introduction, John Wiley & Sons Inc, Asia-Printed.

Dean, G. and B. Read (2001). "Modelling the behaviour of plastics for design under impact." Polymer Testing **20**(6): 677-683.

Donald E. Carlucci, S. S. J. (2008). Ballistics Theory and Design of Guns and Ammunition, CRC Press, Taylor & Francis Group 6000 Broken Sound Parkway NW, Suite 300 Boca Raton.

Donald R. Askeland, P. P. P. (2003). The Science and Engineering of Materials Fourth Edition. USA, Thomson Learning, Brooks/Cole.

Dorogoy, A., D. Rittel, et al. (2010). "A study of inclined impact in polymethylmethacrylate plates." International Journal of Impact Engineering **37**(3): 285-294.

Duan, Y., M. Keefe, et al. (2006). "A numerical investigation of the influence of friction on energy absorption by a high-strength fabric subjected to ballistic impact." International Journal of Impact Engineering **32**(8): 1299-1312.

Fischer, T. (2009). Materials Science for Engineering Students. Canada, Elsevier.

Gama, B. A. and J. W. Gillespie Jr (2011). "Finite element modeling of impact, damage evolution and penetration of thick-section composites." International Journal of Impact Engineering **38**(4): 181-197.

Halsey, K. J. W. G. a. D. H. J. (1982). AMMUNITION (including grenades and mines), BRASSEY'S PUBLISHERS LIMITED.

Hoo Fatt, M. S. and D. Sirivolu (2010). "A wave propagation model for the high velocity impact response of a composite sandwich panel." International Journal of Impact Engineering **37**(2): 117-130.

Iqbal, M. A., A. Chakrabarti, et al. (2010). "3D numerical simulations of sharp nosed projectile impact on ductile targets." International Journal of Impact Engineering **37**(2): 185-195.

Kishore (2010). Rubber Cultivation In Malaysia. kish.in/rubber_cultivation_in_malaysia/.

Krishnan, K., S. Sockalingam, et al. (2010). "Numerical simulation of ceramic composite armor subjected to ballistic impact." Composites Part B: Engineering **41**(8): 583-593.

Lamberts, A. P. T. M. J. (2007). Numerical Simulation of Ballistic Impacts On Ceramic Material, Eindhoven University of Technology, .

Li, Q., J.-c. Zhao, et al. (2009). "Fatigue life prediction of a rubber mount based on test of material properties and finite element analysis." Engineering Failure Analysis **16**(7): 2304-2310.

Loew, R. and P. Meier (2007). "Simulation of reiterated mechanical load of silicone rubber." Finite Elements in Analysis and Design **43**(6-7): 453-462.

Logan, D. L. (2002). A First Course in the Finite Element Method 3rd Edition, Brooks/Cole, 511 Forest Lodge Road Pacific Grove, CA 93950 USA.

M, S. (2011). "Simulation of high velocity impact in fluid-filled containers using finite elements with adaptive coupling to smoothed particle hydrodynamics." International Journal of Impact Engineering **38**(6): 511-520.

McHenry, M. D. G. a. M. E. (2010). Structure Of Materials: An Introduction to Crystallography, Diffraction, and Symmetry, Cambridge University Press.

Nyström, U. and K. Gylltoft (2011). "Comparative numerical studies of projectile impacts on plain and steel-fibre reinforced concrete." International Journal of Impact Engineering **38**(2-3): 95-105.

Omar, M. b. (2003). Effects of Barrel Coppering In Lead Free Bullets, Royal Military Collage of Science, Shrivenham, Swindon, UK. **MSc. Explosive Ordnance Engineering**.

Ong, C. W., C. W. Boey, et al. (2011). "Advanced layered personnel armor." International Journal of Impact Engineering **38**(5): 369-383.

Qasim H, S. (2009). "Impact resistance of a rectangular polycarbonate armor plate subjected to single and multiple impacts." International Journal of Impact Engineering **36**(9): 1128-1135.

R. Barauskas, M. K. (2005). "Collision Detection and Response of Yarns In Computational Models of Woven Structures." Mathematical Modelling and Analysis.

Reddy, J. N. (1984). An Introduction To The Finite Element Method, McGraw-Hill Company.

Roberts, B. a. B., JB (1977). The Relationship Between Uniaxial and Equibiaxial Fatigue in Gum and Carbon Black Filled Vulcanizates. Proceedings of Rubbercon '77.

Sands, J. M., C. G. Fountzoulas, et al. (2009). "Modelling transparent ceramics to improve military armour." Journal of the European Ceramic Society **29**(2): 261-266.

Terry J Gander, C. Q. C. (2000). Jane's Ammunition Handbook 2000 - 2001, Jane's Information Group Limited, Sentinel House,163 Brighton Road, Coulsdon Surrey CR5 2YH UK.

Wang, Y., Y. Miao, et al. (2010). "Digital element approach for simulating impact and penetration of textiles." International Journal of Impact Engineering **37**(5): 552-560.

Yunus, D. Z. b. (2009). Sambutan Majlis Jasamu Dikenang dan Perhimpunan Pagi di Kompleks Induk STRIDE, Kajang. Buletin Dalaman BUDI STRIDE. Kajang, Selangor, STRIDE. **BUDI 3/2009:** 3 - 5.

Zeng, H. B., S. Pattofatto, et al. (2010). "Perforation of sandwich plates with graded hollow sphere cores under impact loading." International Journal of Impact Engineering **37**(11): 1083-1091.

APPENDIX

Results of Penetration of Simulation

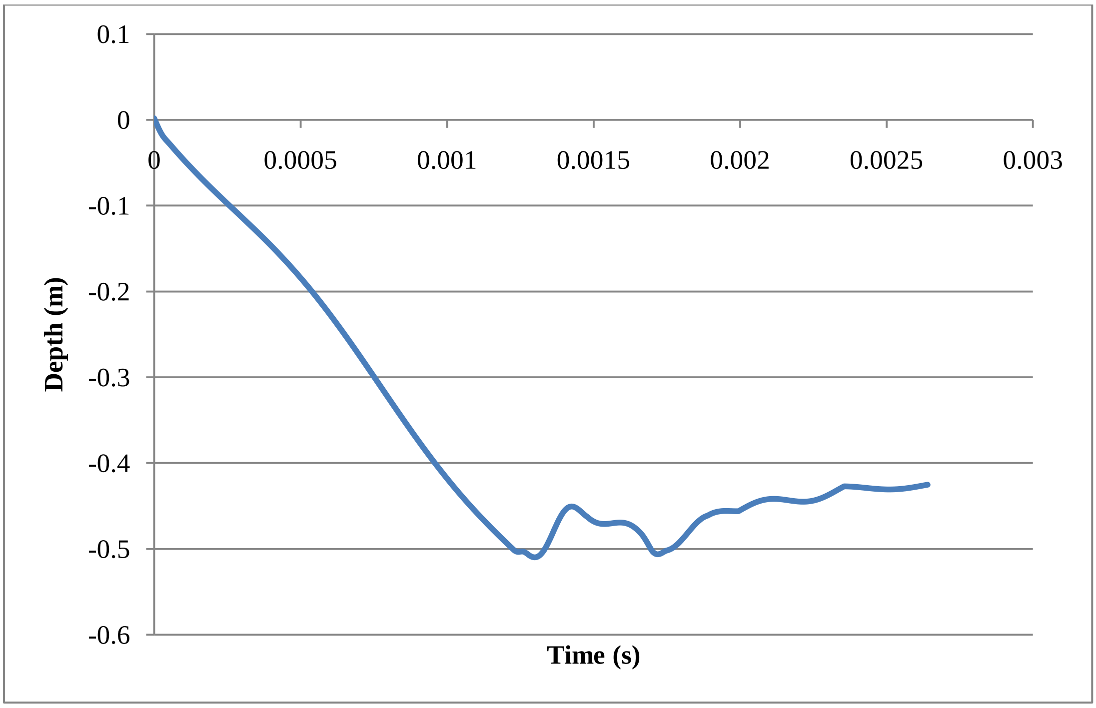

Figure A1: Penetration vs Time of Constant A 1.0 x 0.89 MPa with Panel Thickness 500 mm

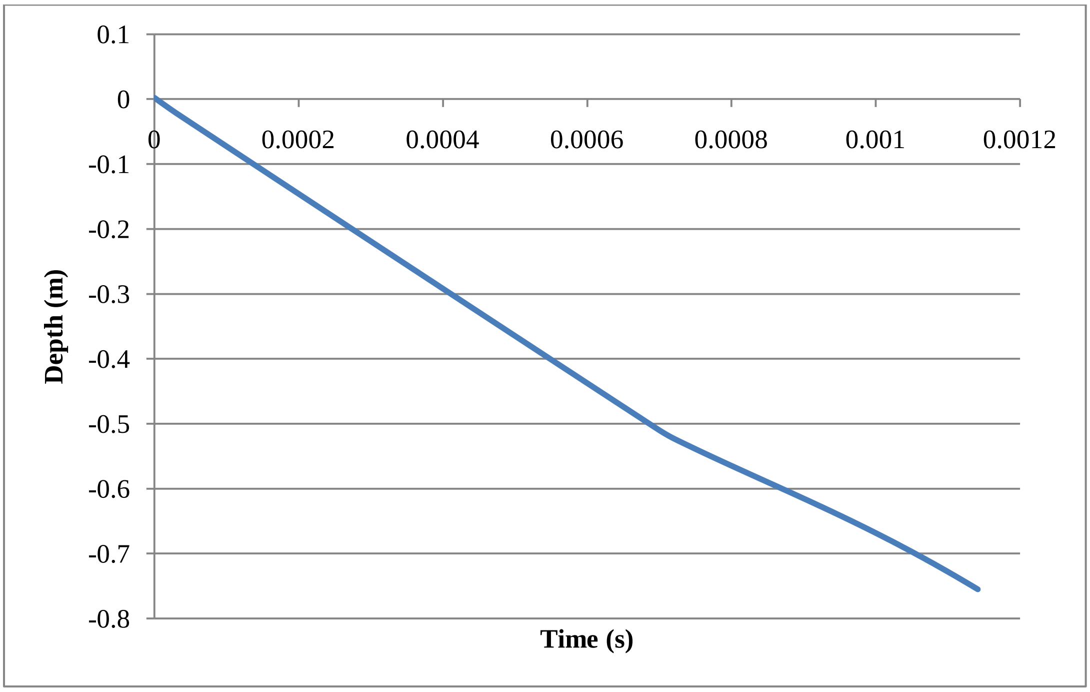

Figure A2: Penetration vs Time of Constant A 1.2 x 0.89 MPa with Panel Thickness 500 mm

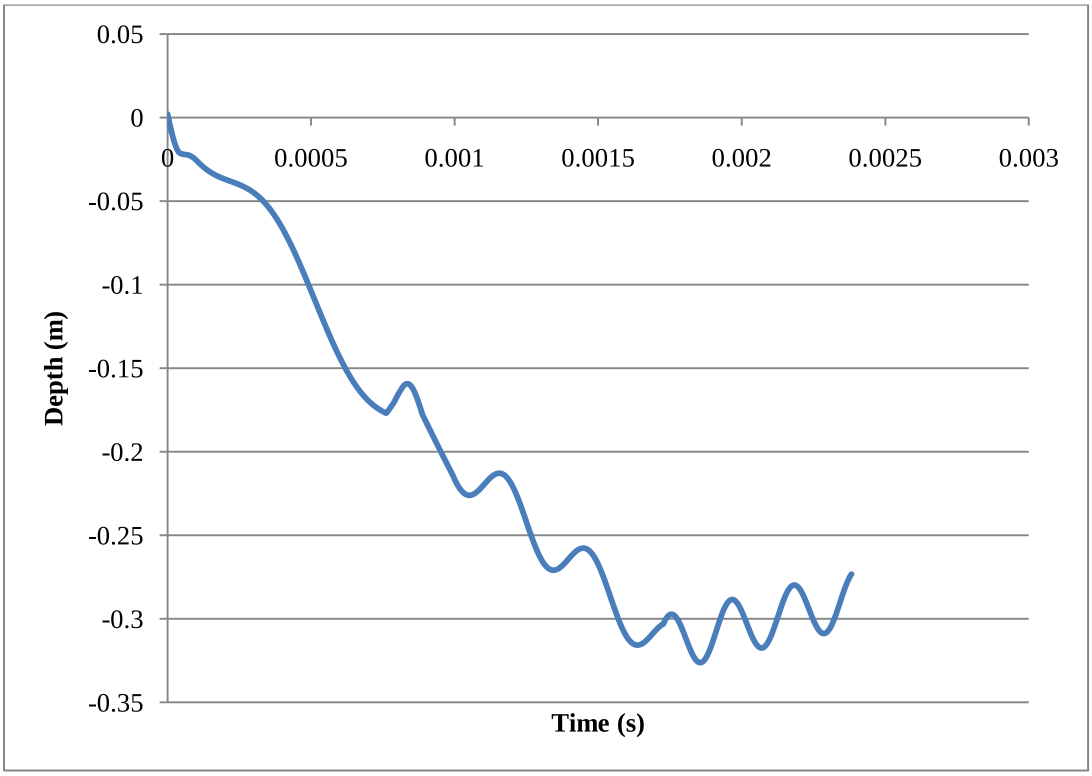

Figure A3: Penetration vs Time of Constant A 1.4 x 0.89 MPa with Panel Thickness 500 mm

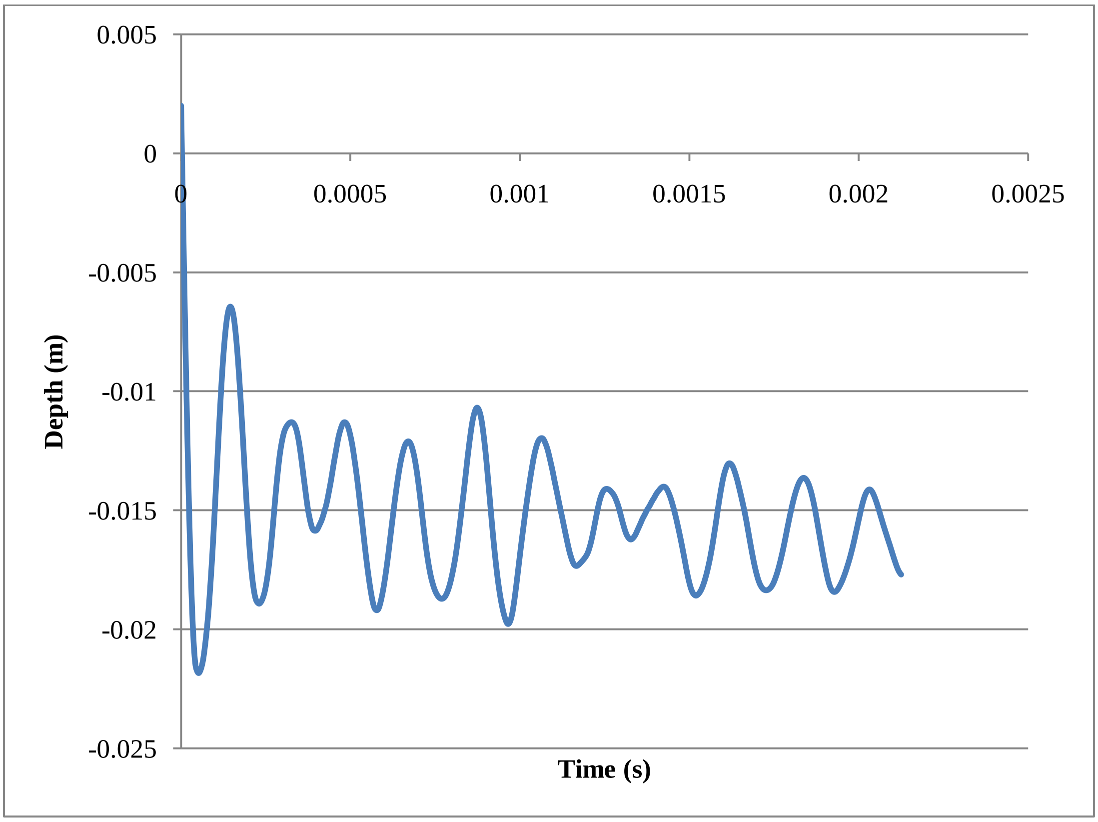

Figure A4: Penetration vs Time of Constant A 1.6 x 0.89 MPa with Panel Thickness 500 mm

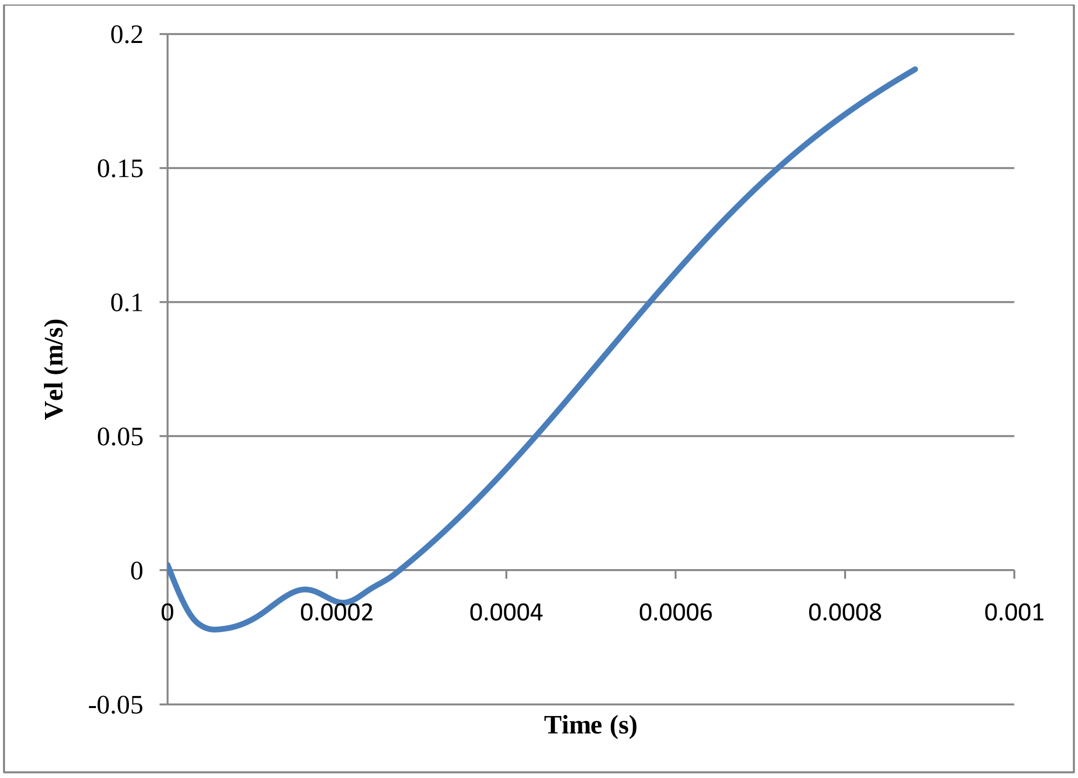

Figure A5: Penetration vs Time of Constant A 1.8 x 0.89 MPa with Panel Thickness 500 mm

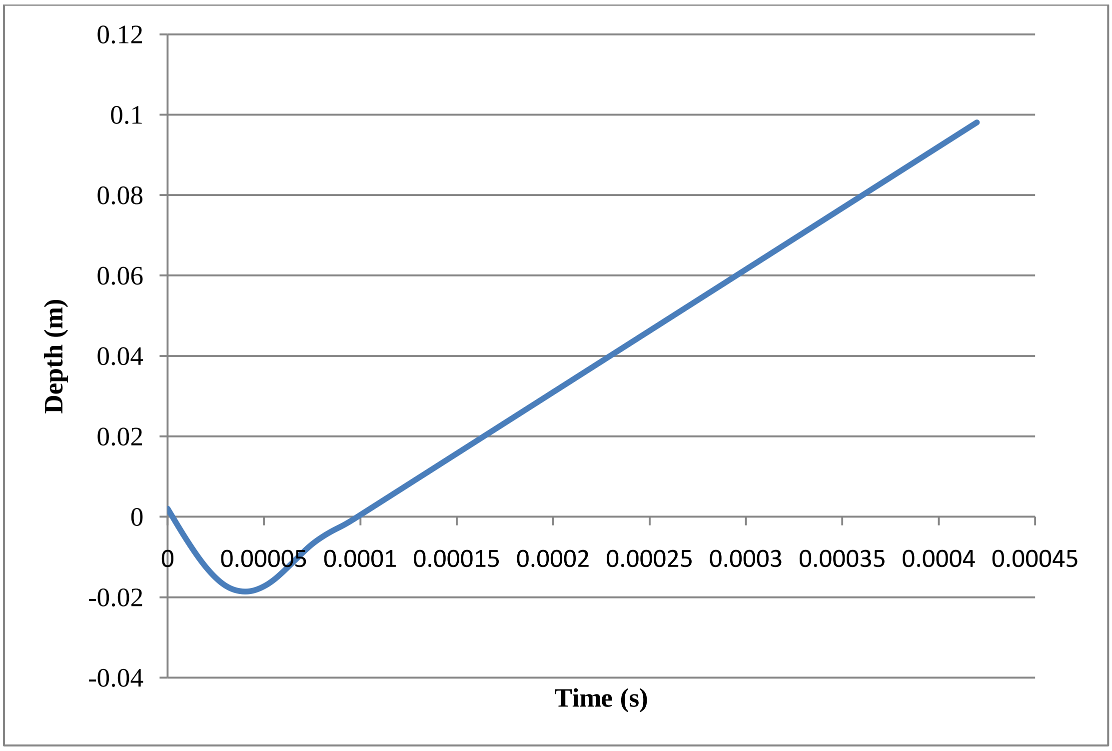

Figure A6: Penetration vs Time of Constant A 2.0 x 0.89 MPa with Panel Thickness 500 mm

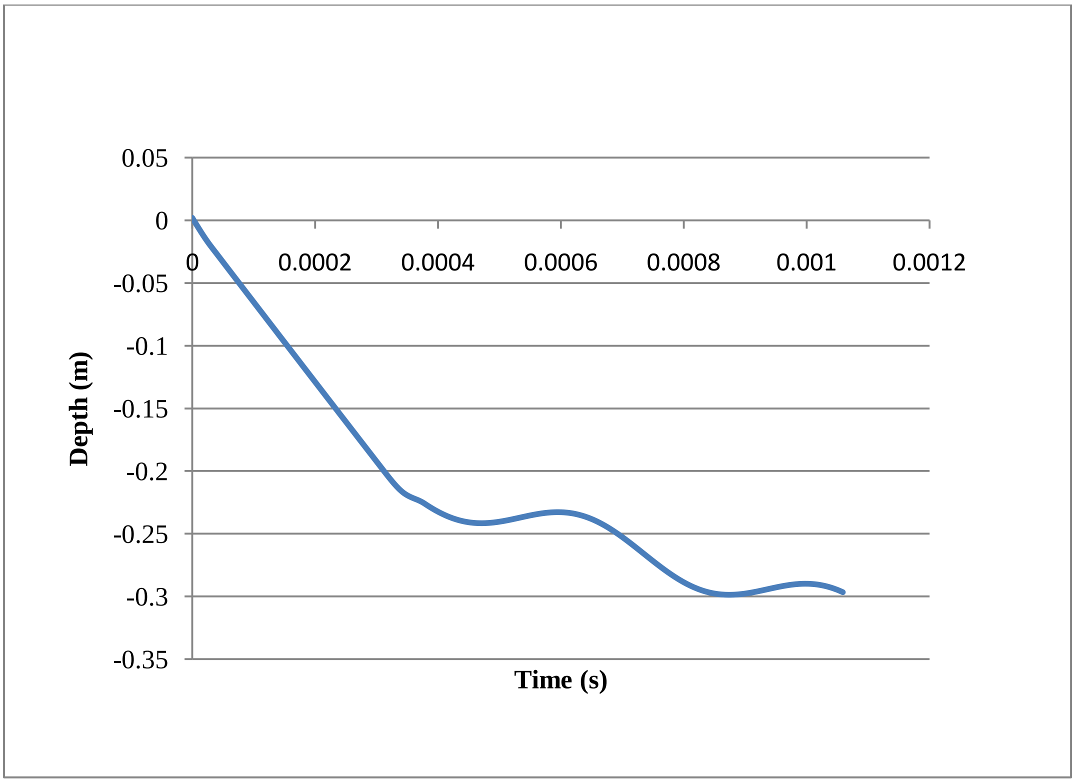

Figure A7: Penetration vs Time of Constant A 1.4 x 0.89 MPa with Panel Thickness 200 mm

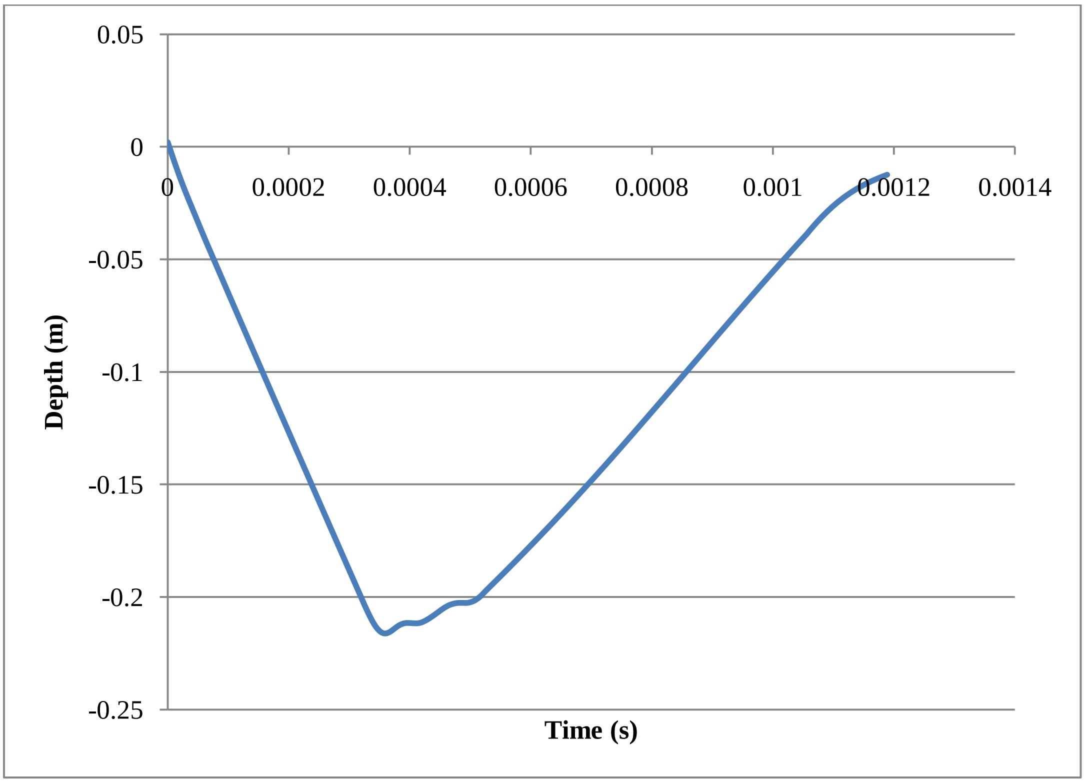

Figure A8: Penetration vs Time of Constant A 1.5 x 0.89 MPa with Panel Thickness 200 mm

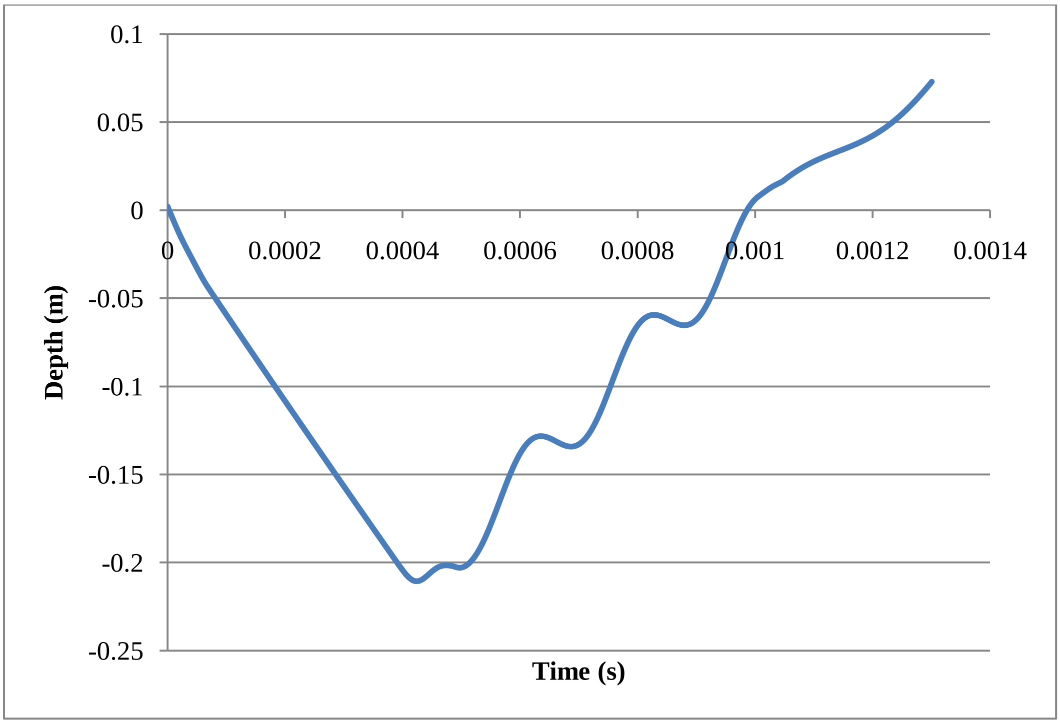

Figure A9: Penetration vs Time of Constant A 1.6 x 0.89 MPa with Panel Thickness 200 mm

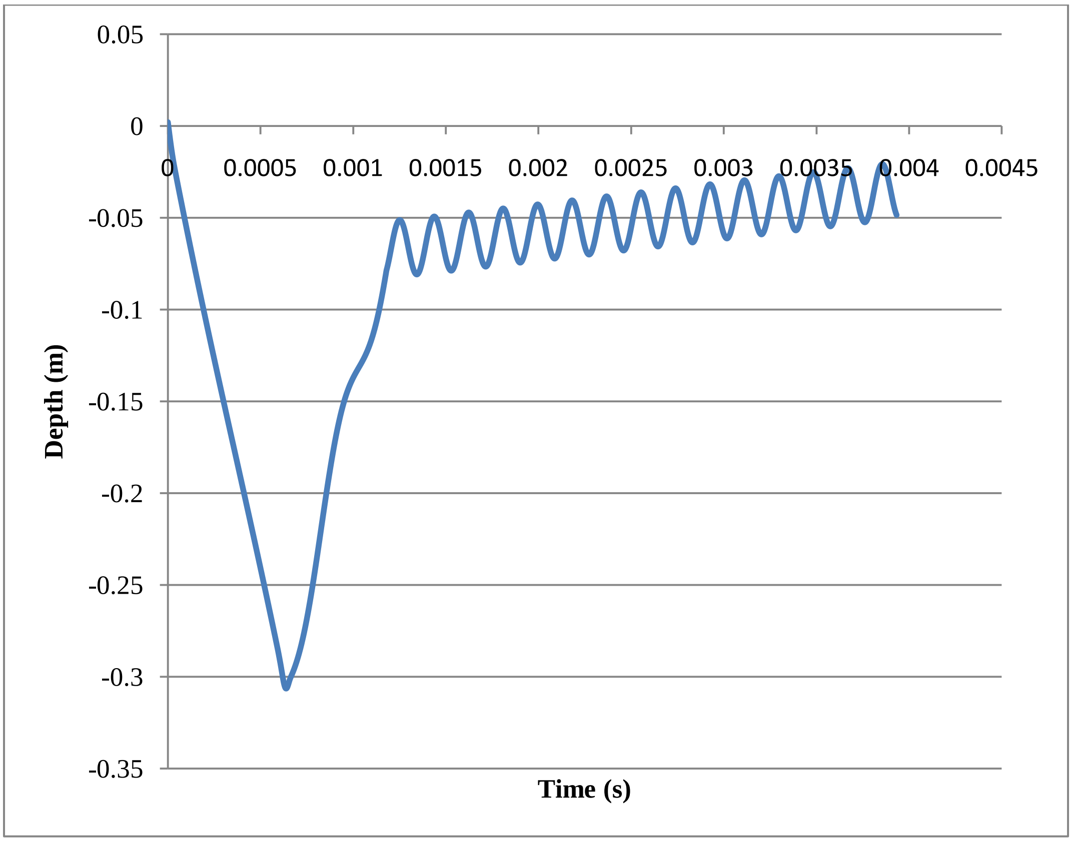

Figure A10: Penetration vs Time of Constant A 1.4 x 0.89 MPa with Panel Thickness 300 mm

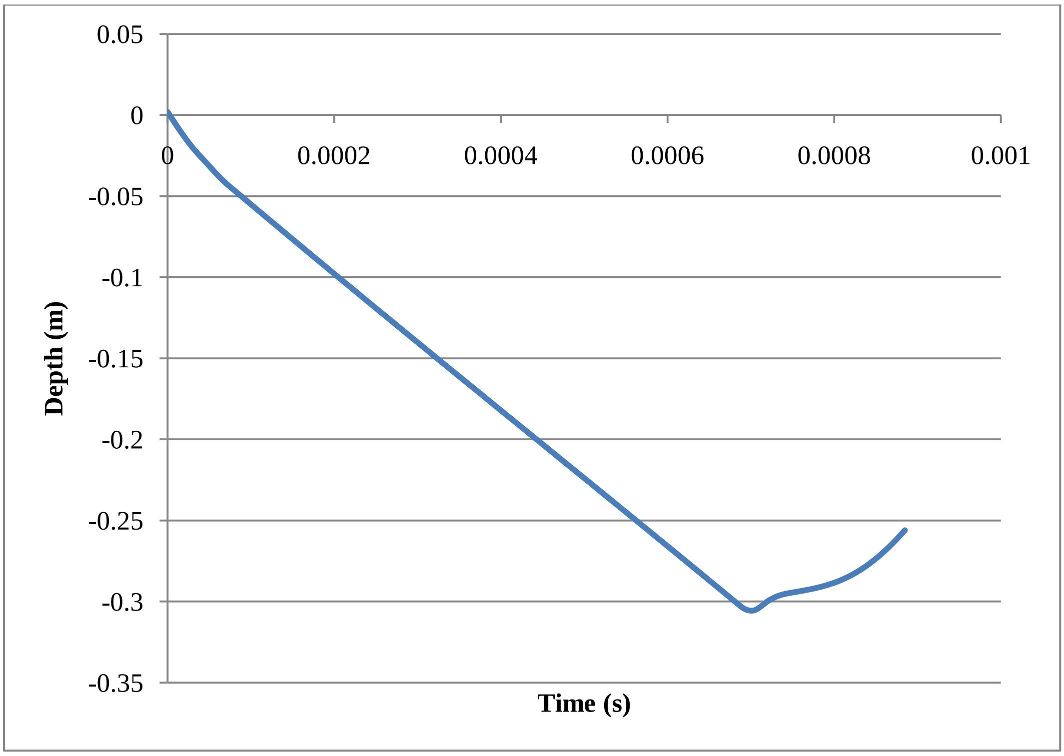

Figure A11: Penetration vs Time of Constant A 1.6 x 0.89 MPa with Panel Thickness 300 mm

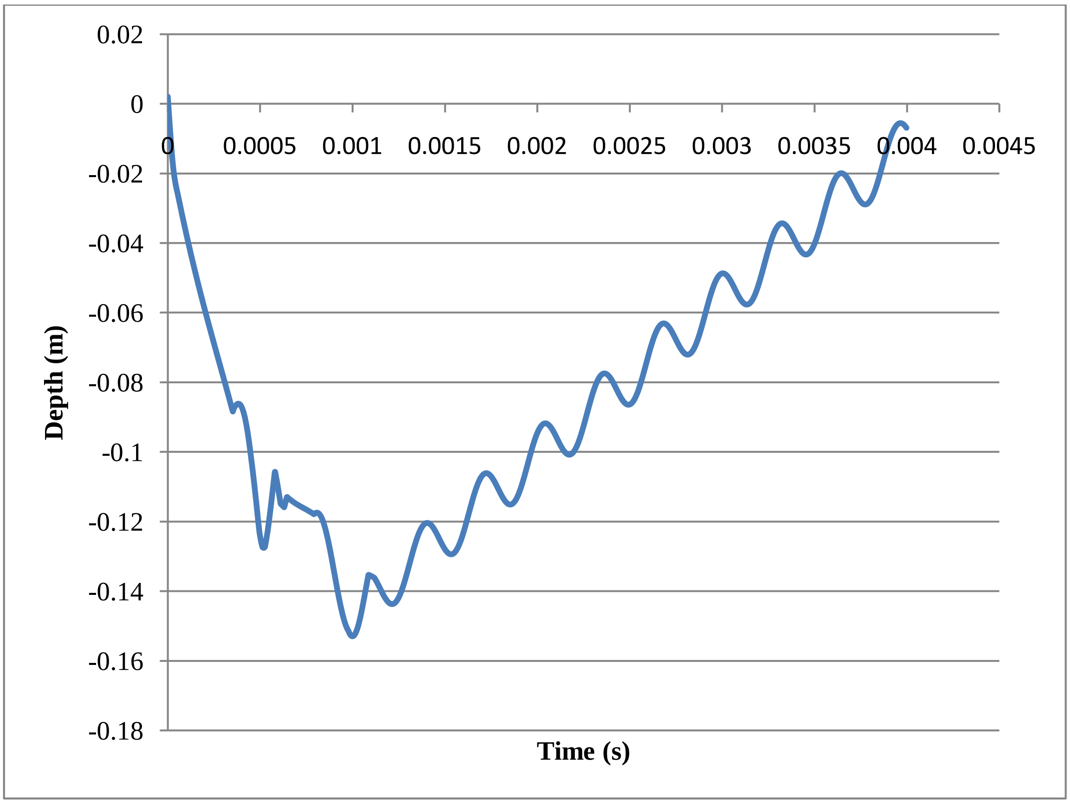

Figure A12: Penetration vs Time of Constant A 1.8 x 0.89 MPa with Panel Thickness 300 mm

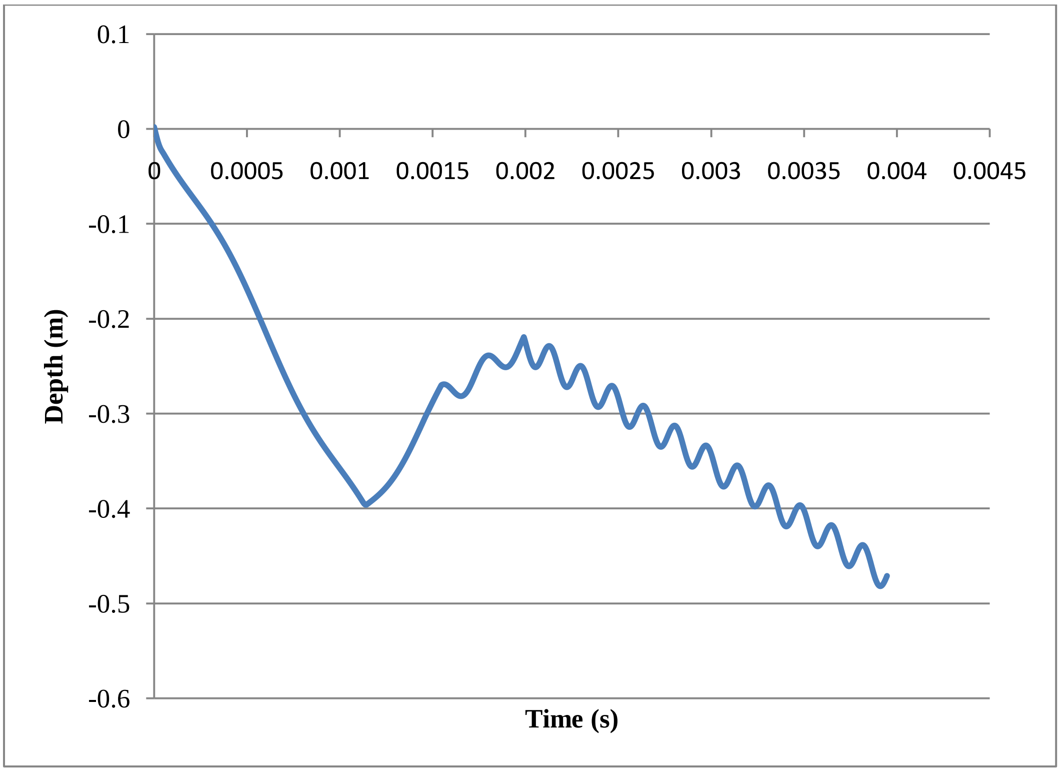

Figure A13: Penetration vs Time of Constant A 1.4 x 0.89 MPa with Panel Thickness 400 mm

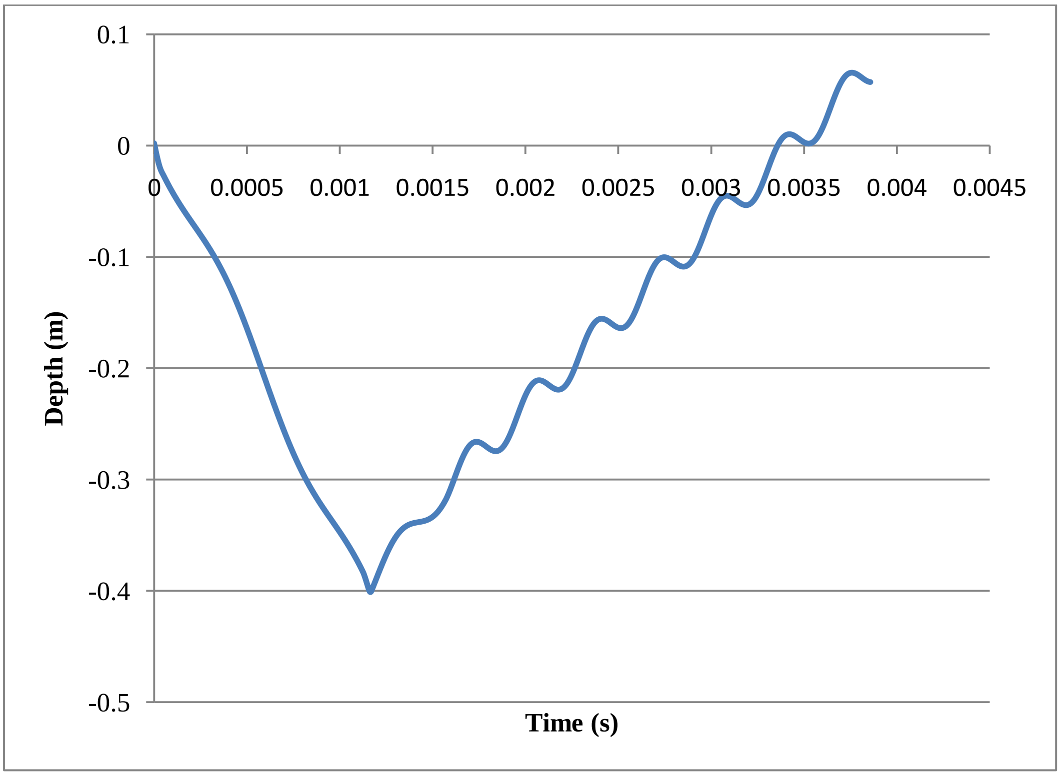

Figure A14: Penetration vs Time of Constant A 1.5 x 0.89 MPa with Panel Thickness 400 mm

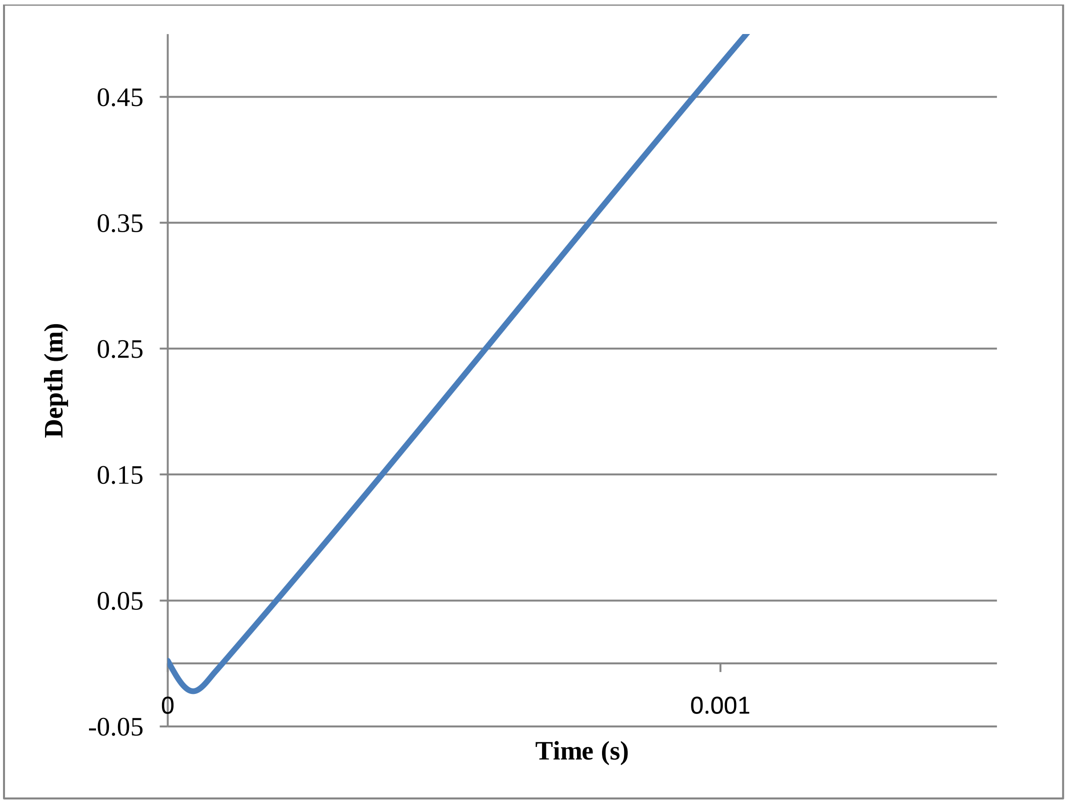

Figure A 15: Penetration vs Time of Constant A 1.6 x 0.89 MPa with Panel Thickness 400 mm

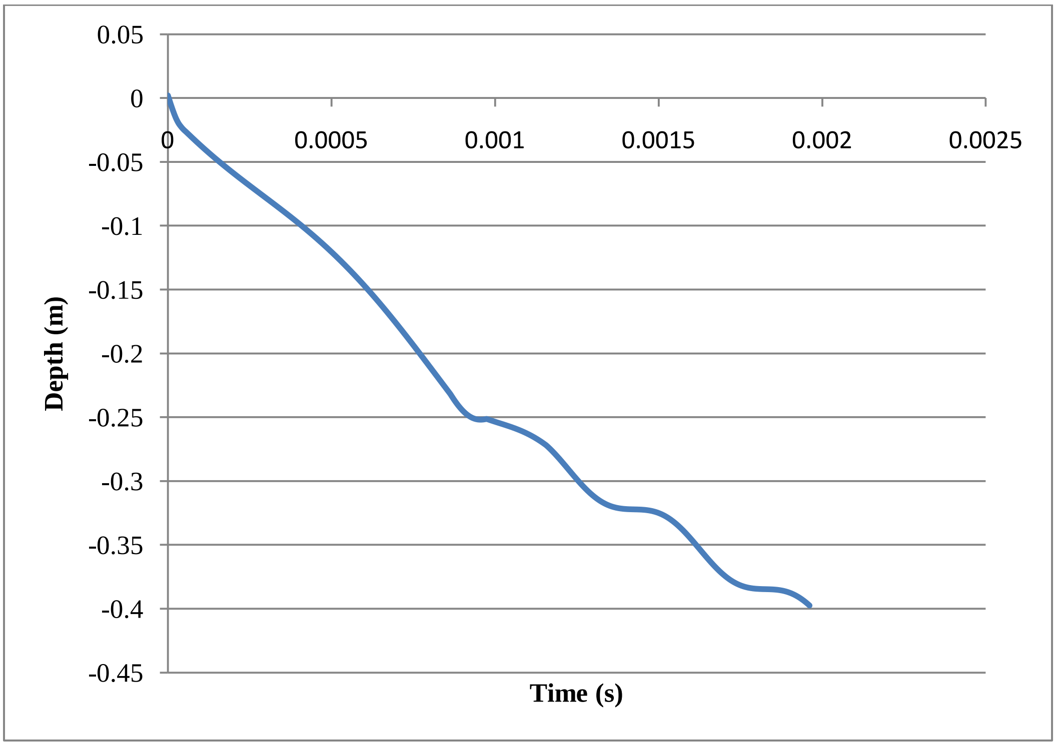

Figure A16: Penetration vs Time of Constant A 1.4 x 0.89 MPa with Panel Thickness 500 mm and LVC 0.0001

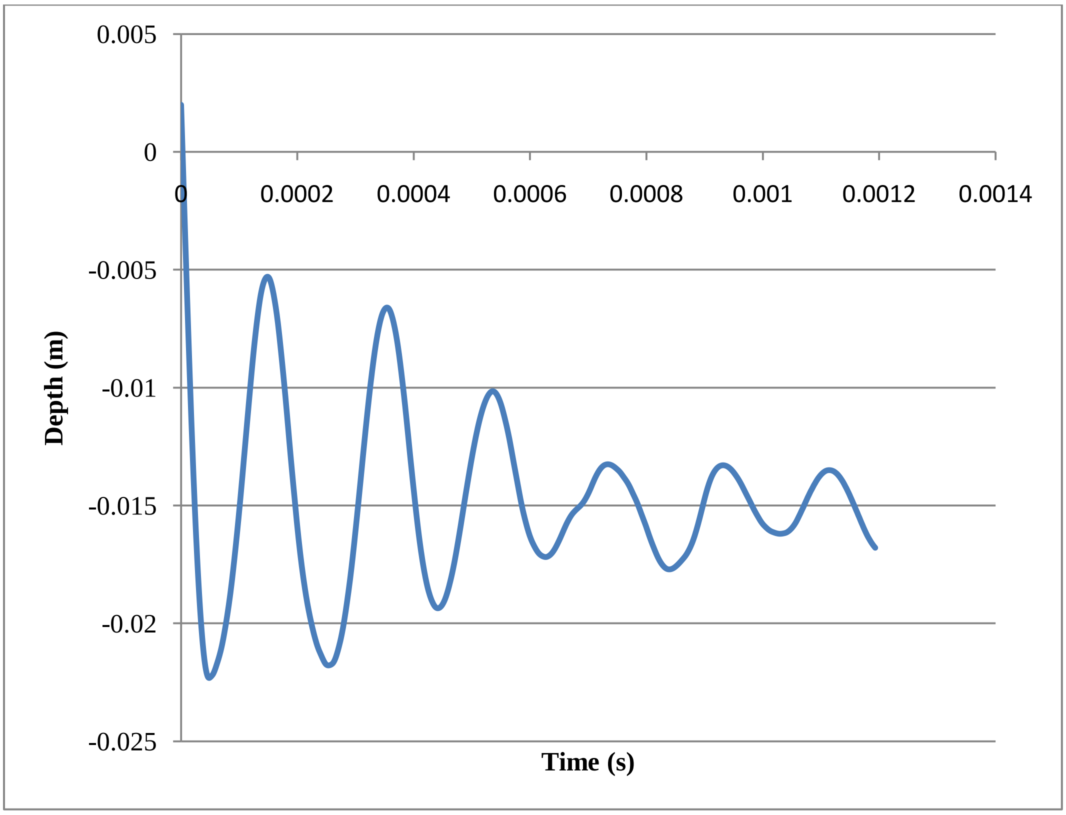

Figure A17: Penetration vs Time of Constant A 1.4 x 0.89 MPa with Panel Thickness 500 mm and LVC 0.001

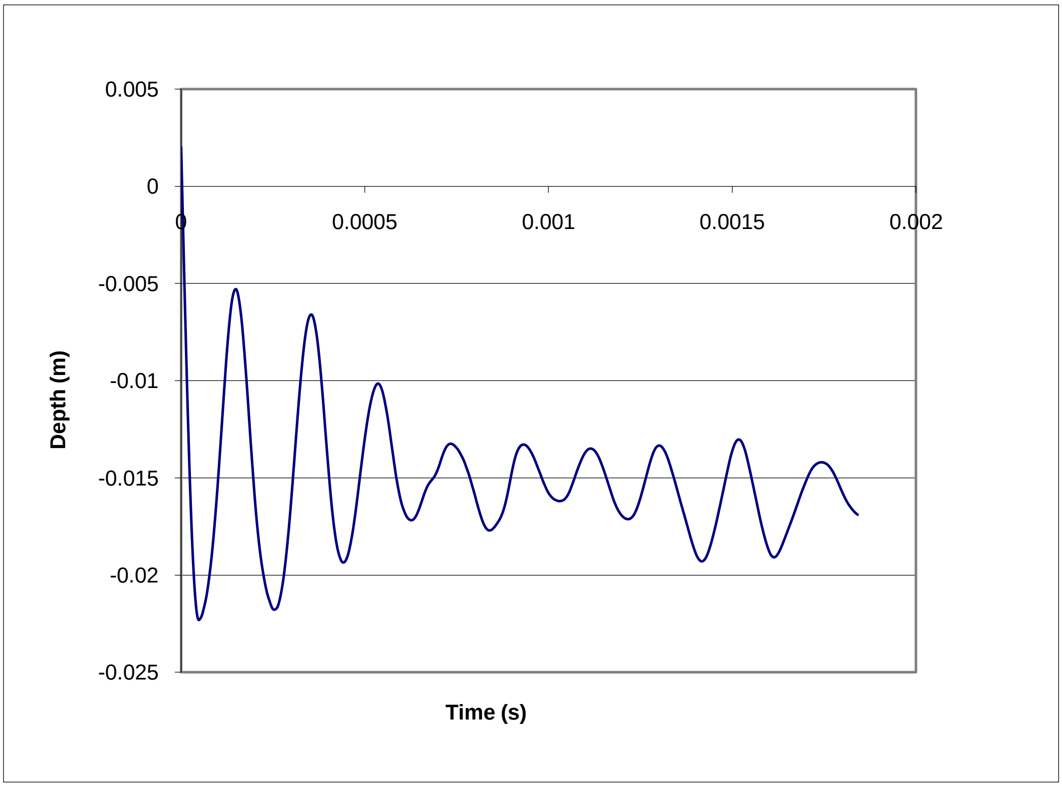

Figure A18: Penetration vs Time of Constant A 1.4 x 0.89 MPa with Panel Thickness 500 mm and LVC 0.01

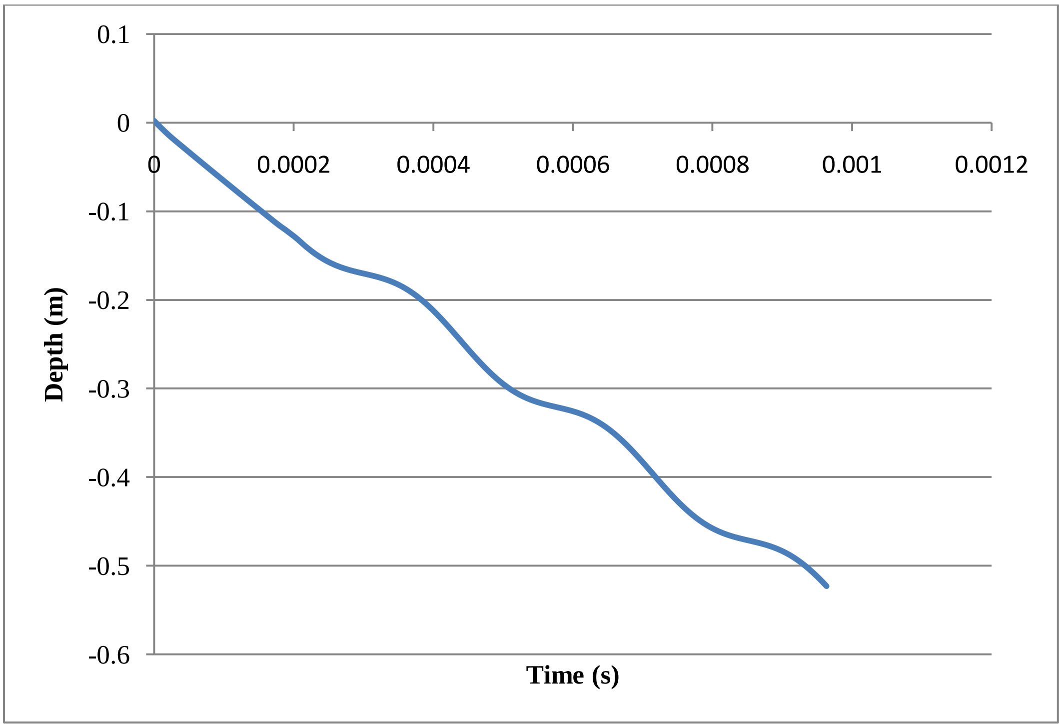

Figure A19: Penetration vs Time of Sandwich Panel 4 Layers Rubber-Stainless Alloy 304 with Panel Thickness 110 mm

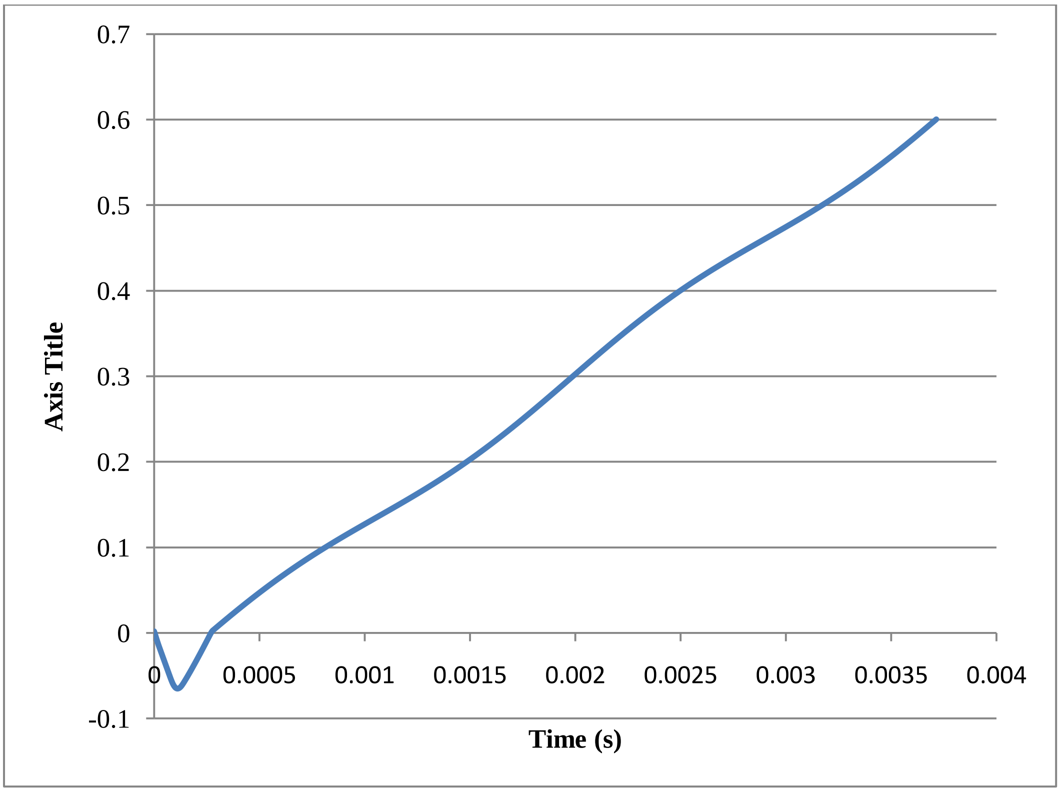

Figure A20: Penetration vs Time of Sandwich Panel 4 Layers Rubber-Steel Alloy 4140 with Panel Thickness 110 mm

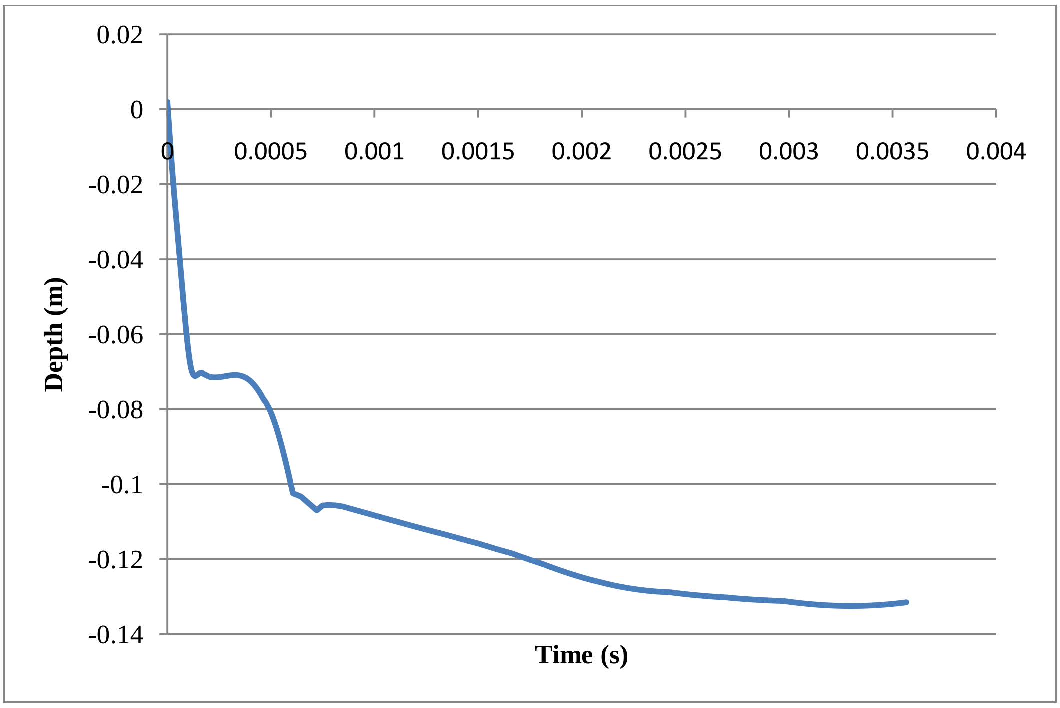

Figure A21: Penetration vs Time of Sandwich Panel 6 Layers Rubber-Stainless Alloy 304 with Panel Thickness 165 mm

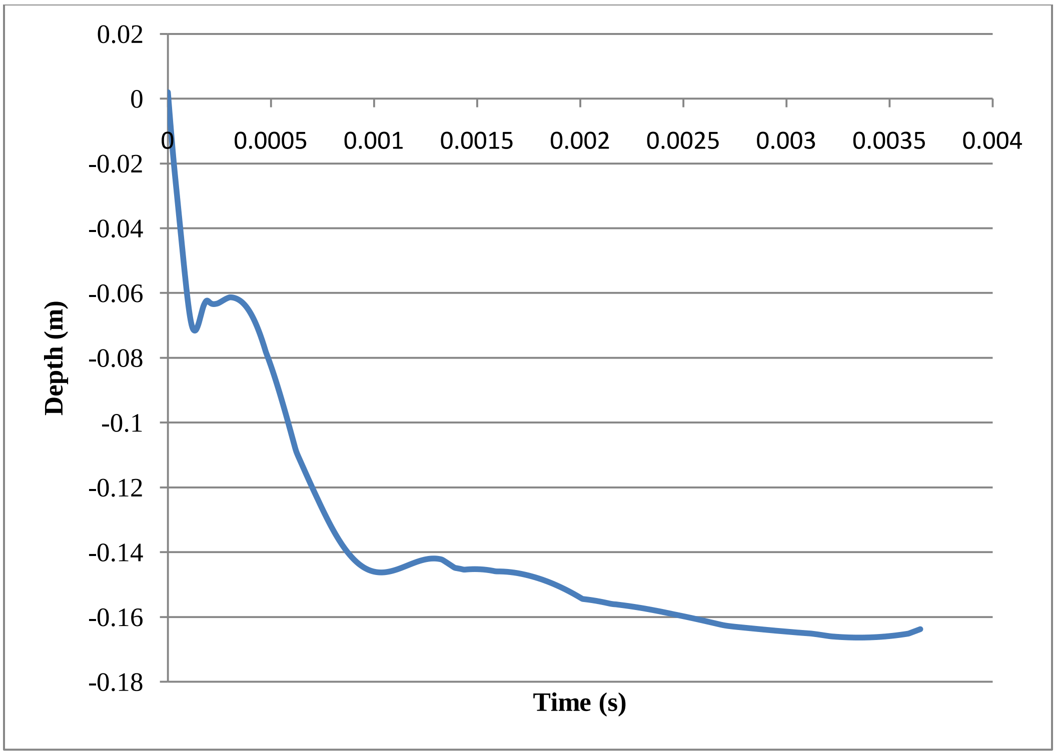

Figure A22: Penetration vs Time of Sandwich Panel 6 Layers Rubber-Steel Alloy 4140 with Panel Thickness 165 mm

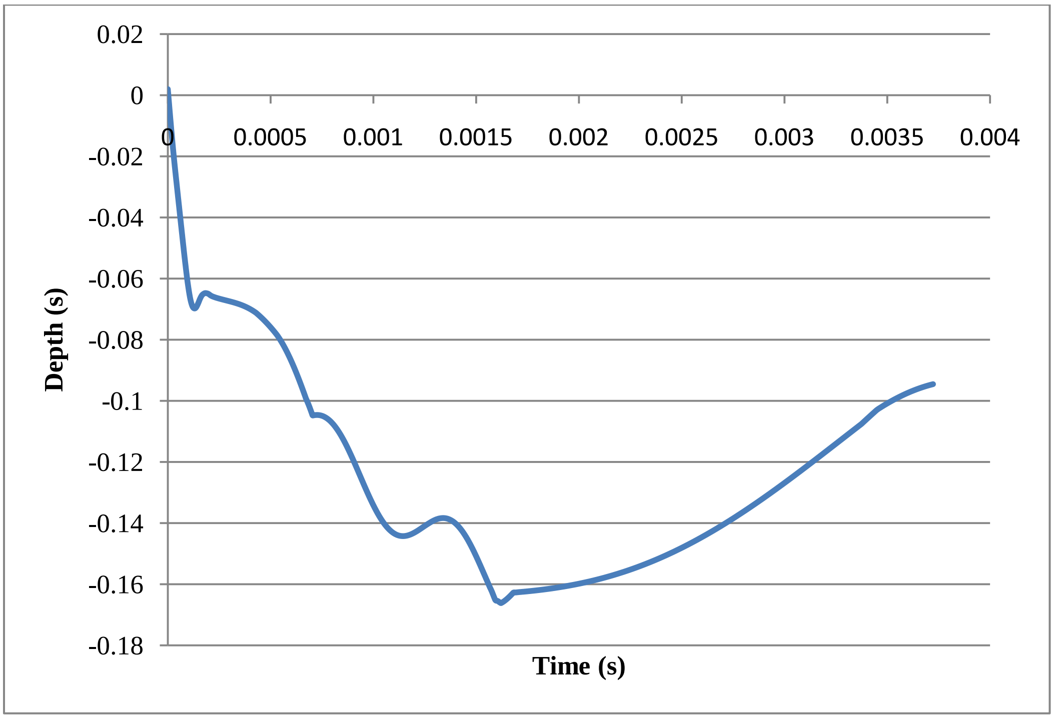

Figure A23: Penetration vs Time of Sandwich Panel 8 Layers Rubber-Stainless Alloy 304 with Panel Thickness 220 mm

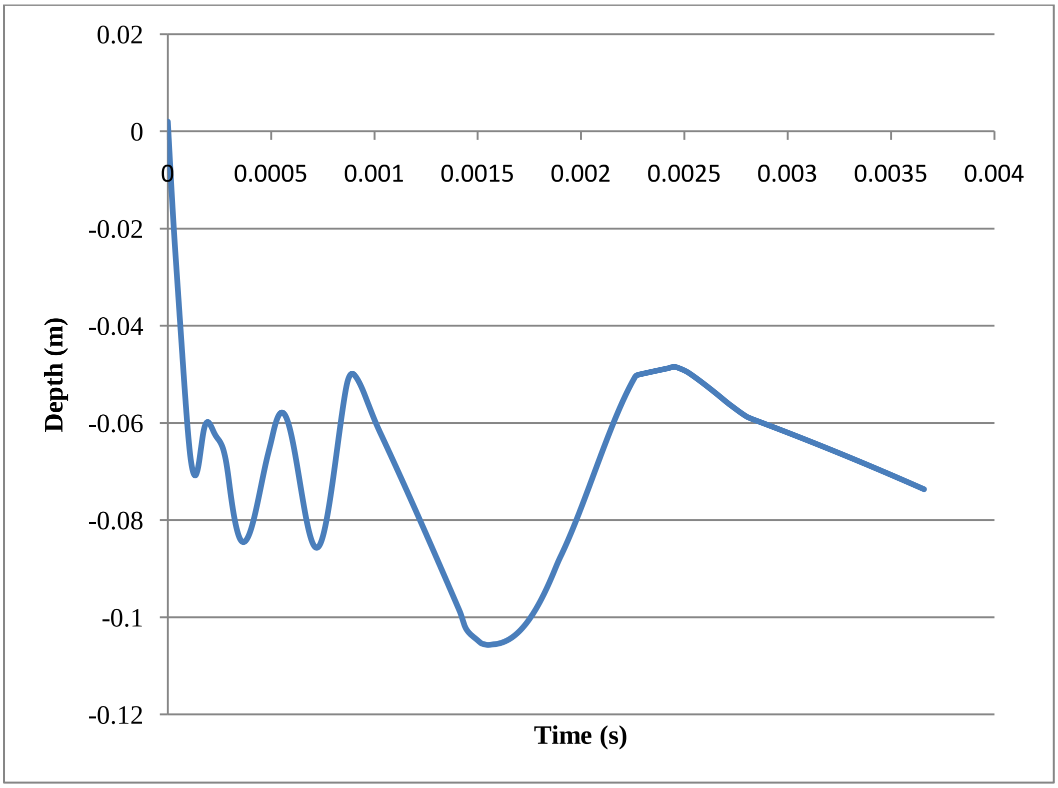

Figure A24: Penetration vs Time of Sandwich Panel 8 Layers Rubber-Steel Alloy 4140 with Panel Thickness 220 mm

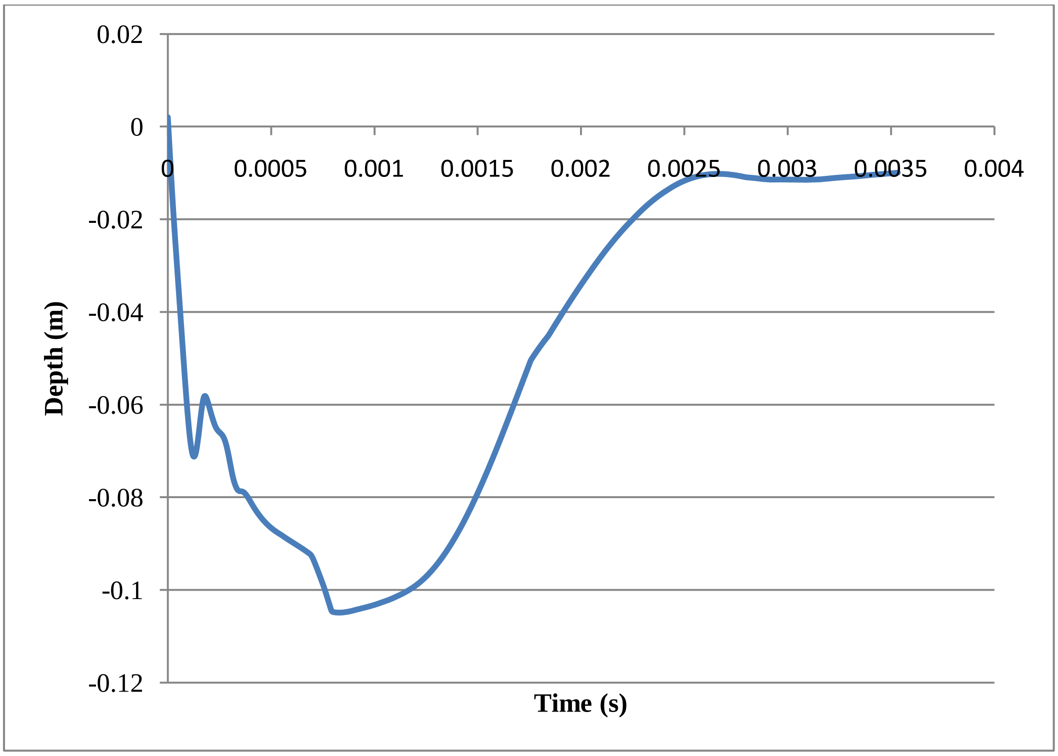

Figure A25: Penetration vs Time of Sandwich Panel 6 Layers Rubber-Steel Alloy 4140 with Panel Thickness 165 mm and Yield Strength Reduced 20%

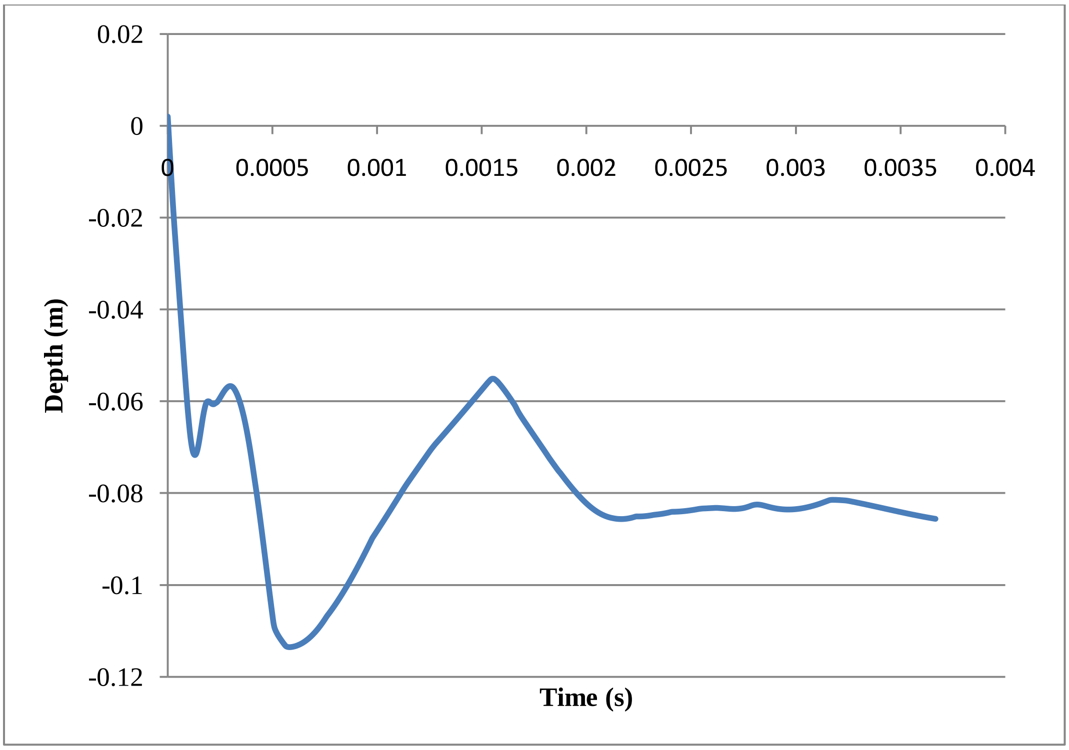

Figure A26: Penetration vs Time of Sandwich Panel 6 Layers Rubber-Steel Alloy 4140 with Panel Thickness 165 mm and Yield Strength Reduced 40%

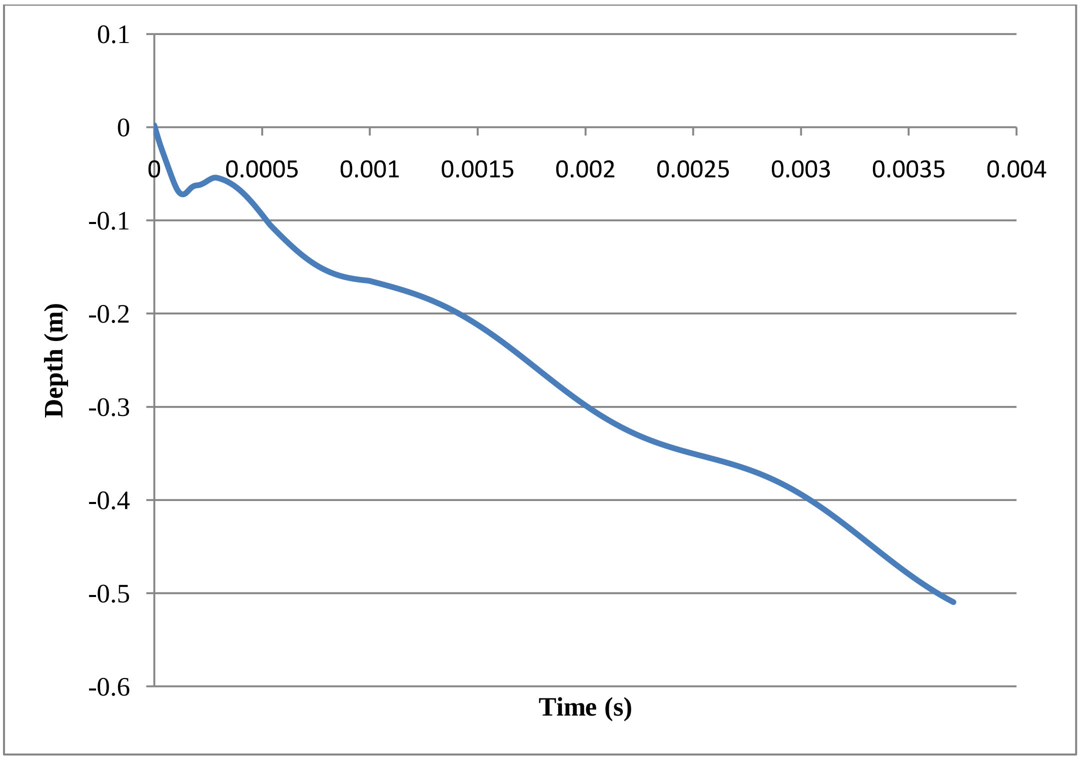

Figure A27: Penetration vs Time of Sandwich Panel 6 Layers Rubber-Steel Alloy 4140 with Panel Thickness 165 mm and Yield Strength Reduced 60%

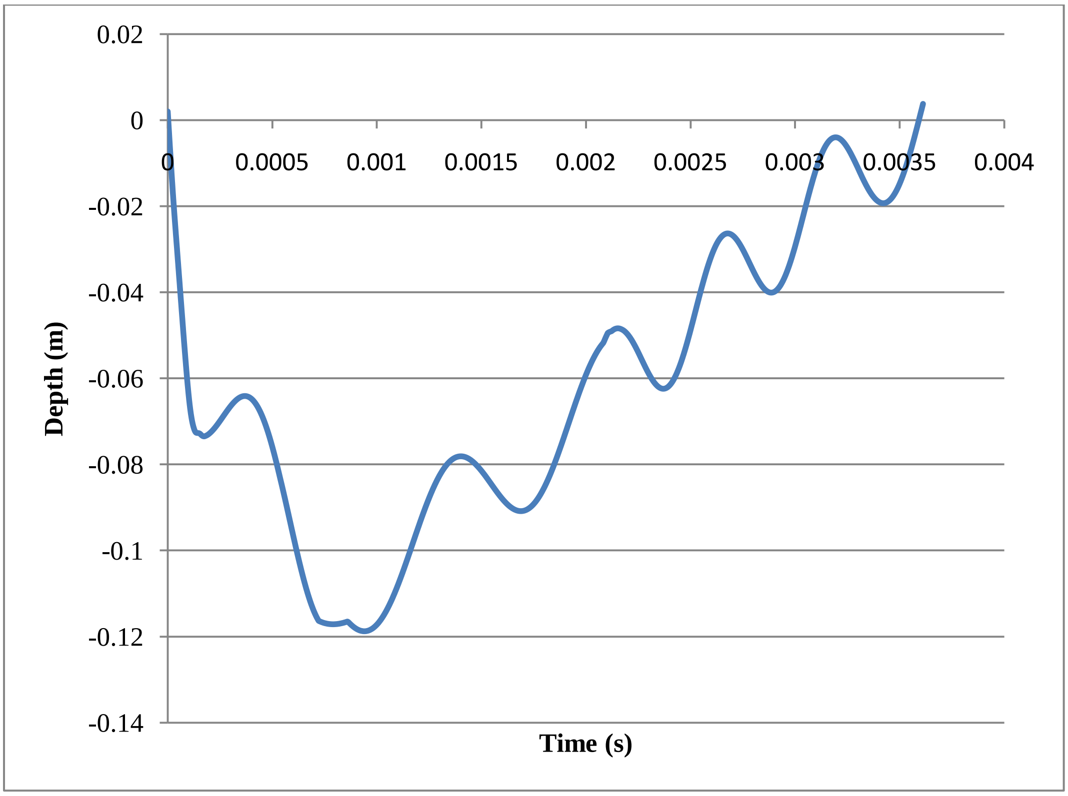

Figure A28: Penetration vs Time of Sandwich Panel 6 Layers Rubber-Steel Alloy 4140 with Panel Thickness 165 mm and % of Plastic Elongation 0.4

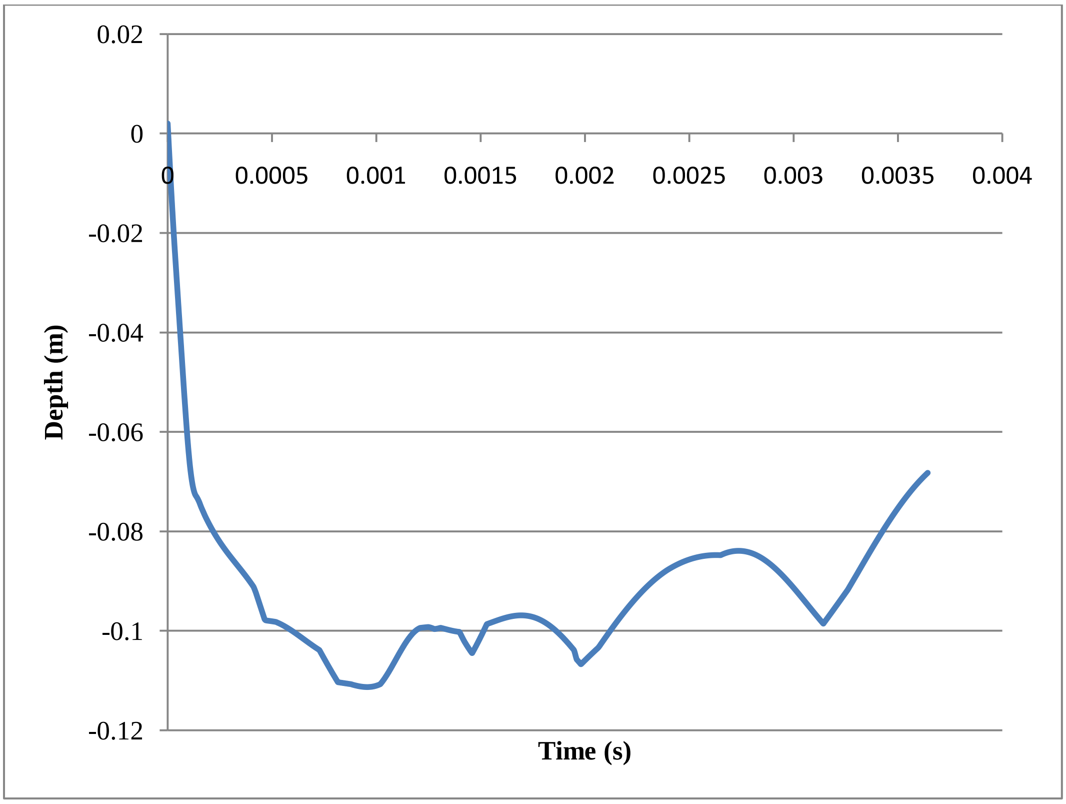

Figure A29: Penetration vs Time of Sandwich Panel 6 Layers Rubber-Steel Alloy 4140 with Panel Thickness 165 mm and % of Plastic Elongation 0.6

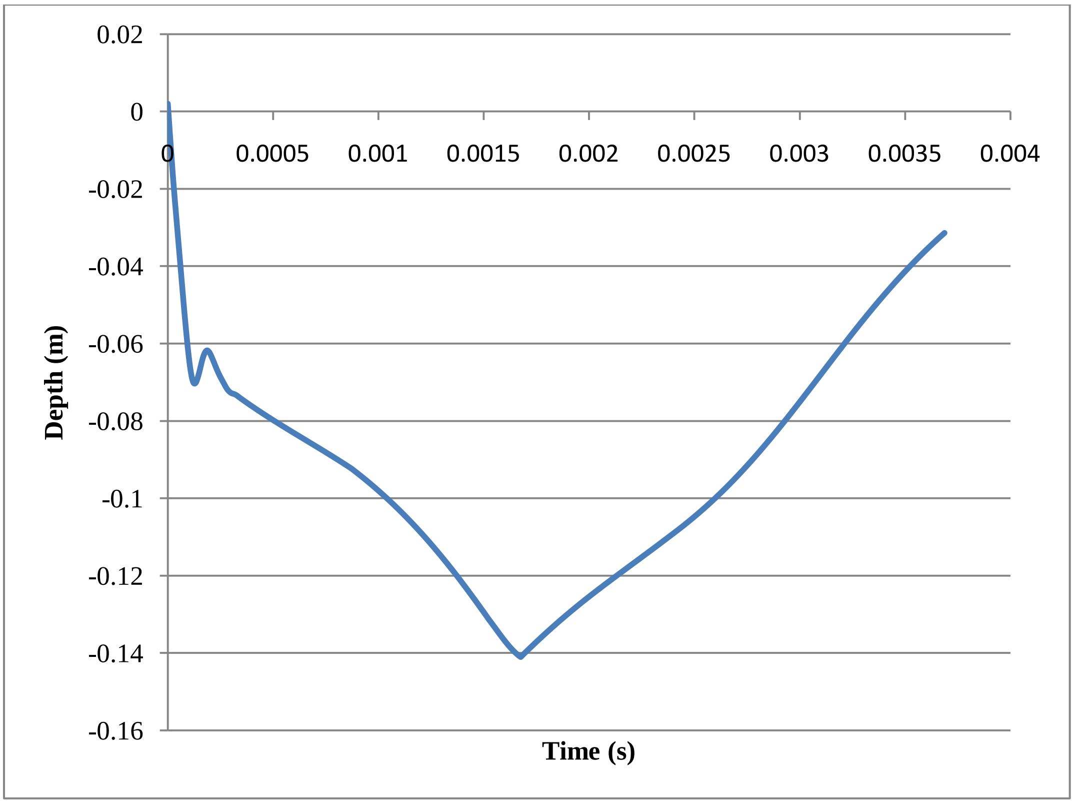

Figure A30: Penetration vs Time of Sandwich Panel 6 Layers Rubber-Steel Alloy 4140 with Panel Thickness 165 mm and % of Plastic Elongation 0.8